

522

NACA TN 2096

0065402



NATIONAL ADVISORY COMMITTEE FOR AERONAUTICS

TECHNICAL NOTE 2096

THE EFFECTS OF AMOUNT AND TYPE OF CAMBER ON THE VARIATION
WITH MACH NUMBER OF THE AERODYNAMIC CHARACTERISTICS OF
A 10-PERCENT-THICK NACA 64A-SERIES AIRFOIL SECTION

By James L. Summers and Stuart L. Treon

Ames Aeronautical Laboratory
Moffett Field, Calif.



Washington
May 1950

AFMTC
TECHNICAL LIBRARY
MAY 25 1950

319.98141



NATIONAL ADVISORY COMMITTEE FOR AERONAUTICS

TECHNICAL NOTE 2096

THE EFFECTS OF AMOUNT AND TYPE OF CAMBER ON THE VARIATION
WITH MACH NUMBER OF THE AERODYNAMIC CHARACTERISTICS OF
A 10-PERCENT-THICK NACA 64A-SERIES AIRFOIL SECTION

By James I. Summers, and Stuart L. Treon

SUMMARY

The results of a wind-tunnel investigation to determine the effect of varying the amount and type of camber on the section characteristics of 10-percent-chord-thick NACA 64A-series profiles are presented. The airfoil sections were cambered for design section lift coefficients of 0.3, 0.6, and 0.9 on the NACA $a=1.0$ mean line and for 0.3 and 0.6 on the NACA $a=0.4$ mean line. Mach numbers were varied from 0.3 to approximately 0.9, with corresponding Reynolds numbers from 1.0×10^6 to 2.0×10^6 .

It was found, in general, that increases in camber to 0.9 design section lift coefficient affected section characteristics in a manner which would ordinarily be anticipated. Increases in camber resulted in large increases in lift- and drag-divergence Mach numbers at high values of lift coefficient and in augmentation of the maximum lift coefficient. The variation of lift-curve slope with Mach number was most favorable, at a given lift coefficient, for the airfoil having a design section lift coefficient equal to the given value. At Mach numbers greater than those for lift divergence, increasing camber adversely affected the variation with Mach number of the slope of the pitching-moment curve, but had little effect on the variation with Mach number of the angle of attack required for a given lift coefficient greater than zero. At low and moderate Mach numbers, the improvements in lift-drag ratio ordinarily expected of camber were noted; but, at Mach numbers of 0.8 and above, camber provided either little improvement or had a detrimental effect on lift-drag ratio.

In general, the aerodynamic characteristics of the airfoil sections having the $a=0.4$ mean line were found to be inferior to those of the $a=1.0$ mean line airfoil sections.

INTRODUCTION

Information available at present concerning the aerodynamic characteristics at high subsonic Mach numbers of highly cambered airfoil sections is limited. The present investigation was undertaken in the Ames 1- by 3-1/2-foot high-speed wind tunnel to determine the effects of variation of the amount and type of camber on the characteristics of 10-percent-chord-thick NACA 64A-series airfoil sections. Lift, drag, and pitching-moment data were obtained at Mach numbers ranging from 0.3 to approximately 0.9 for sections having, for the NACA a=1.0 mean line, values of design section lift coefficient of 0.3, 0.6, and 0.9, and, for the NACA a=0.4 mean line, values of 0.3 and 0.6.

NOTATION

a	mean-line designation, fraction of chord from leading edge over which design load is uniform
a_0	section lift-curve slope, per degree
c	airfoil chord, feet
c_d	section drag coefficient
c_l	section lift coefficient
c_l/c_d	section lift-drag ratio
c_{l_i}	design section lift coefficient
$c_{l_{max}}$	maximum section lift coefficient
$c_{m_{c/4}}$	section pitching-moment coefficient about the quarter-chord point
M	free-stream Mach number
M_d	drag-divergence Mach number, defined as the Mach number at which $\left(\frac{dc_d}{dM} \right)_{\alpha_0 = \text{constant}} = 0.1$
M_l	lift-divergence Mach number, defined as the Mach number at which $\left(\frac{d^2c_l}{dM^2} \right)_{\alpha_0 = \text{constant}} = 0$
V	free-stream velocity, feet per second
v	local velocity, feet per second
x	distance along chord from leading edge, feet

y	distance perpendicular to chord, feet
α_0	section angle of attack, degrees
α_1	section angle of attack at design section lift coefficient, degrees

APPARATUS AND METHODS

The investigation was conducted in the Ames 1- by 3-1/2-foot high-speed wind tunnel which is a two-dimensional-flow, low-turbulence, closed-throat tunnel.

The airfoil sections¹ investigated are designated as:

NACA 64A010
NACA 64A310
NACA 64A310, $a=0.4$
NACA 64A610
NACA 64A610, $a=0.4$
NACA 64A910

All models were of 6-inch chord and 12-inch span and were constructed of aluminum alloy. The calculated coordinates for these airfoil sections are given in tables I to VI. Section profiles and theoretical pressure distributions, calculated by the methods of references 1 and 2 for incompressible and inviscid flow, are shown in figure 1.

The models were supported in the tunnel by circular glass plates and completely spanned the 1-foot dimension of the test section. To obtain variation of angle of attack, these end plates were constructed so as to be free to rotate, care being taken to retain the continuity of the test-section walls. Tight-fitting rubber gaskets between the model and the end plates sealed the gap, preserving two-dimensional flow.

Measurements of the lift, drag, and quarter-chord pitching moment were made simultaneously at angles of attack varying from approximately -10° to $+14^\circ$ in 2° increments, and at -1° and $+1^\circ$. For each airfoil section, the range of angle of attack was sufficient to encompass both a negative lift and a positive maximum lift at the low and moderate Mach numbers. At the higher Mach numbers, maximum lift could not be obtained because of the force limit on the balance. Mach number variation was from 0.3 to approximately 0.9. The corresponding Reynolds numbers ranged from about 1.0×10^6 to 2.0×10^6 .

¹Where mean line is not indicated for cambered airfoil sections, the basic loading is uniform ($a=1.0$ mean line).

The airfoil lift and quarter-chord pitching-moment data were obtained by use of a manometer which integrated the force reactions of the air on the floor and ceiling of the tunnel test section. These data were corrected to account for the finite length of test section by a method similar to that described in reference 2. Airfoil drag was determined from wake surveys made with a rake of total-head tubes.

ACCURACY OF MEASUREMENT

Although measurements of the lift, drag, quarter-chord pitching moment, and angle of attack were all affected by inaccuracies inherent in the testing procedure, the magnitude of these inaccuracies is not considered sufficiently great to affect the conclusions drawn from the results. The instrumentation employed in the measurement of lift and quarter-chord pitching moment is characterized by large tare values, resulting in inaccurate measurements of small values of force. However, analysis indicates that, at 0.3 Mach number, lift and quarter-chord pitching-moment coefficients are accurate within ± 0.008 and ± 0.016 , respectively, and, at 0.9 Mach number, within ± 0.002 and ± 0.003 , respectively.

A bubble-type protractor, in conjunction with an adjustable template placed on the airfoil surface, was employed to obtain the desired angle of attack. Errors inherent in the initial setting of this template and in the airfoil fabrication could result in a maximum error of 0.1° in the angle of attack. Also, since the protractor could be read no closer than the nearest 0.1° , a possibility of an additional 0.05° error in the angle-of-attack setting exists from this cause.

An examination of the contours of the 6-inch-chord models indicated, although the models were smooth and fair, that on the average the airfoil ordinates differed from the calculated values by approximately 0.6 percent of the calculated value. At certain stations, however, the difference amounted to as much as 3 percent of the calculated ordinate because of scattered surface irregularities.

RESULTS AND DISCUSSION

All the data in the present report have been corrected for wind-tunnel-wall interference by the method of reference 3. The data obtained at the highest test Mach numbers, however, are subject to some uncertainty because of the possible influence of wind-tunnel choking effects. This region of influence is indicated in the figures by the dashed portions of the curves at the highest Mach numbers.

The respective variations with Mach number of section lift, drag, and quarter-chord pitching-moment coefficients at constant angles of attack

are shown in figures 2, 3, and 4. The angle-of-attack values shown in these figures are subject to the previously discussed inaccuracies in the angle-of-attack setting, one result of which is the failure of the NACA 64A010 airfoil section to display zero section lift coefficient at zero angle of attack (fig. 2(a)).

Lift- and Drag-Divergence Characteristics

Plots of the lift- and drag-divergence Mach numbers as functions of lift coefficient (obtained from figs. 2 and 3) are presented in figures 5 and 6, respectively, for the airfoil sections having the $a=1.0$ mean line. From these figures, it is noticed that increasing camber extends the range of lift coefficient over which reasonably high values of lift- and drag-divergence Mach numbers are realized, and that the loss both of lift- and drag-divergence Mach numbers accruing from an increase of design lift coefficient from 0 to 0.3 is quite moderate, amounting to less than 0.02. For these reasons, it may be concluded that camber can be employed to obtain a high-divergence Mach number at a high value of lift coefficient, and that the drag penalty arising from use of a moderate amount of camber for this airfoil section is not great.

Furthermore, it is noted from figures 5 and 6 that, for any value of lift coefficient, drag divergence always occurs at a lower Mach number than lift divergence for all the airfoils embodying the $a=1.0$ mean line, the possible exception being the NACA 64A910 airfoil section for which the data are too limited to justify a categorical statement. For the NACA 64A610 airfoil section having the $a=0.4$ mean line, however, this desirable characteristic is not evident at values of lift coefficient greater than 0.7. (See figs. 7 and 8.) It is also to be noted that both the lift- and drag-divergence Mach numbers of the airfoil sections with the $a=0.4$ mean line are always less (at positive lift coefficients below 0.8) than those of the sections with the $a=1.0$ mean line.

Lift Characteristics

Lift coefficient as a function of angle of attack is plotted in figure 9 at constant values of Mach number for the various airfoil sections. The effects of amount and type of camber on these characteristics are more clearly shown as variations with Mach number of maximum lift coefficient (figs. 10 and 11), lift-curve slope (figs. 12 and 13), and angle of attack for constant lift coefficient (figs. 14 and 15). Because of the relatively low Reynolds numbers of the present investigation, the values of maximum lift coefficient at Mach numbers below approximately 0.6 are not representative of those at full scale. At the higher Mach numbers, however, scale of the tests does not significantly affect the maximum lift results. (See reference 4.)

As indicated in figure 10, increasing camber produced an anticipated increase in maximum lift coefficient, the magnitude of the improvement amounting to roughly two-thirds of the value of the design section lift coefficient. From a comparison of the curves of figure 11, it is shown that the airfoil sections utilizing the $a=1.0$ mean line have somewhat higher values of maximum lift coefficients above 0.65 Mach number than do those having the $a=0.4$ mean line.

The variations of lift-curve slope with Mach number for the airfoil sections having the $a=1.0$ mean line are compared in figure 12. In general, the more favorable variation of lift-curve slope with Mach number at a given lift coefficient is realized with the airfoil cambered to have a design section lift coefficient equal to the given value. The angle of attack required to maintain a given lift coefficient (fig. 14) increased rapidly at the higher Mach numbers. For any value of lift coefficient, the Mach number at which this change occurs (somewhat after lift divergence) decreases with increasing amount of camber. Above this Mach number, however, the rate of change of angle of attack with Mach number is essentially unaffected by amount of camber at values of lift coefficient greater than zero.

The airfoil sections with the $a=1.0$ mean line have better over-all lift-curve-slope variation throughout the Mach number range than do the airfoil sections with the $a=0.4$ mean line (fig. 13). In addition, in a given Mach number range, the variation of angle of attack for a given lift coefficient is somewhat less (fig. 15).

Drag Characteristics

Drag coefficient as a function of lift coefficient is presented in figure 16 at several Mach numbers for the various airfoil sections. The improvement in lift-drag ratio ordinarily accompanying increases in amount of camber is apparent at the low and moderate Mach numbers. However, this advantage of camber disappears with increasing Mach number until, at Mach numbers of approximately 0.8 and higher, the effect of camber is either negligible or detrimental. These characteristics are illustrated in figure 17 in which is shown the effect of amount of camber on lift-drag ratio at Mach numbers of 0.5 and 0.8. As can be seen from a comparison at Mach numbers greater than 0.7 of the drag-coefficient curves of figure 16, at any common lift coefficient, the drag of the airfoil sections having the $a=0.4$ mean line is appreciably greater than those of the corresponding airfoil sections having the $a=1.0$ mean line.

Pitching-Moment Characteristics

Pitching-moment coefficient plotted against lift coefficient for several Mach numbers is shown in figure 18 for the several airfoil sections. At Mach numbers greater than those for lift divergence, the average slopes of the pitching-moment curves increase negatively somewhat more rapidly with Mach number as the amount of camber is increased. Less variation with Mach number of the slopes of the pitching-moment curves is noted for the airfoil sections having the $a=0.4$ mean line. As was expected, the sections having the $a=0.4$ mean line also display a smaller value of pitching-moment coefficient at zero lift than do the airfoil sections having the $a=1.0$ mean line.

CONCLUSIONS

The results of a wind-tunnel investigation of several cambered 10-percent-chord-thick NACA 64A-series airfoil sections at Mach numbers from 0.3 to approximately 0.9 and corresponding Reynolds numbers from 1.0×10^6 to 2.0×10^6 lead to the following conclusions:

1. An increase in camber from 0 to 0.9 design section lift coefficient resulted in large increases in the range of lift coefficient over which reasonably high values of lift- and drag-divergence Mach numbers are realized with only small or moderate losses in the lift- and drag-divergence Mach numbers at the lower values of lift coefficient.
2. Maximum lift coefficient increased with amount of camber, the increase, at Mach numbers greater than 0.6, being roughly two-thirds the value of the design section lift coefficient.
3. For a given value of lift coefficient, the variation of lift-curve slope with Mach number was the most favorable for the airfoil section cambered to have a design lift coefficient equal to the given value.
4. For lift coefficients greater than zero and for Mach numbers greater than those for lift divergence, the rate of change of angle of attack with Mach number was little affected by increases in the amount of camber.
5. Increasing amounts of camber produced, at Mach numbers less than 0.8, the increases in lift-drag ratio ordinarily expected; but, above this Mach number, the effect of such increases was negligible or detrimental.
6. The variation with Mach number of the average slope of the pitching-moment-coefficient curves became somewhat greater, at Mach numbers greater than those for lift divergence, as the amount of camber was increased.

7. In general, it was found that the aerodynamic characteristics of the airfoil sections having the NACA $a=0.4$ mean line were somewhat inferior to those of the sections having the NACA $a=1.0$ mean line.

Ames Aeronautical Laboratory,
National Advisory Committee for Aeronautics;
Moffett Field, Calif.

REFERENCES

1. Theodorsen, T., and Garrick, I. E.: General Potential Theory of Arbitrary Wing Sections. NACA Rep. 452, 1933.
2. Abbott, Ira H., von Doenhoff, Albert E., and Stivers, Louis S., Jr.: Summary of Airfoil Data. NACA Rep. 824, 1945.
3. Allen, H. Julian, and Vincenti, Walter G.: Wall Interference in a Two-Dimensional-Flow Wind Tunnel, with Consideration of the Effect of Compressibility. NACA Rep. 782, 1944.
4. Spreiter, John R., and Steffen, Paul J.: Effect of Mach and Reynolds Numbers on Maximum Lift Coefficient. NACA TN 1044, 1946.

TABLE I.— COORDINATES OF THE NACA 64A010 AIRFOIL SECTION

[Coordinates given in percent of airfoil chord]

Upper surface		Lower surface	
Station	Ordinate	Station	Ordinate
0	0	0	0
.5	.804	.5	-.804
.75	.969	.75	-.969
1.25	1.225	1.25	-1.225
2.5	1.688	2.5	-1.688
5.0	2.327	5.0	-2.327
7.5	2.805	7.5	-2.805
10	3.199	10	-3.199
15	3.813	15	-3.813
20	4.272	20	-4.272
25	4.606	25	-4.606
30	4.837	30	-4.837
35	4.968	35	-4.968
40	4.995	40	-4.995
45	4.894	45	-4.894
50	4.684	50	-4.684
55	4.388	55	-4.388
60	4.021	60	-4.021
65	3.597	65	-3.597
70	3.127	70	-3.127
75	2.623	75	-2.623
80	2.103	80	-2.103
85	1.582	85	-1.582
90	1.062	90	-1.062
95	.541	95	-.541
100	.021	100	-.021

L.E. radius: 0.687 percent c



TABLE II.— COORDINATES OF THE NACA 64A310 AIRFOIL SECTION

[Coordinates given in percent of airfoil chord]

Upper surface		Lower surface	
Station	Ordinate	Station	Ordinate
0	0	0	0
.399	.873	.601	-.723
.638	1.068	.862	-.858
1.123	1.379	1.377	-1.057
2.353	1.961	2.647	-1.403
4.837	2.759	5.163	-1.847
7.332	3.436	7.668	-2.164
9.832	3.970	10.168	-2.420
14.842	4.819	15.158	-2.809
19.859	5.464	20.141	-3.076
24.879	5.946	25.121	-3.262
29.902	6.294	30.098	-3.378
34.927	6.513	35.073	-3.423
39.952	6.601	40.048	-3.389
44.977	6.536	45.023	-3.252
50.000	6.338	50.000	-3.030
55.021	6.030	54.979	-2.746
60.039	5.627	59.961	-2.415
65.053	5.142	64.947	-2.052
70.063	4.584	69.937	-1.668
75.069	3.964	74.931	-1.280
80.070	3.296	79.930	-.908
85.065	2.582	84.935	-.580
90.056	1.836	89.944	-.286
95.038	1.014	94.962	-.065
100.000	0	100.000	0

L.E. radius: 0.687 percent c



TABLE III.— COORDINATES OF THE NACA 64A310,
a=0.4 AIRFOIL SECTION

[Coordinates given in percent of airfoil chord]

Upper surface		Lower surface	
Station	Ordinate	Station	Ordinate
0	0	0	0
.354	.900	.646	-.682
.586	1.110	.914	-.800
1.064	1.441	1.436	-.981
2.284	2.083	2.716	-1.265
4.759	3.013	5.241	-1.615
7.251	3.734	7.749	-1.854
9.752	4.337	10.248	-2.041
14.769	5.297	15.231	-2.315
19.799	6.025	20.201	-2.509
24.838	6.566	25.162	-2.640
29.884	6.946	30.116	-2.726
34.938	7.170	35.062	-2.766
40.011	7.227	39.989	-2.763
45.078	7.075	44.922	-2.711
50.118	6.762	49.882	-2.604
55.141	6.321	54.859	-2.451
60.152	5.776	59.848	-2.260
65.151	5.154	64.849	-2.034
70.140	4.466	69.860	-1.782
75.123	3.731	74.877	-1.509
80.100	2.977	79.900	-1.225
85.074	2.219	84.926	-.941
90.048	1.469	89.952	-.653
95.022	.732	94.978	-.350
100.000	.021	100.000	-.021

L.E. radius: 0.687 percent c



TABLE IV.— COORDINATES OF THE NACA 64A610
AIRFOIL SECTION

[Coordinates given in percent of airfoil chord]

Upper surface		Lower surface	
Station	Ordinate	Station	Ordinate
0	0	0	0
.303	.930	.697	-.630
.530	1.154	.970	-.734
1.000	1.520	1.500	-.878
2.209	2.221	2.791	-1.105
4.676	3.252	5.324	-1.356
7.166	4.057	7.834	-1.513
9.666	4.733	10.334	-1.631
14.685	5.831	15.315	-1.769
19.718	6.651	20.282	-1.875
24.758	7.285	25.242	-1.915
29.804	7.749	30.196	-1.917
34.853	8.056	35.147	-1.876
39.903	8.207	40.097	-1.781
44.953	8.179	45.047	-1.609
50.000	7.993	50.000	-1.375
55.042	7.673	54.958	-1.103
60.078	7.233	59.922	-.807
65.106	6.686	64.894	-.506
70.126	6.040	69.874	-.208
75.138	5.304	74.862	.066
80.139	4.486	79.861	.290
85.132	3.608	84.868	.454
90.111	2.607	89.889	.495
95.075	1.484	94.925	.412
100.000	0	100.000	0

L.E. radius: 0.687 percent c



TABLE V.— COORDINATES OF THE NACA 64A610,
 $\alpha=0.4$ AIRFOIL SECTION

[Coordinates given in percent of airfoil chord]

Upper surface		Lower surface	
Station	Ordinate	Station	Ordinate
0	0	0	0
.220	.972	.780	-.536
.436	1.227	1.064	-.607
.890	1.643	1.610	-.699
2.077	2.452	2.923	-.816
4.525	3.676	5.475	-.880
7.008	4.642	7.992	-.882
9.509	5.457	10.491	-.865
14.542	6.767	15.458	-.803
19.600	7.769	20.400	-.737
24.677	8.521	25.323	-.669
29.769	9.051	30.231	-.611
34.877	9.370	35.123	-.562
40.022	9.459	39.978	-.531
45.156	9.256	44.844	-.528
50.235	8.836	49.765	-.520
55.282	8.249	54.718	-.509
60.302	7.526	59.698	-.494
65.300	6.704	64.700	-.464
70.280	5.798	69.720	-.430
75.244	4.834	74.756	-.390
80.199	3.846	79.801	-.342
85.148	2.856	84.852	-.300
90.096	1.874	89.904	-.242
95.045	.920	94.955	-.158
100.000	.021	100.000	-.021

L.E. radius: 0.687 percent c



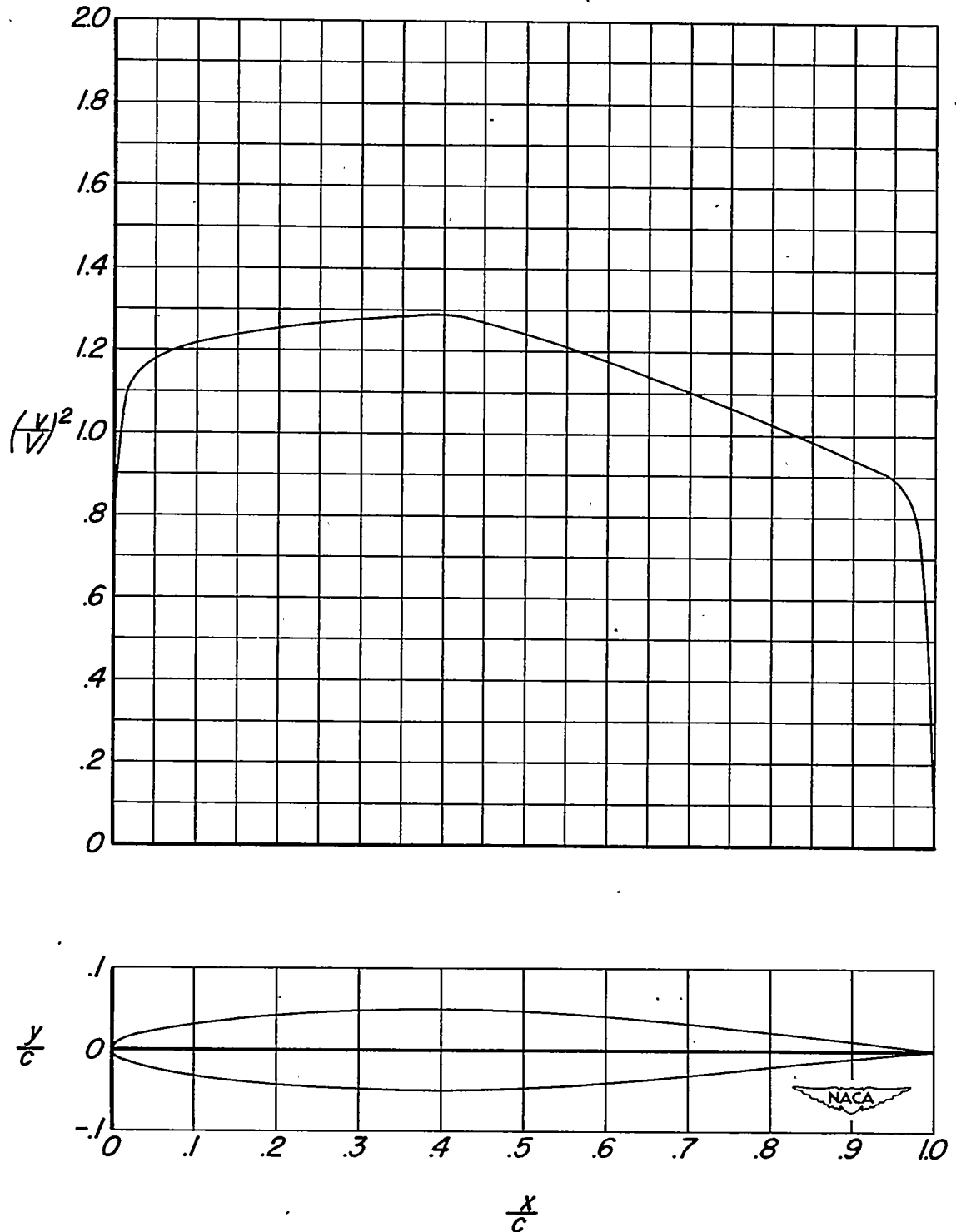
TABLE VI.— COORDINATES OF THE NACA 64A910 AIRFOIL SECTION

[Coordinates given in percent of airfoil chord]

Upper surface		Lower surface	
Station	Ordinate	Station	Ordinate
0	0	0	0
.215	.977	.785	-.527
.430	1.230	1.070	-.600
.884	1.651	1.616	-.688
2.072	2.470	2.928	-.796
4.520	3.699	5.480	-.855
7.003	4.669	7.997	-.853
9.503	5.487	10.497	-.834
14.530	6.814	15.470	-.755
19.578	7.833	20.422	-.669
24.639	8.620	25.361	-.565
29.707	9.202	30.293	-.454
34.780	9.598	35.220	-.328
39.855	9.813	40.145	-.174
44.930	9.822	45.070	.034
50.000	9.648	50.000	.280
55.063	9.316	54.937	.540
60.117	8.839	59.883	.801
65.159	8.228	64.841	1.042
70.189	7.495	69.811	1.253
75.206	6.642	74.794	1.414
80.208	5.675	79.792	1.489
85.195	4.600	84.805	1.460
90.165	3.376	89.835	1.277
95.112	1.951	94.888	.893
100.000	0	100.000	0

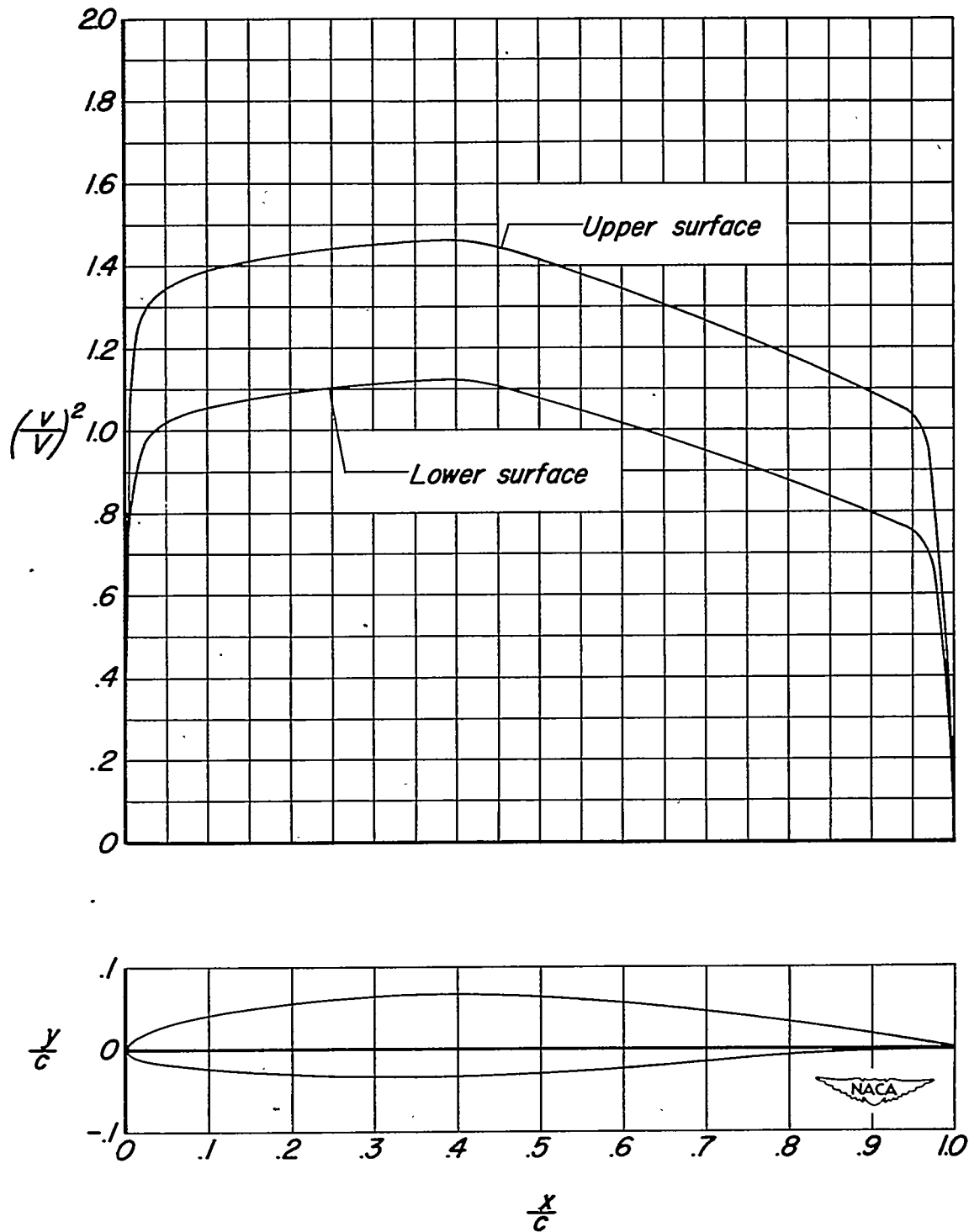
L.E. radius: 0.687 percent c





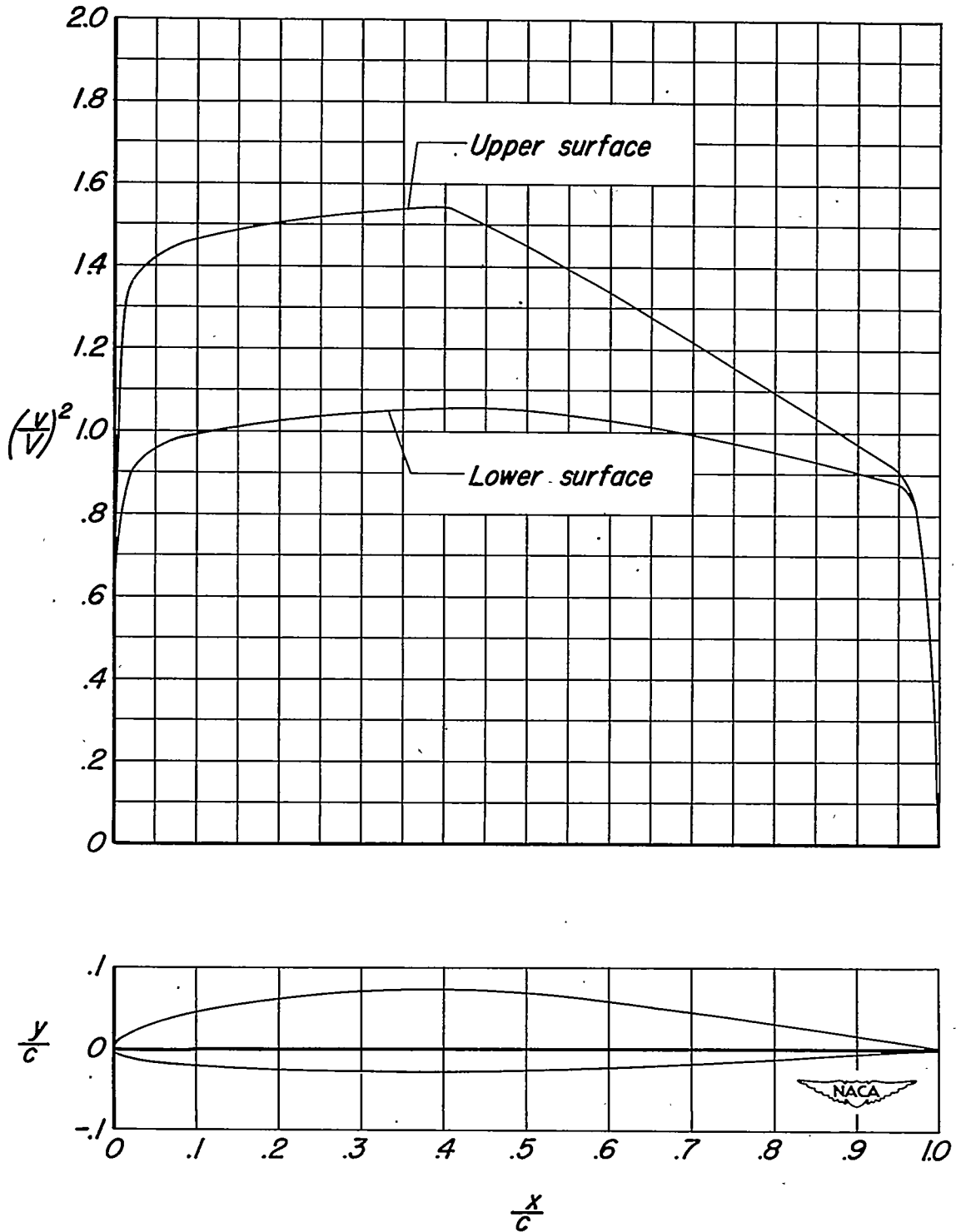
(a) NACA 64A010 airfoil section.

Figure 1 - Airfoil profiles and theoretical pressure distributions .



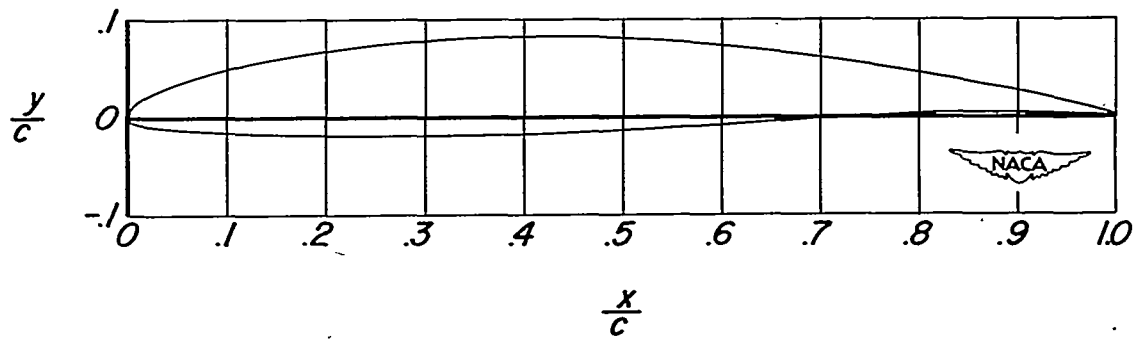
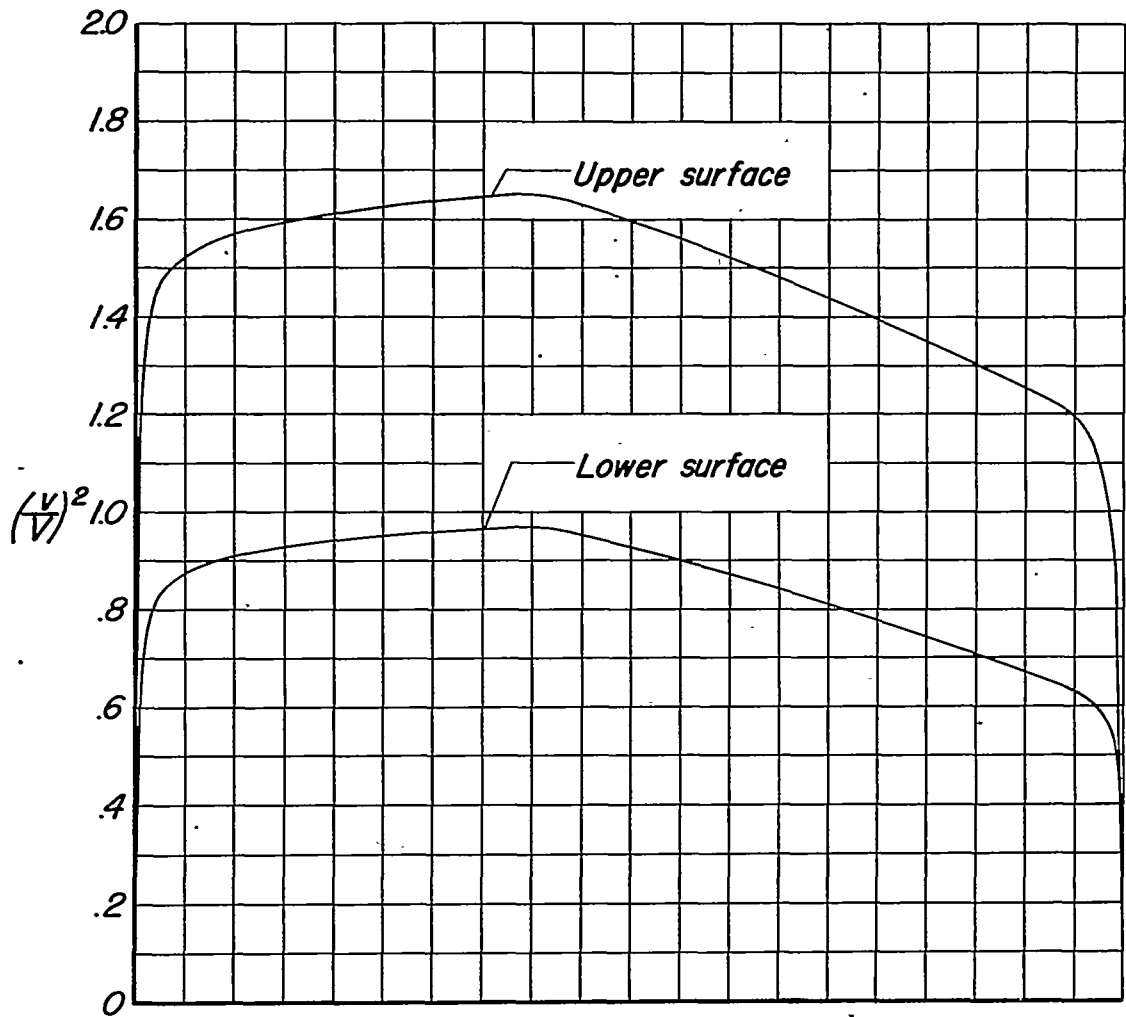
(b) NACA 64A310 airfoil section.

Figure 1 - Continued.



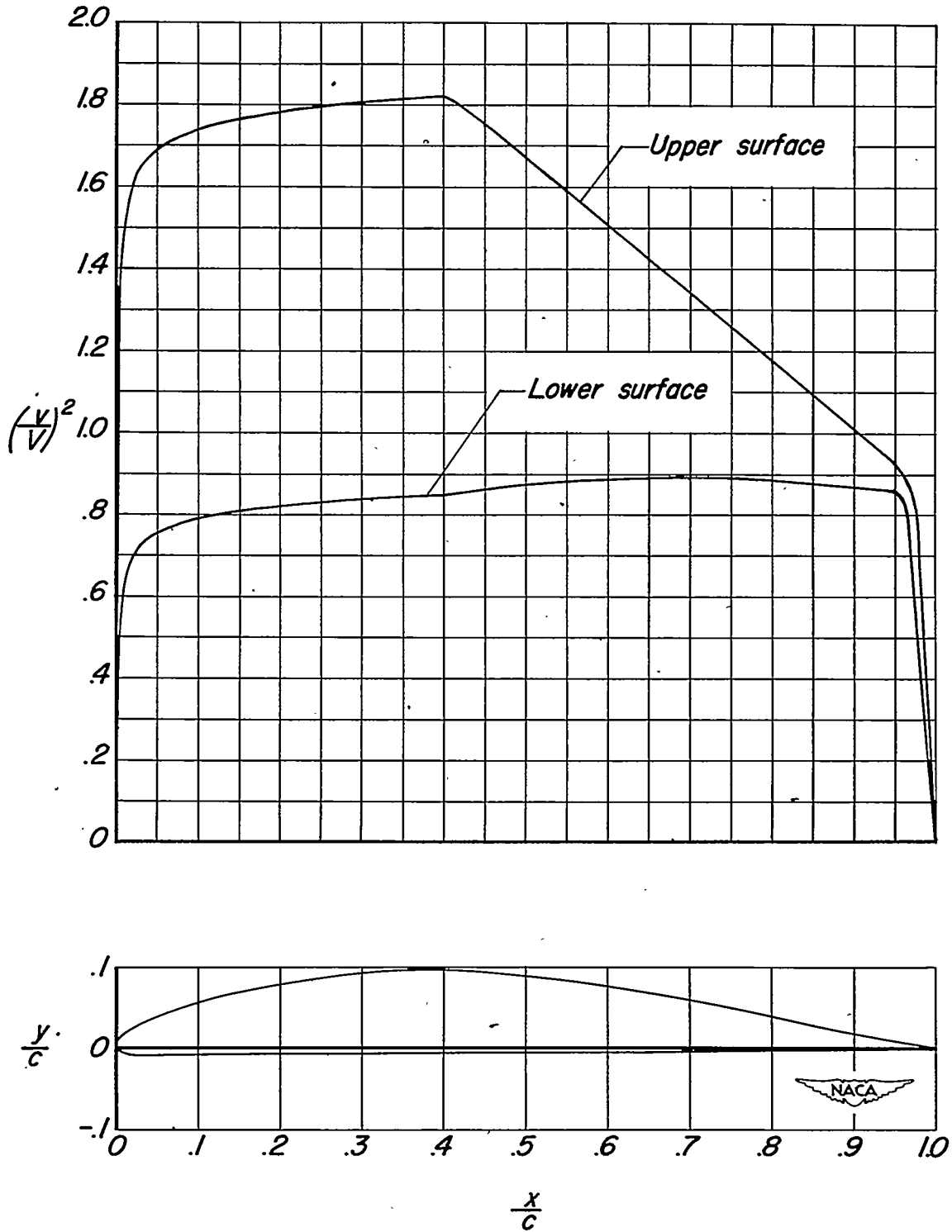
(c) NACA 64A310, $\alpha=0.4$ airfoil section.

Figure 1 - Continued.



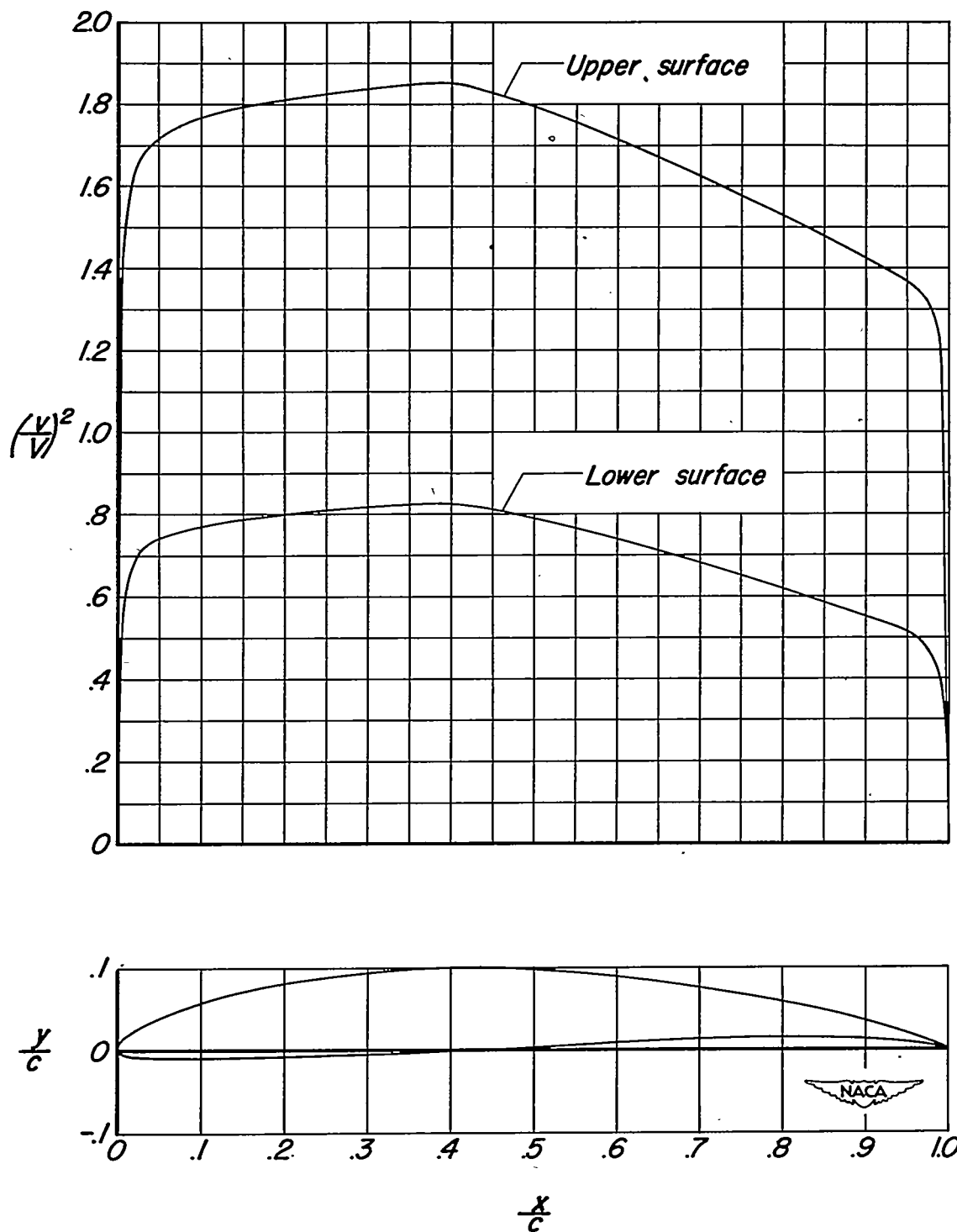
(d) NACA 64A610 airfoil section.

Figure 1 - Continued.



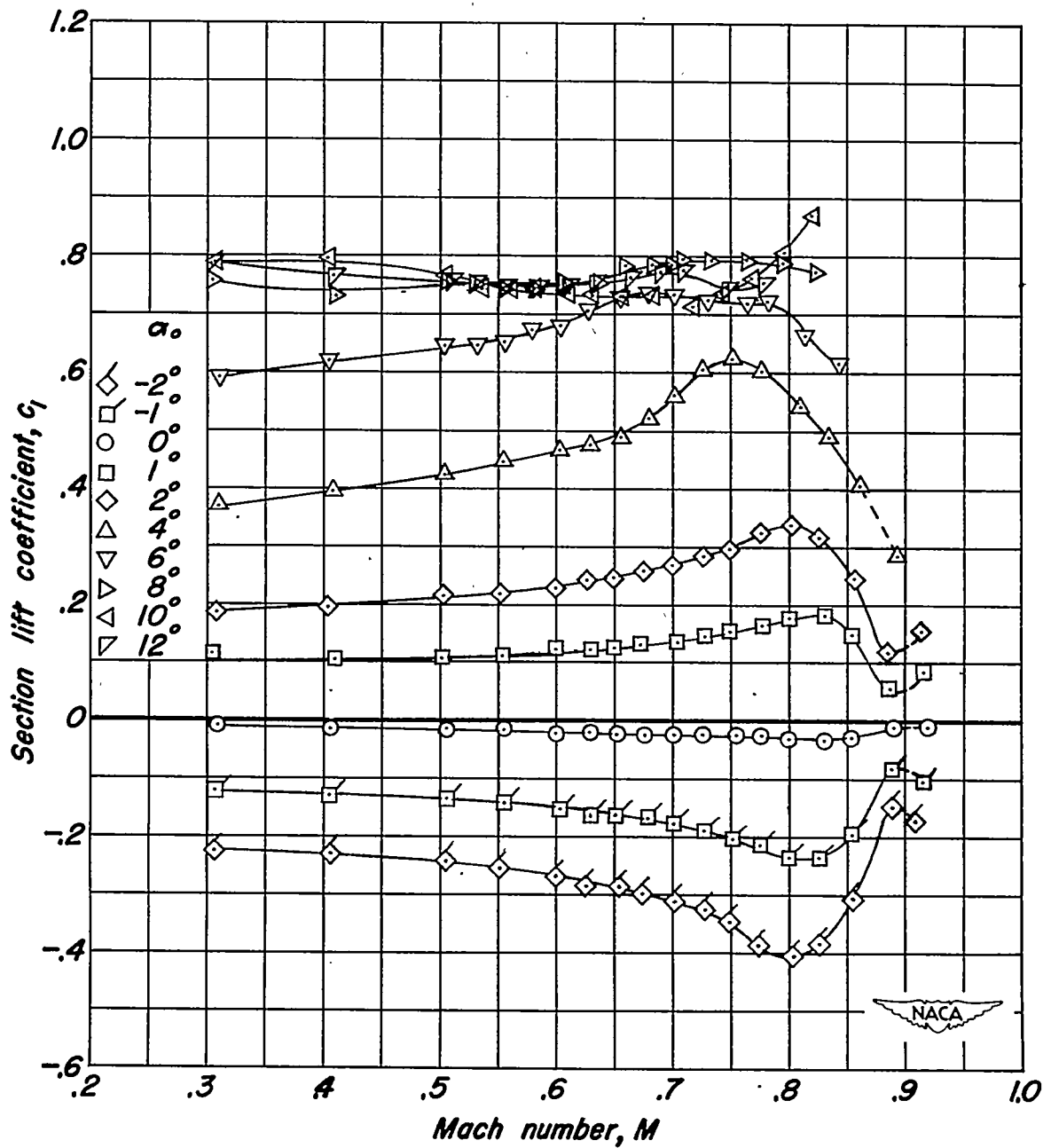
(e) NACA 64A610, $\alpha=0.4$ airfoil section.

Figure 1 - Continued.



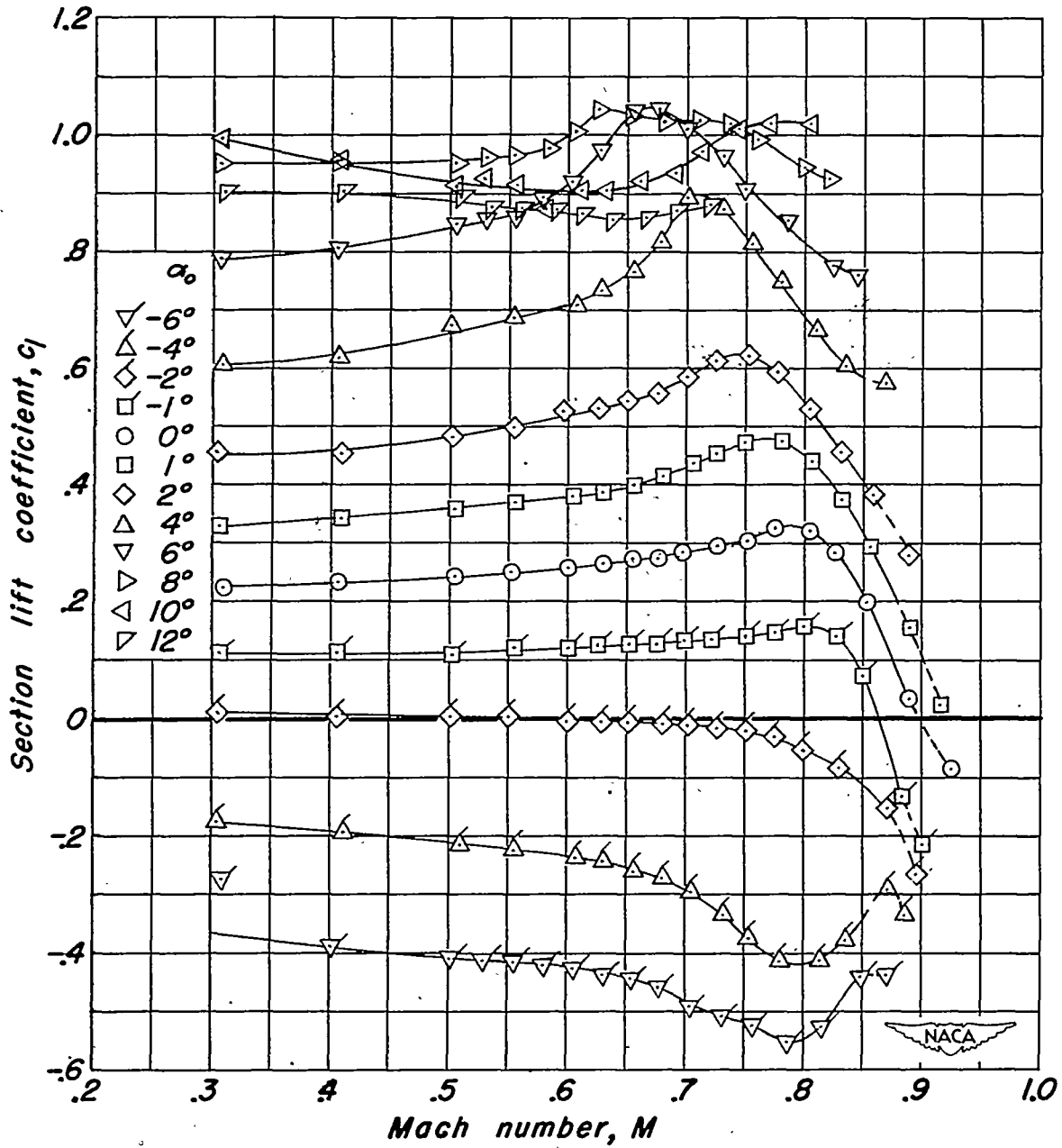
(f) NACA 64A910 airfoil section.

Figure 1 - Concluded.



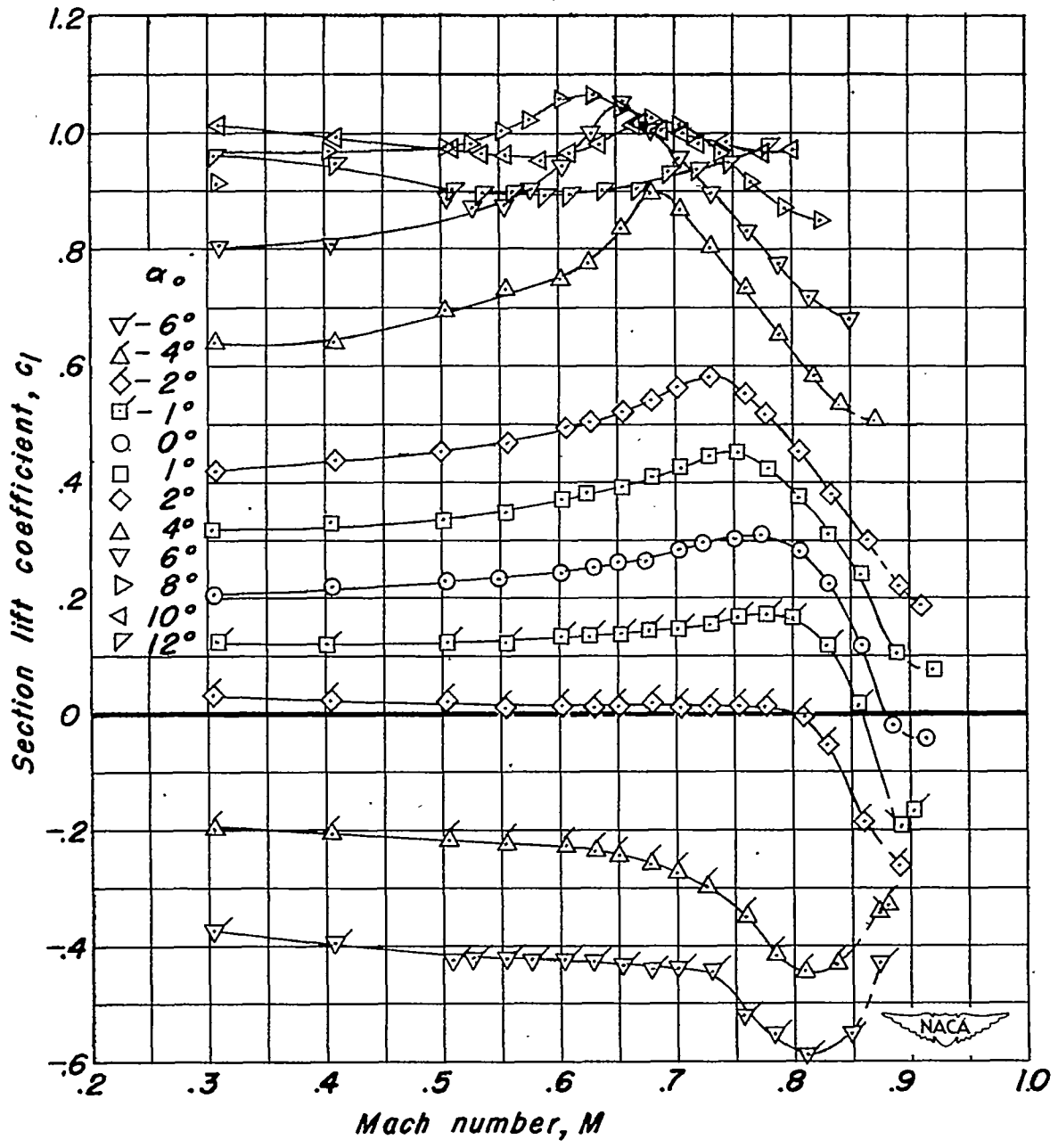
(a) NACA 64A010 airfoil section.

Figure 2.- Variation of section lift coefficient with Mach number at constant section angles of attack.



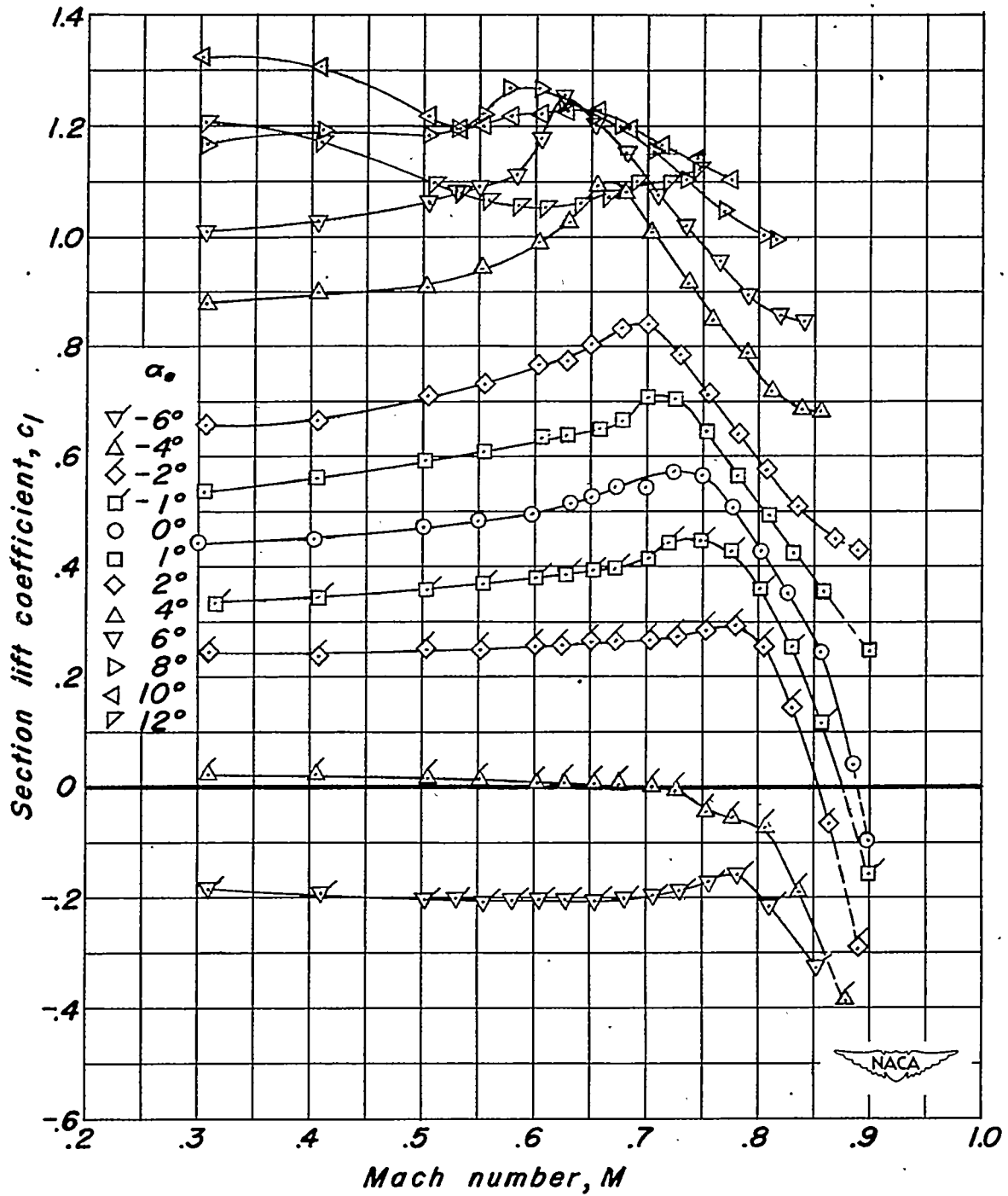
(b) NACA 64A310 airfoil section.

Figure 2 - Continued.



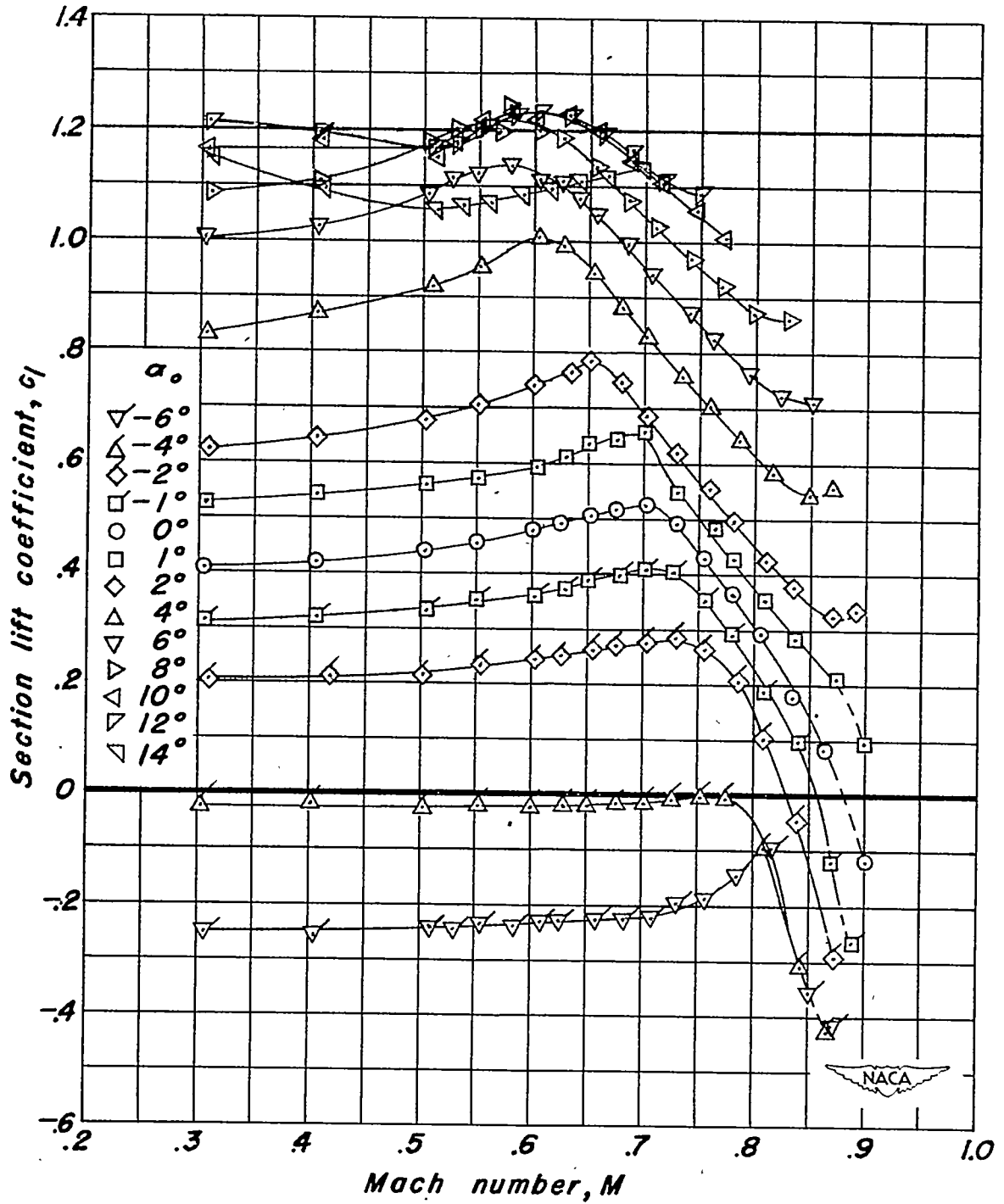
(c) NACA 64A310, $\alpha=0.4$ airfoil section.

Figure 2.-Continued.



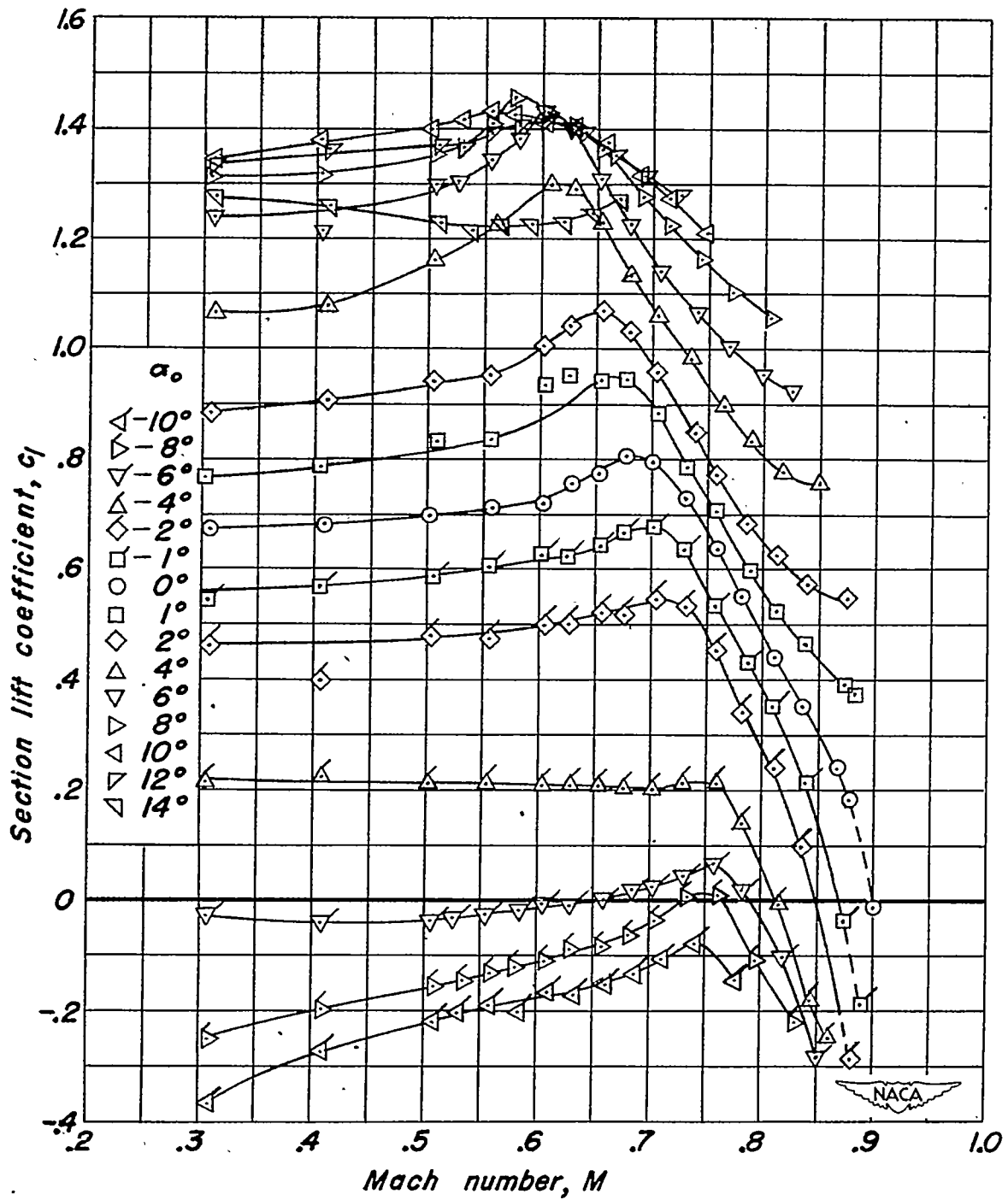
(d) NACA 64A610 airfoil section.

Figure 2.-Continued .



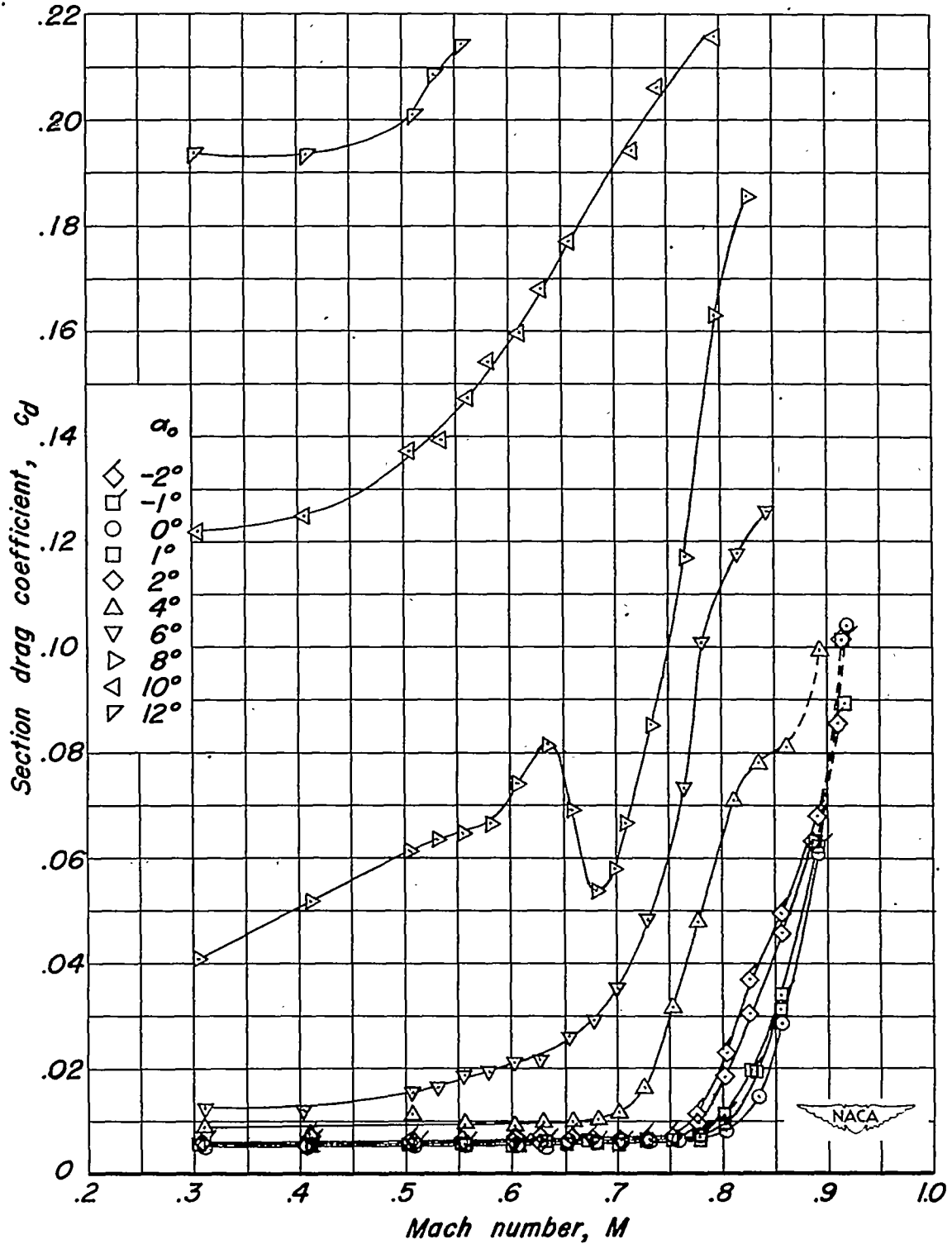
(e) NACA 64A610, $\alpha=0.4$ airfoil section.

Figure 2 - Continued .



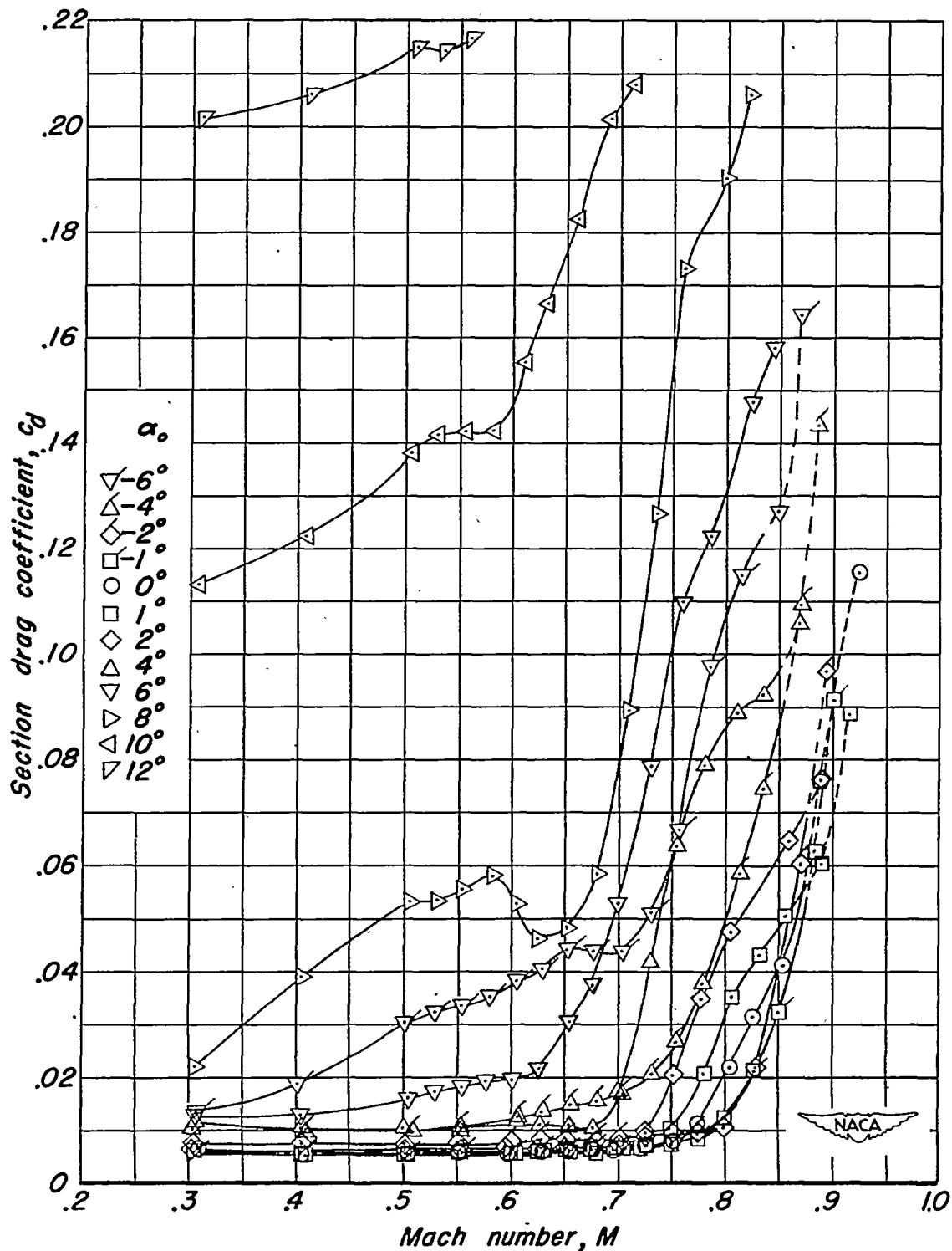
(f) NACA 64A910 airfoil section.

Figure 2.- Concluded.



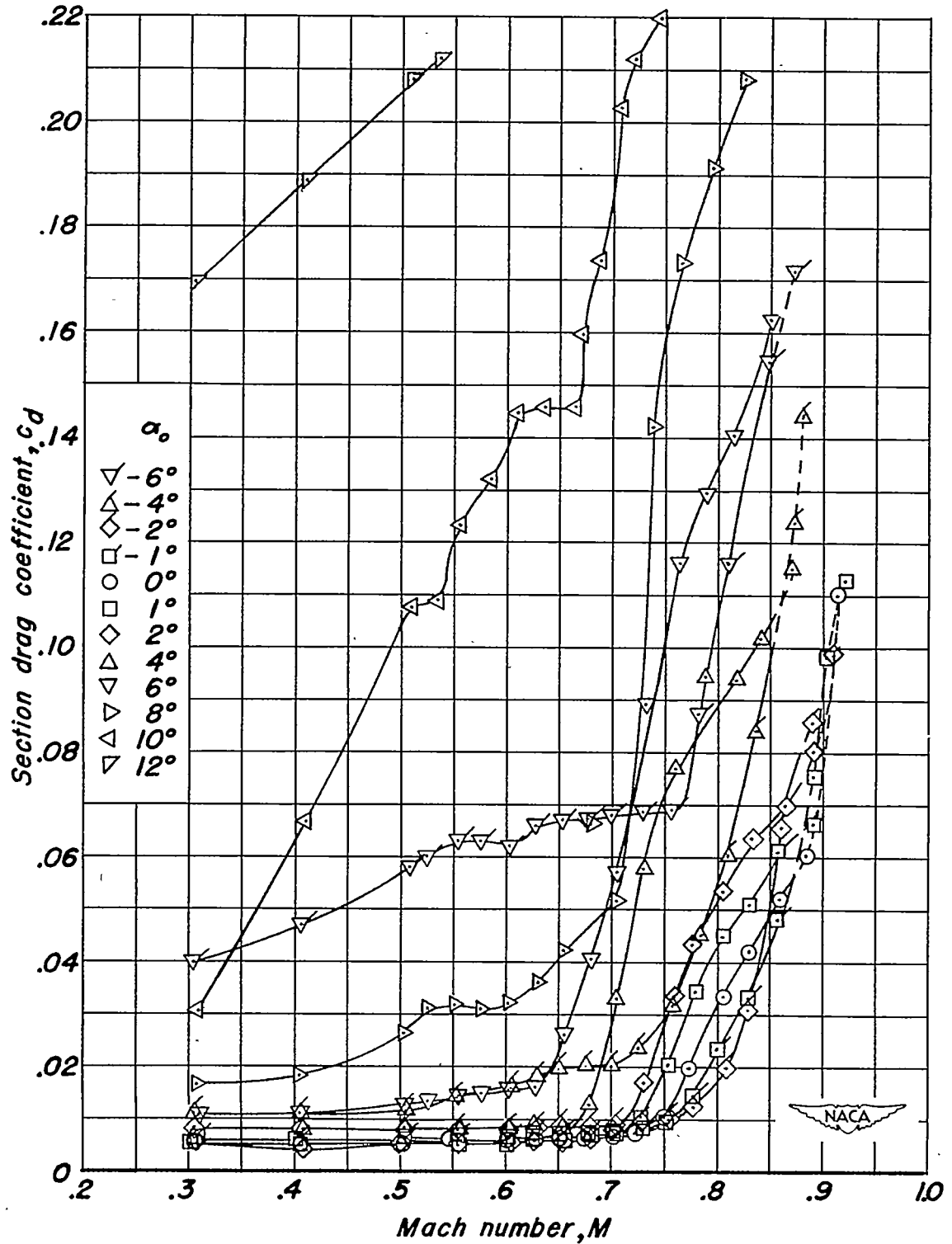
(a) NACA 64A010 airfoil section.

Figure 3.- Variation of section drag coefficient with Mach number at constant section angles of attack.



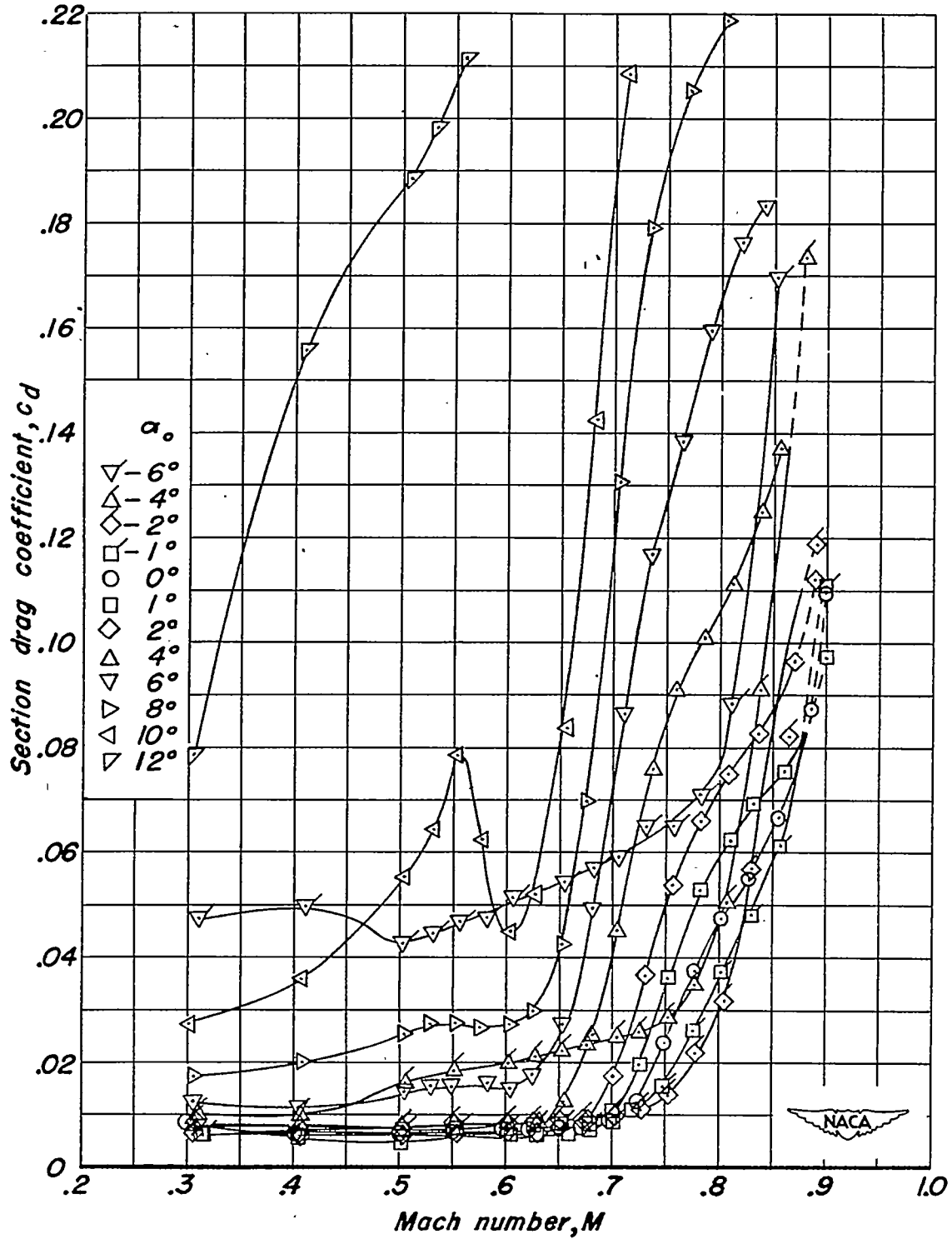
(b) NACA 64A310 airfoil section.

Figure 3.- Continued.



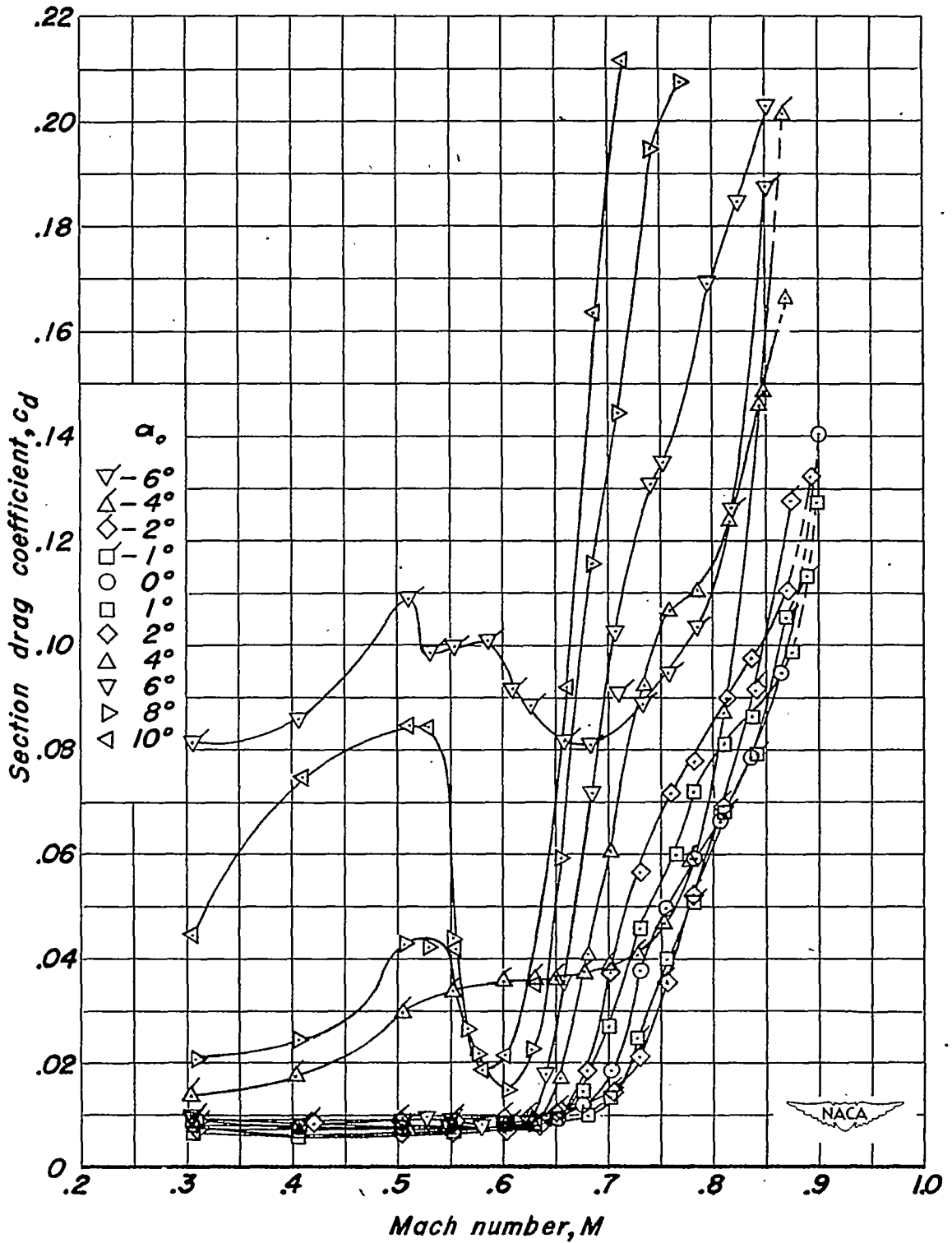
(c) NACA 64A310, $\alpha=0.4$ airfoil section.

Figure 3.- Continued .



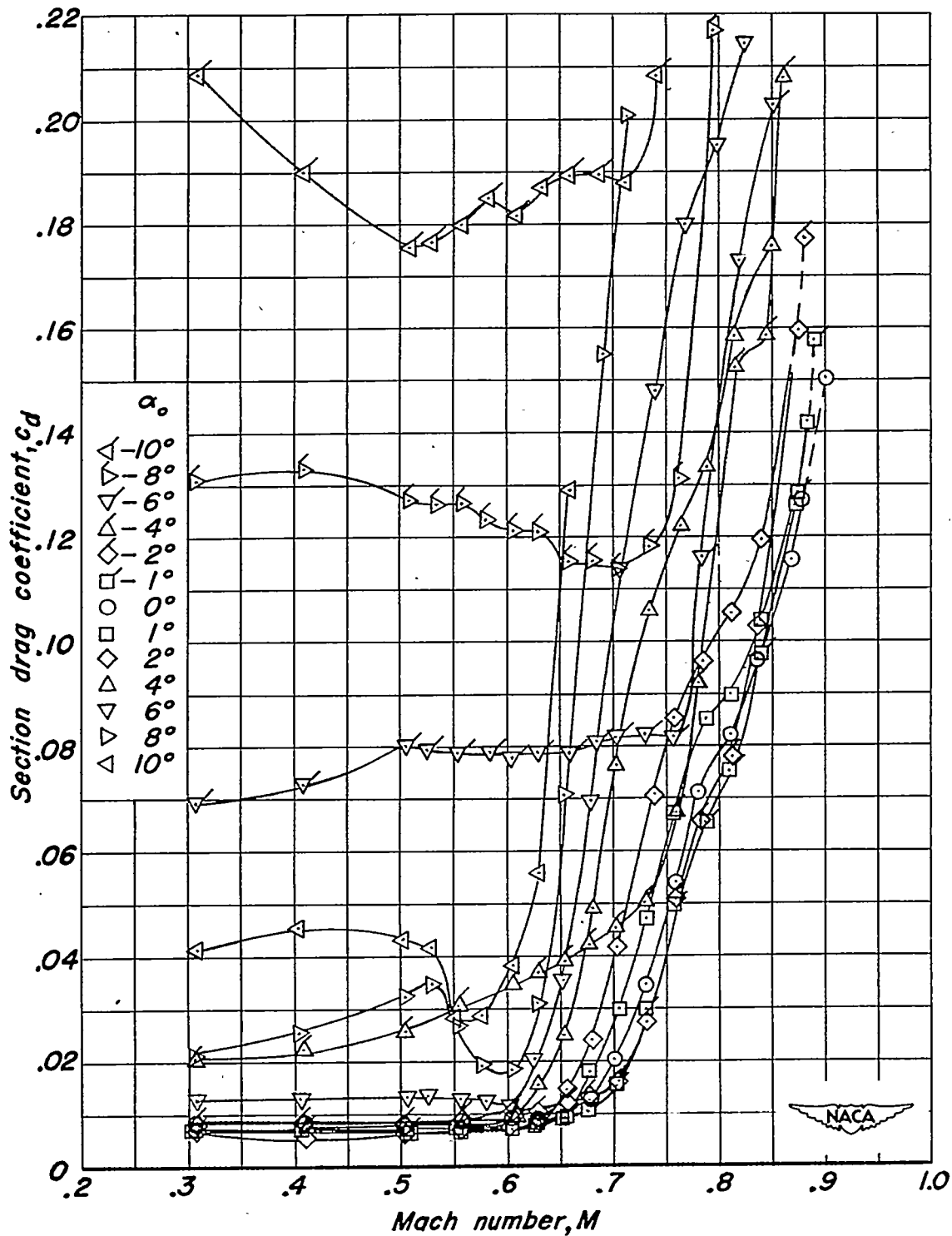
(d) NACA 64A610 airfoil section.

Figure 3 - Continued.



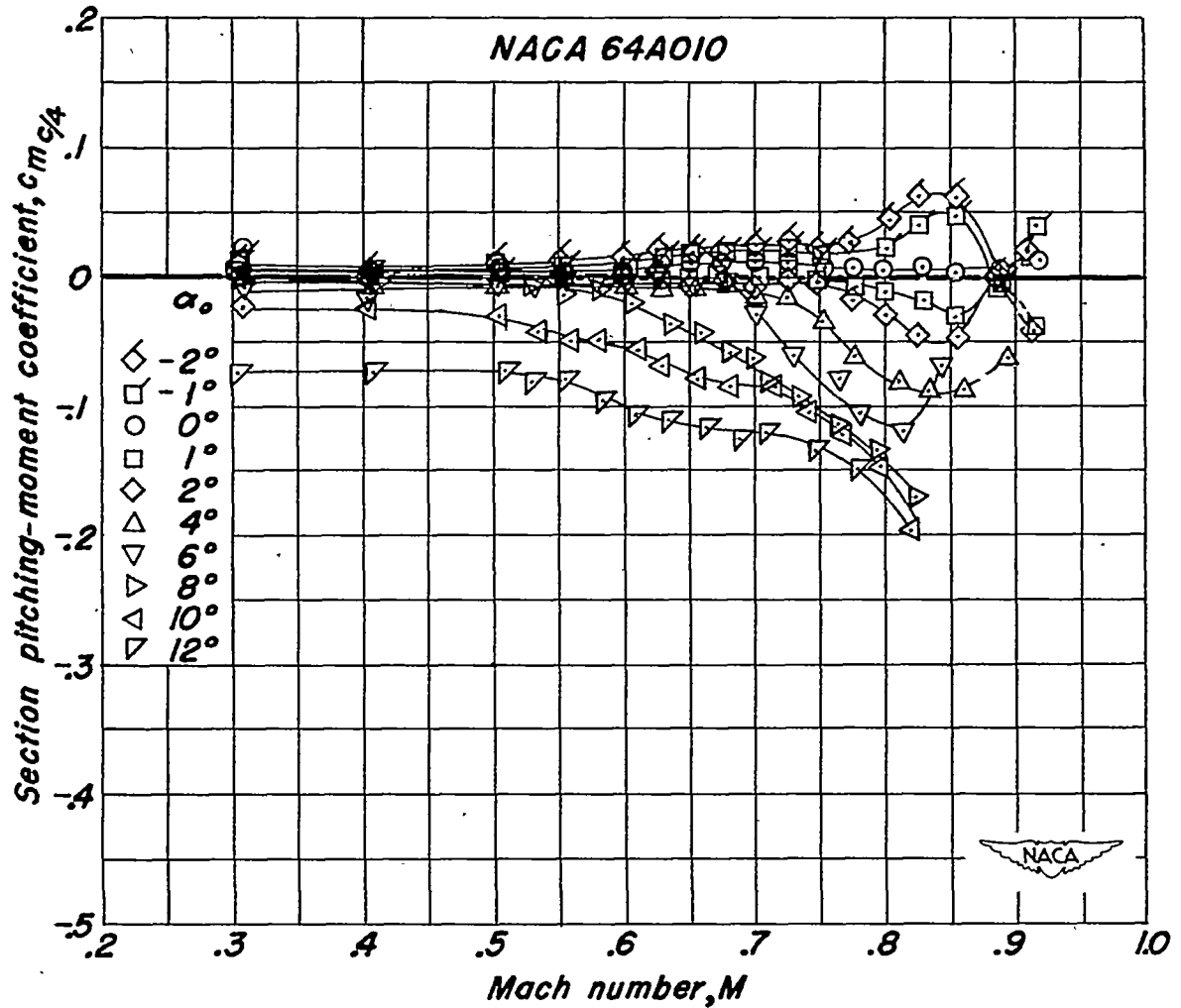
(e) NACA 64A610, $\alpha=0.4$ airfoil section.

Figure 3 - Continued.



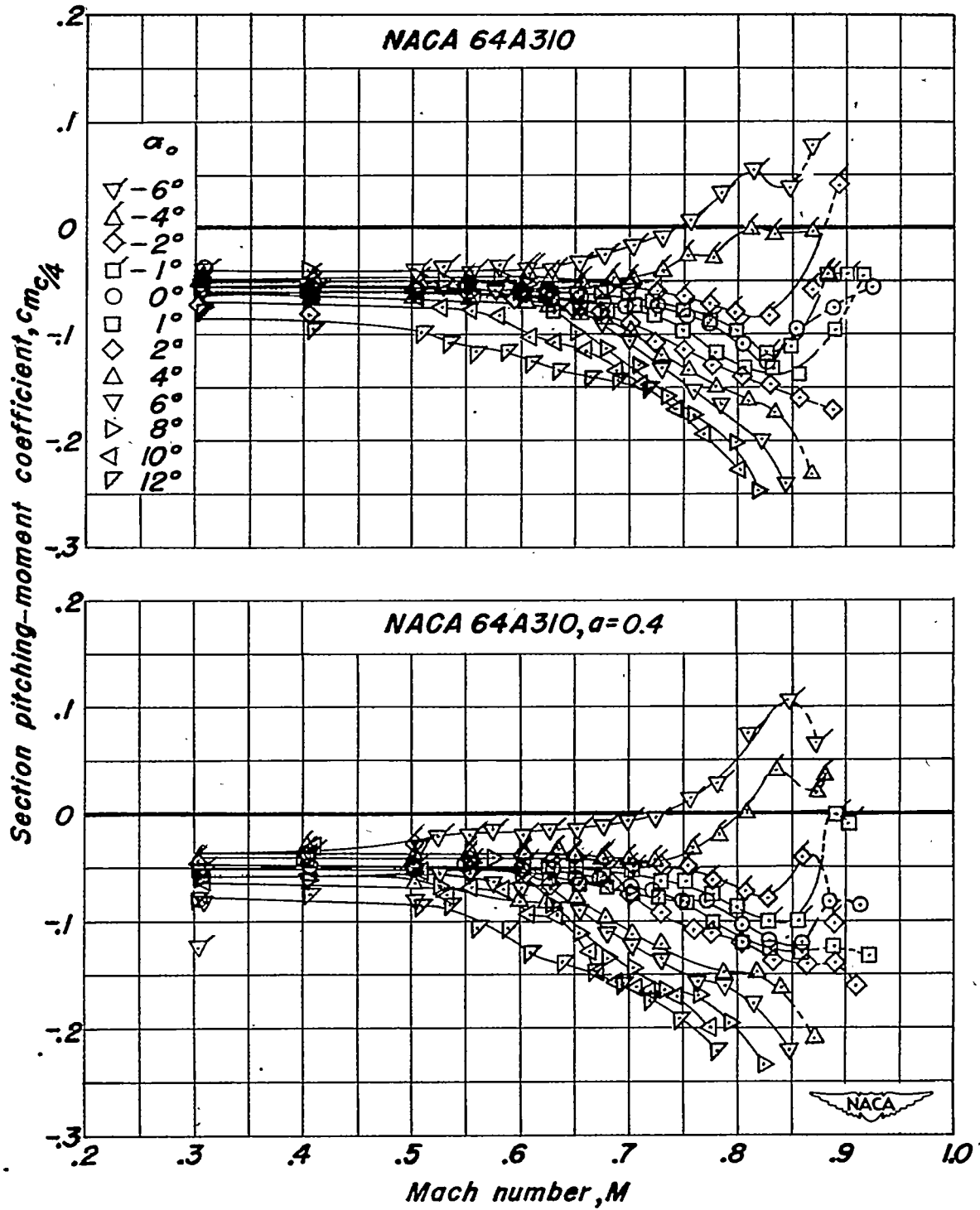
(f) NACA 64A910 airfoil section.

Figure 3.- Concluded .



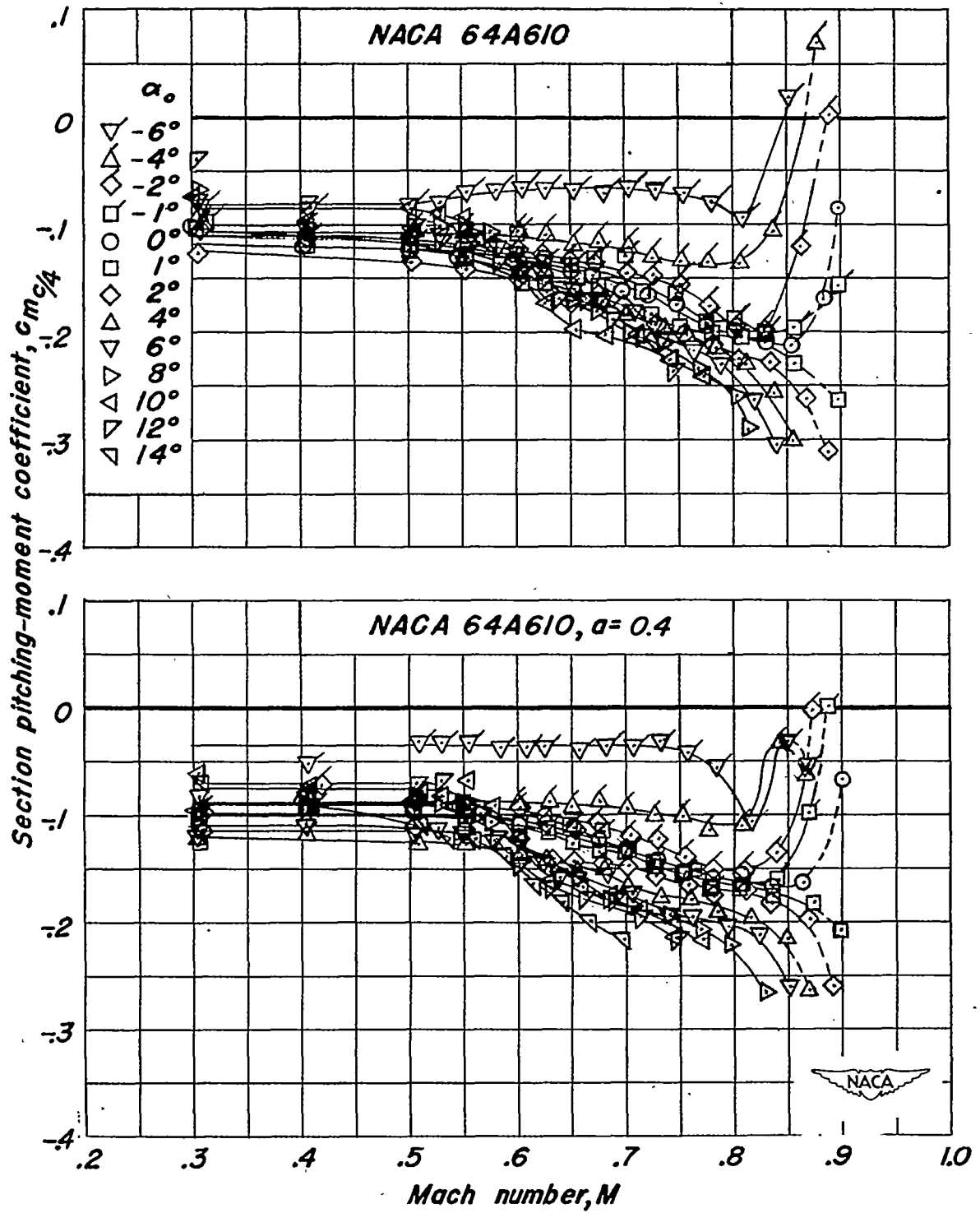
(a) $c_{l, Q}$

Figure 4.- Variation of section pitching-moment coefficient with Mach number at constant section angles of attack.



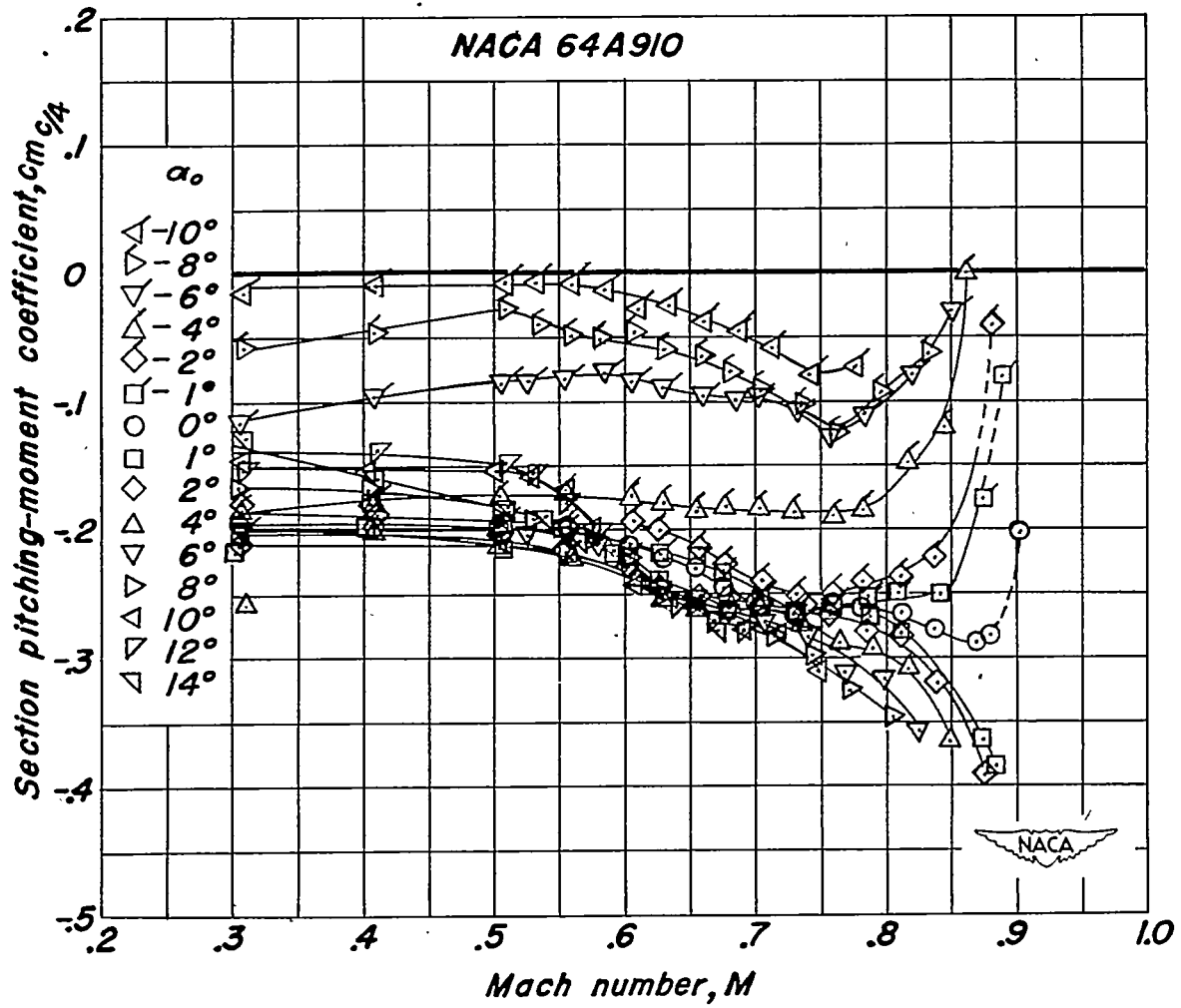
(b) $c_l, 0.3$.

Figure 4- Continued .



(c) $c_l, 0.6$.

Figure 4.- Continued.



(d) $c_{l_i}, 0.9$.

Figure 4- Concluded .

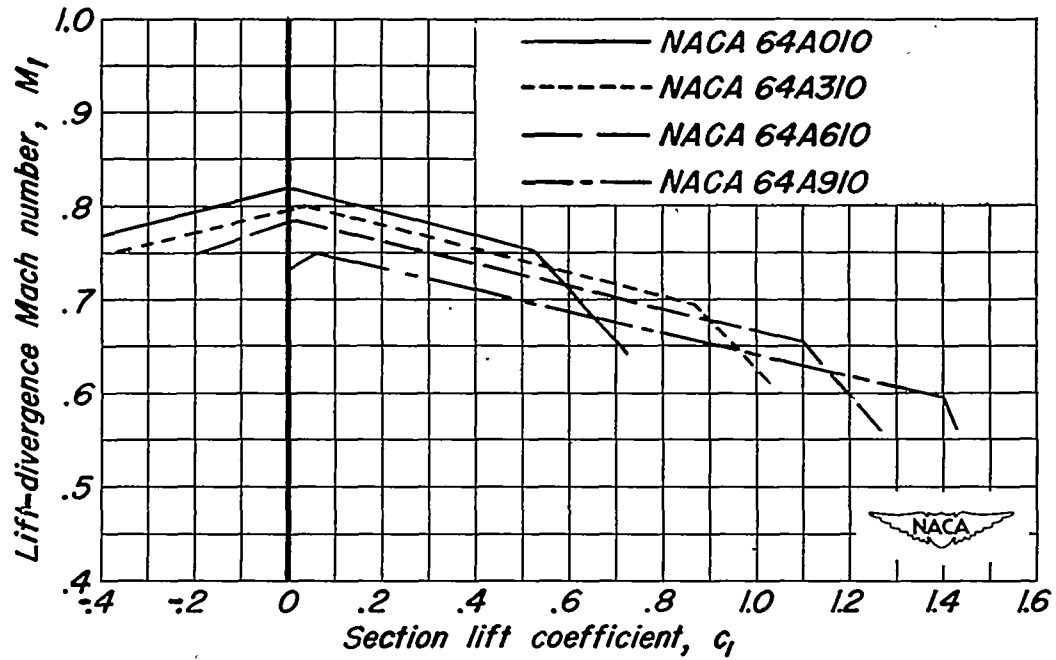


Figure 5.- The effect of the amount of camber on the variation of lift-divergence Mach number with section lift coefficient.

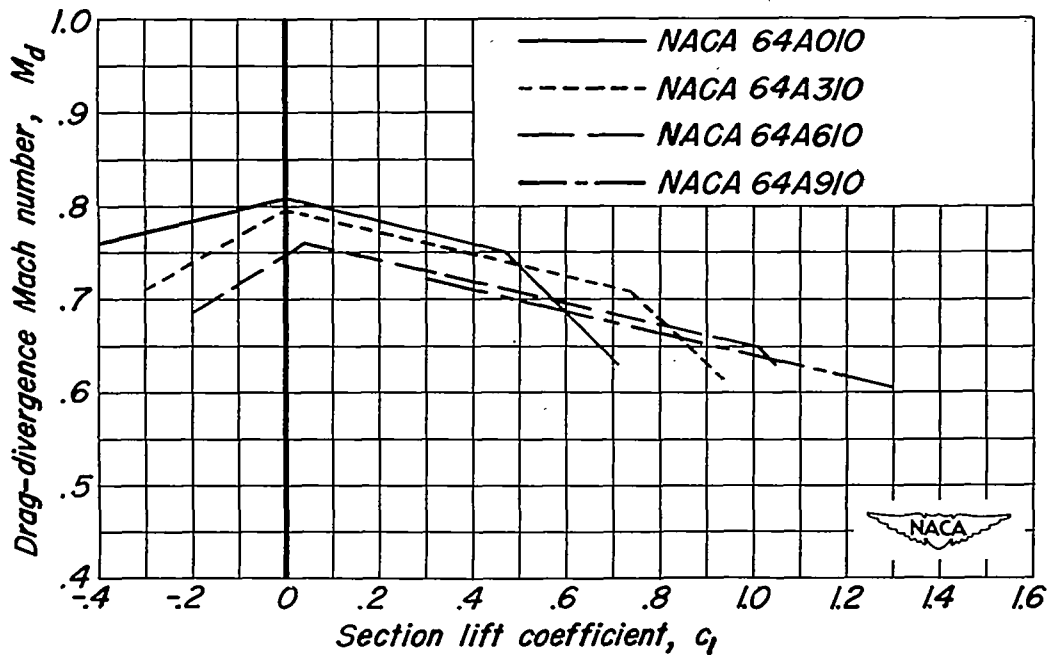


Figure 6.- The effect of the amount of camber on the variation of drag-divergence Mach number with section lift coefficient.

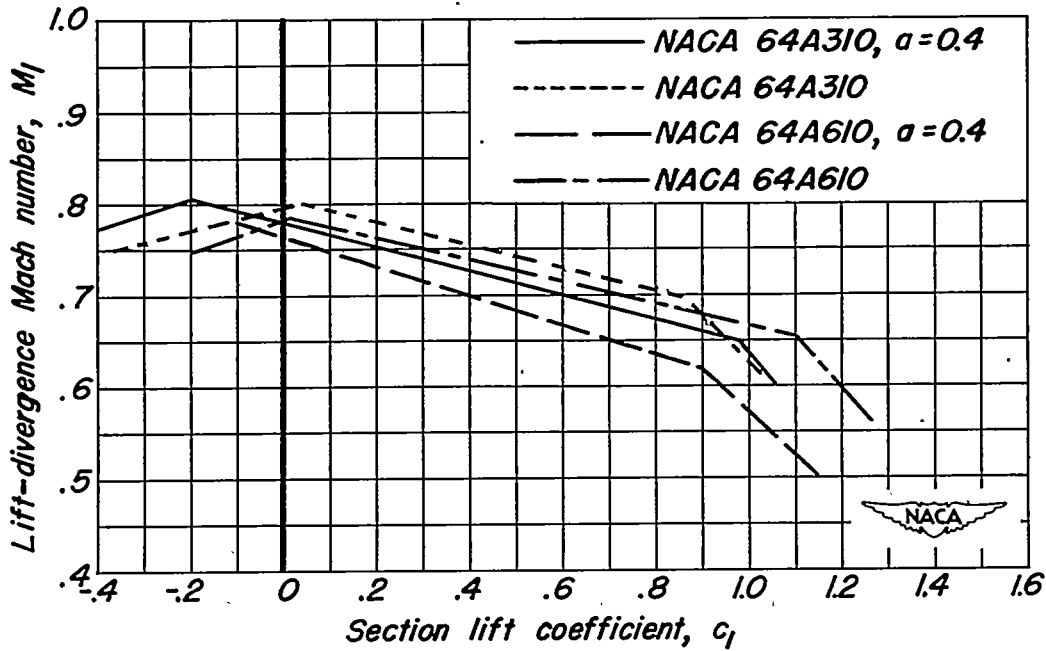


Figure 7.- The effect of the type of camber on the variation of lift-divergence Mach number with section lift coefficient .

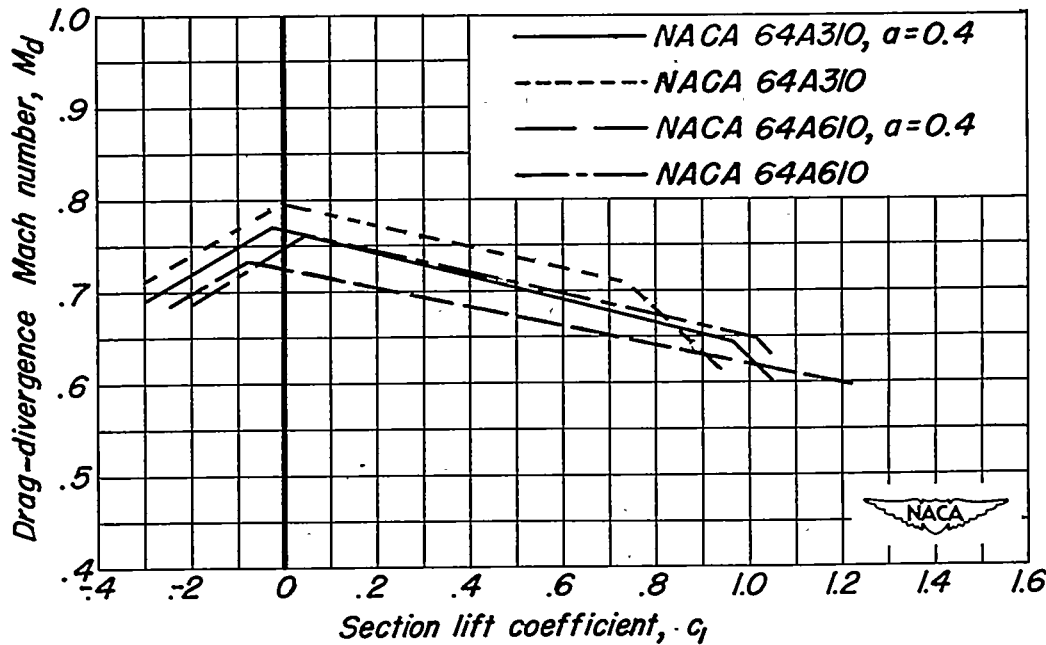
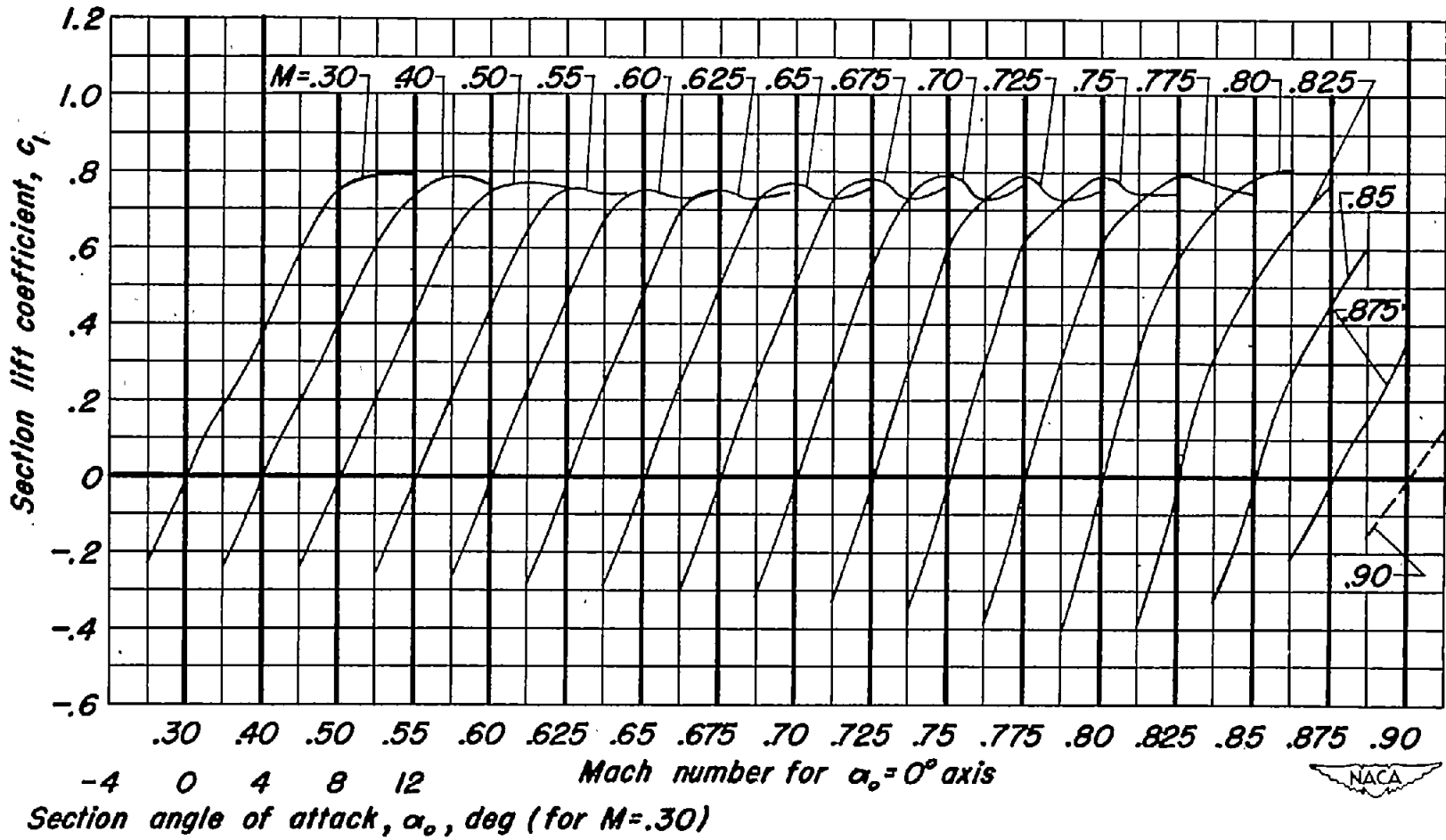
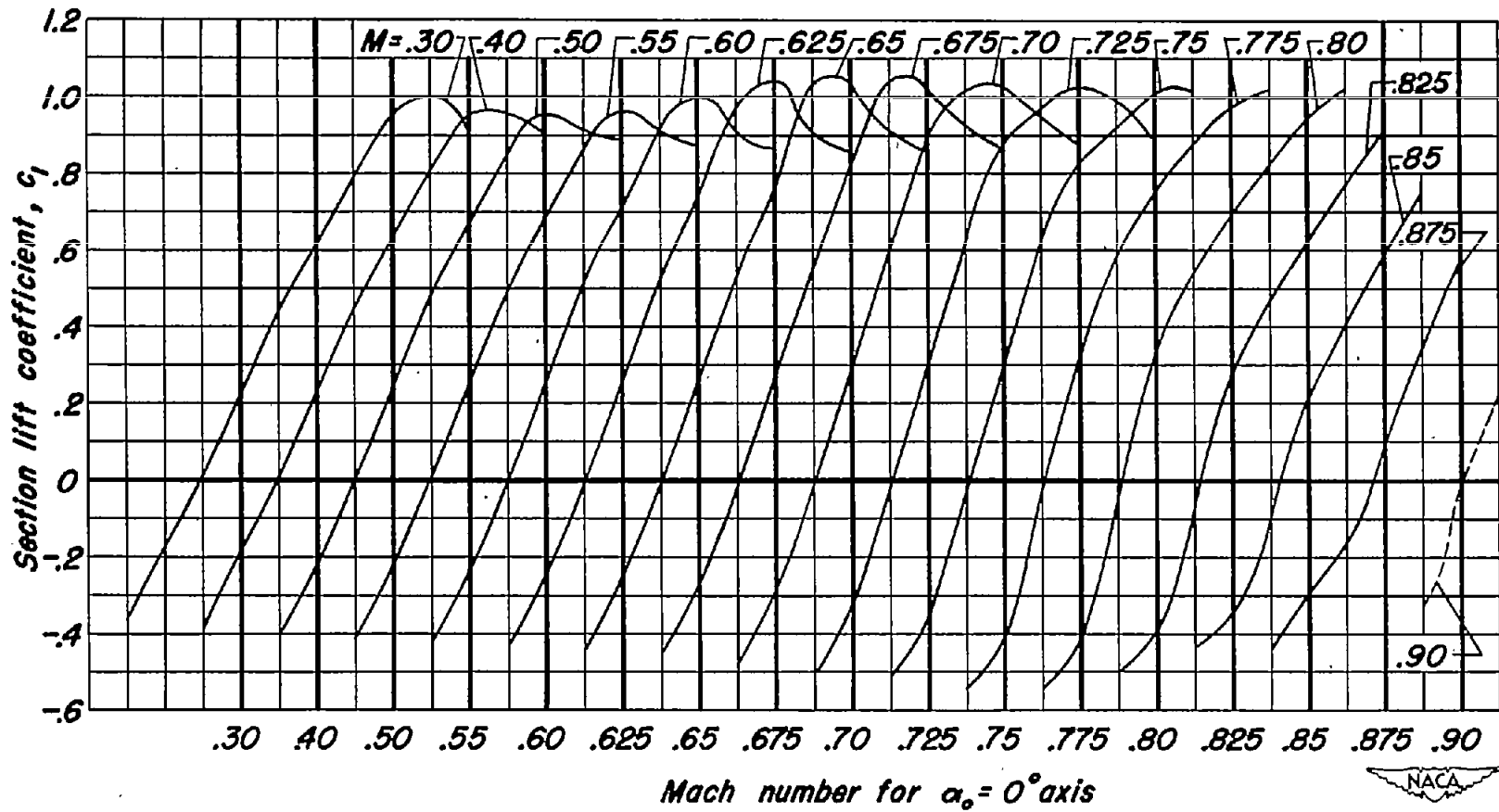


Figure 8.- The effect of the type of camber on the variation of drag-divergence Mach number with section lift coefficient.



(a) NACA 64A010 airfoil section .

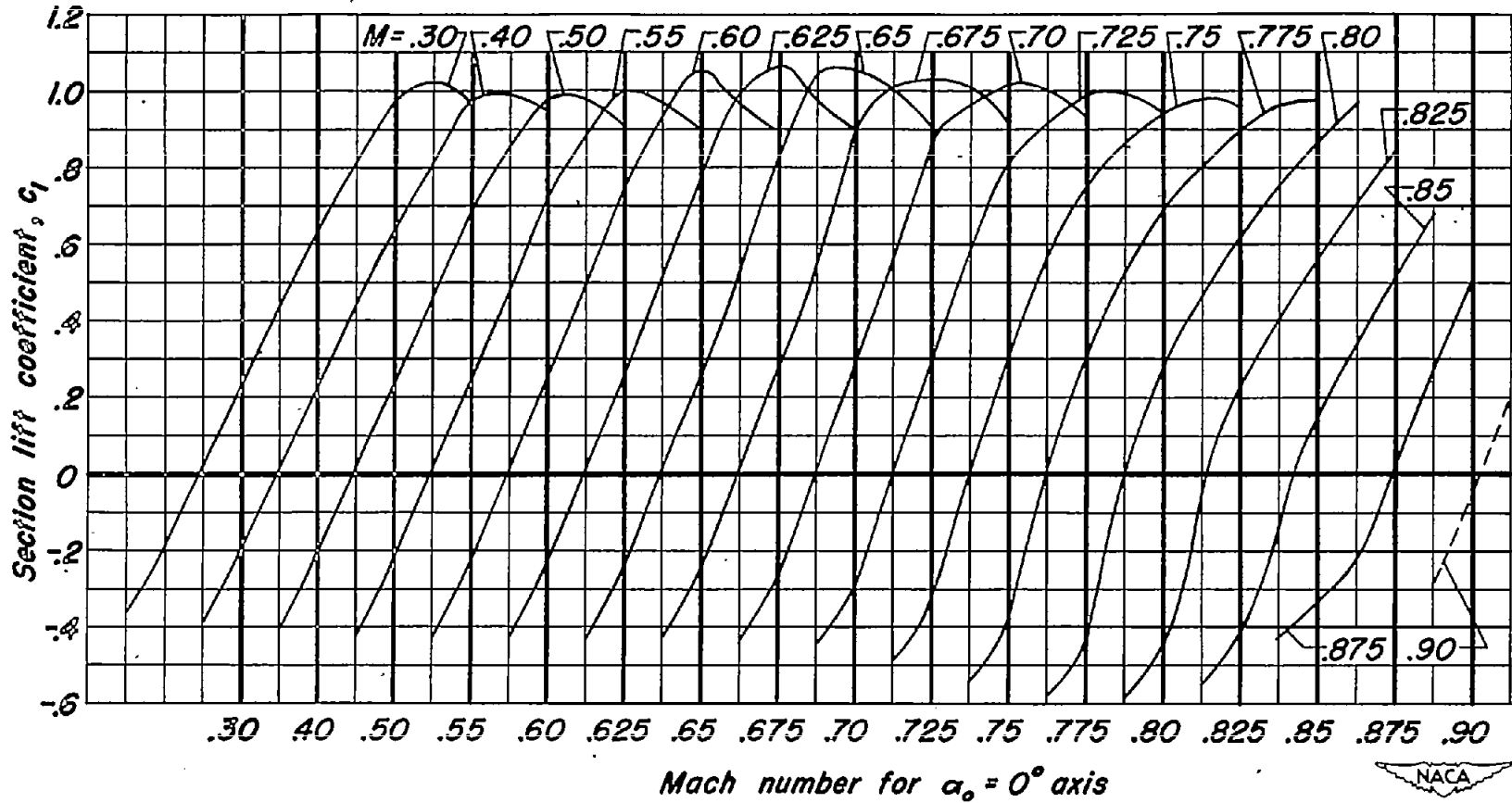
Figure 9 .- Variation of section lift coefficient with section angle of attack at various Mach numbers .



-8 -4 0 4 8 12
 Section angle of attack, α_o , deg (for $M=.30$)

(b) NACA 64A310 airfoil section.

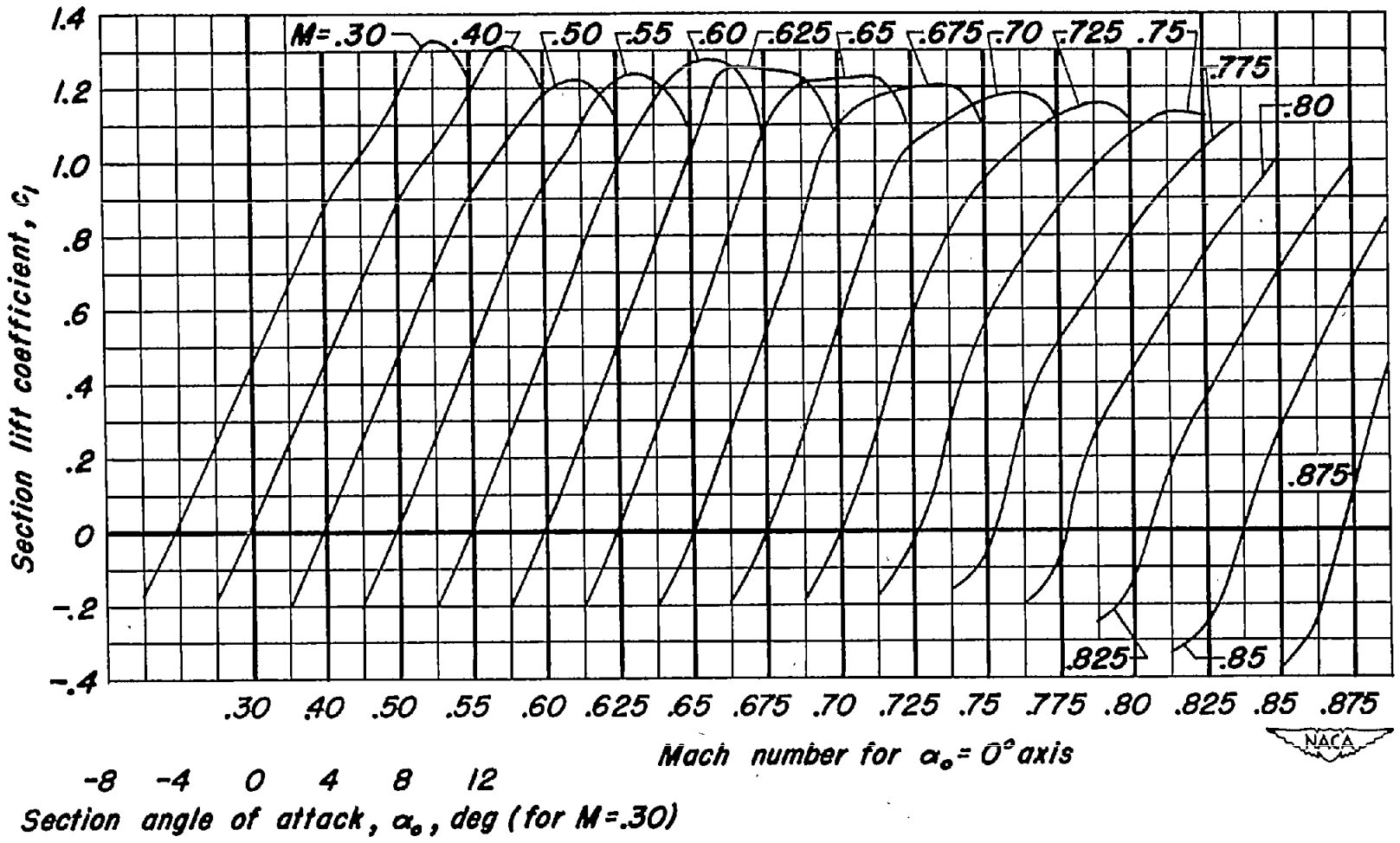
Figure 9 - Continued.



-8 -4 0 4 8 12
 Section angle of attack, α_0 , deg (for $M=.30$)

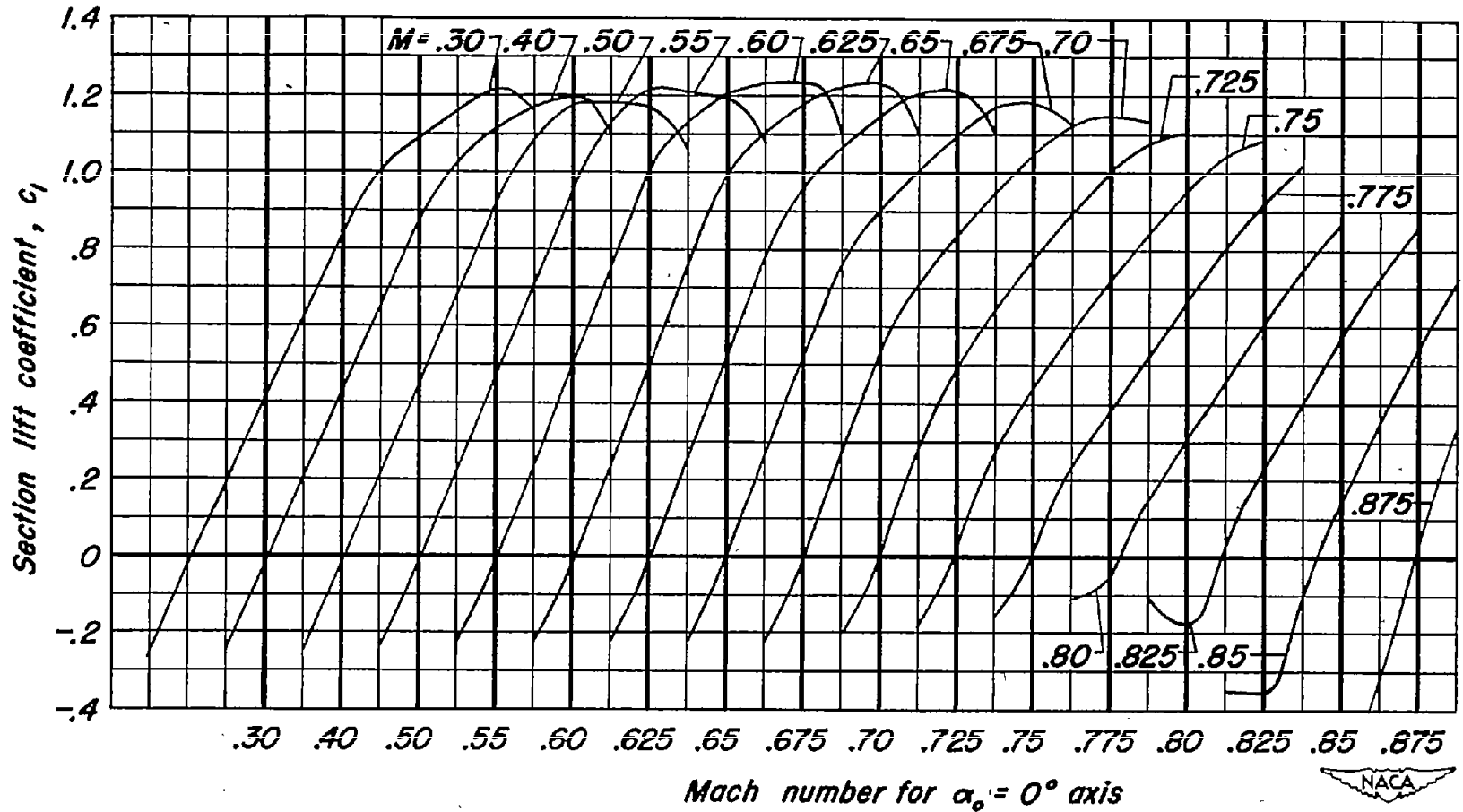
(c) NACA 64A310, $a=0.4$ airfoil section.

Figure 9.- Continued .



(d) NACA 64A610 airfoil section.

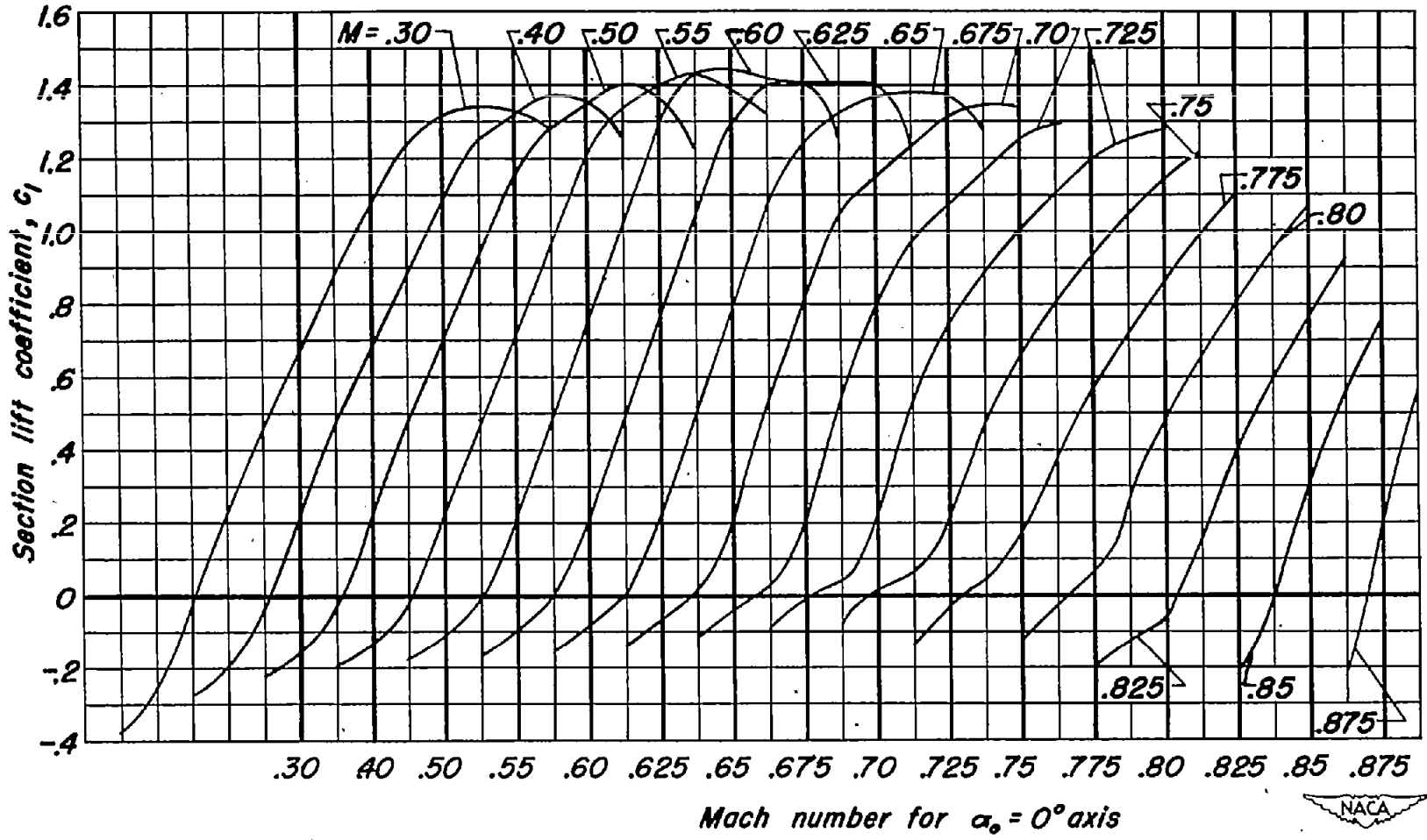
Figure 9.- Continued.



-8 -4 0 4 8 12
 Section angle of attack, α_0 , deg (for $M=.30$)

(e) NACA 64A610 $a=0.4$ airfoil section.

Figure 9.- Continued.



-12 -8 -4 0 4 8 12
 Section angle of attack, α_0 , deg (for $M=0.30$)

(f) NACA 64A910 airfoil section .

Figure 9.- Concluded.

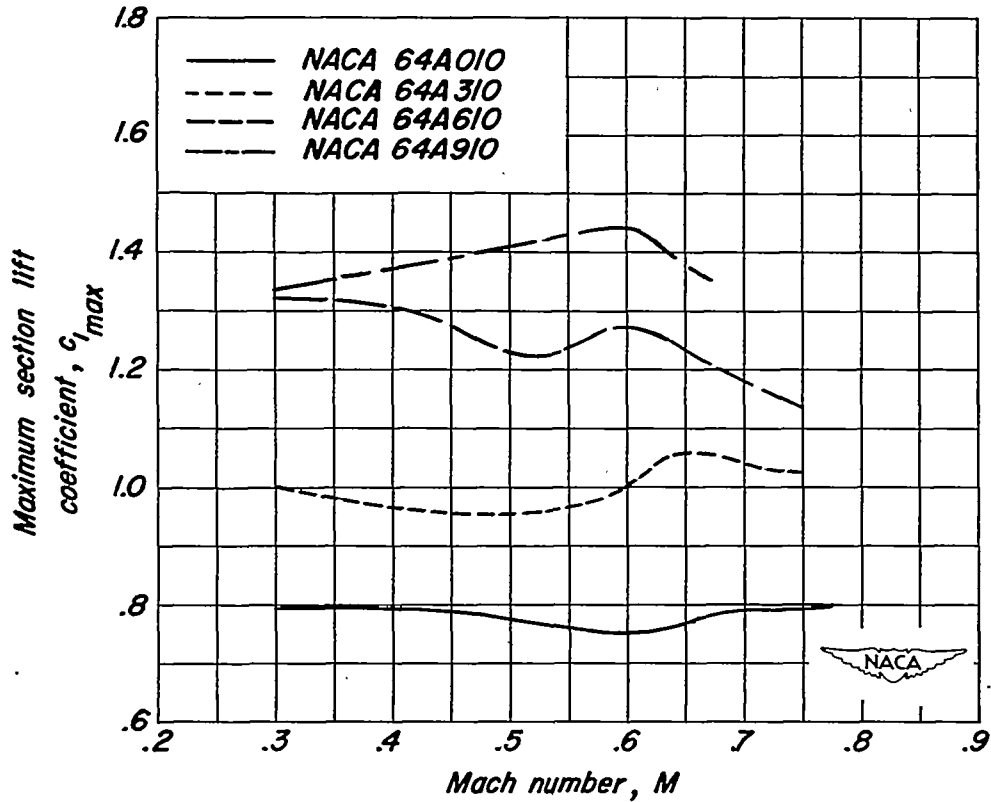


Figure 10.- The effect of the amount of camber on the variation of maximum section lift coefficient with Mach number.

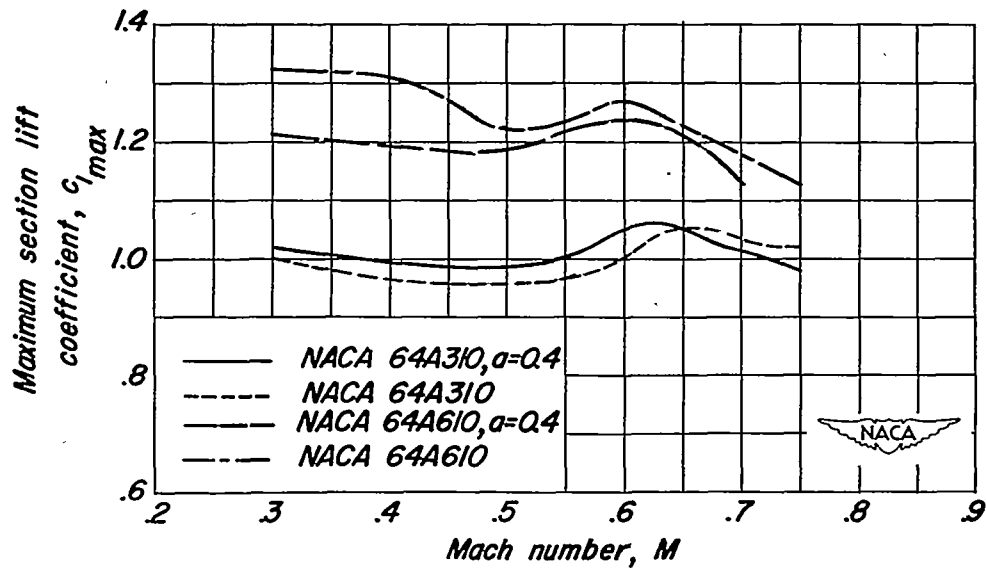


Figure 11.- The effect of the type of camber on the variation of maximum section lift coefficient with Mach number.

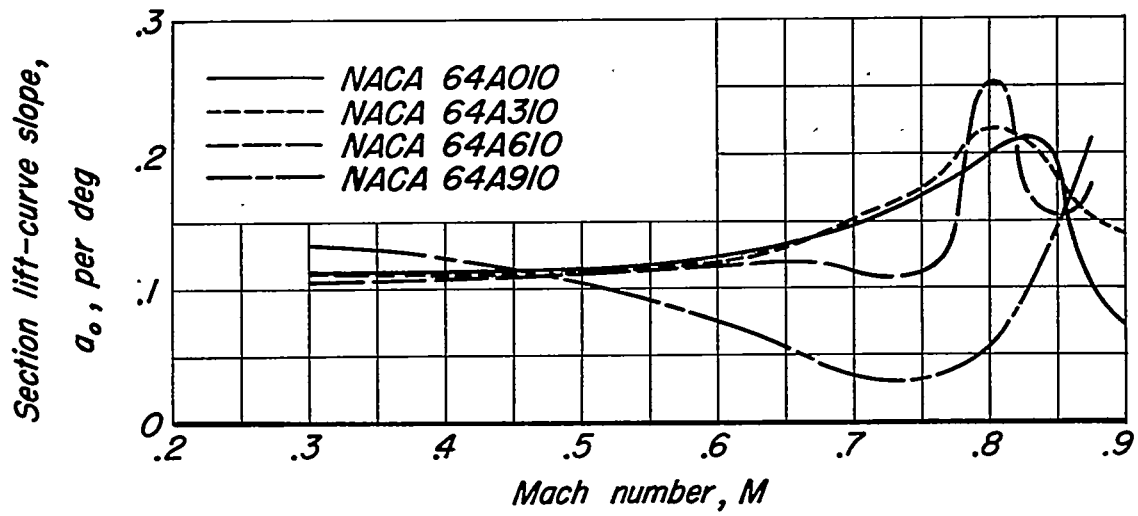
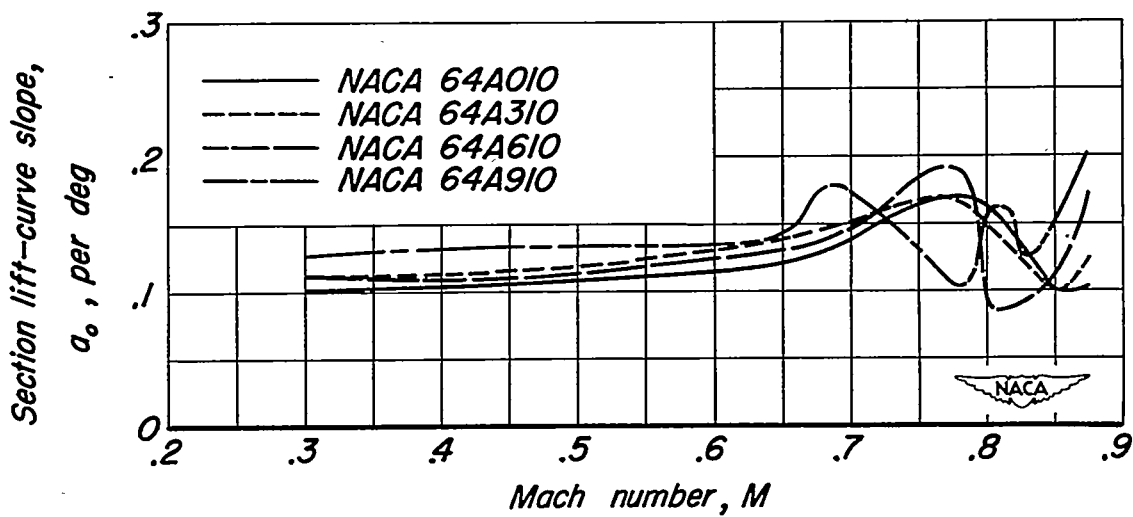
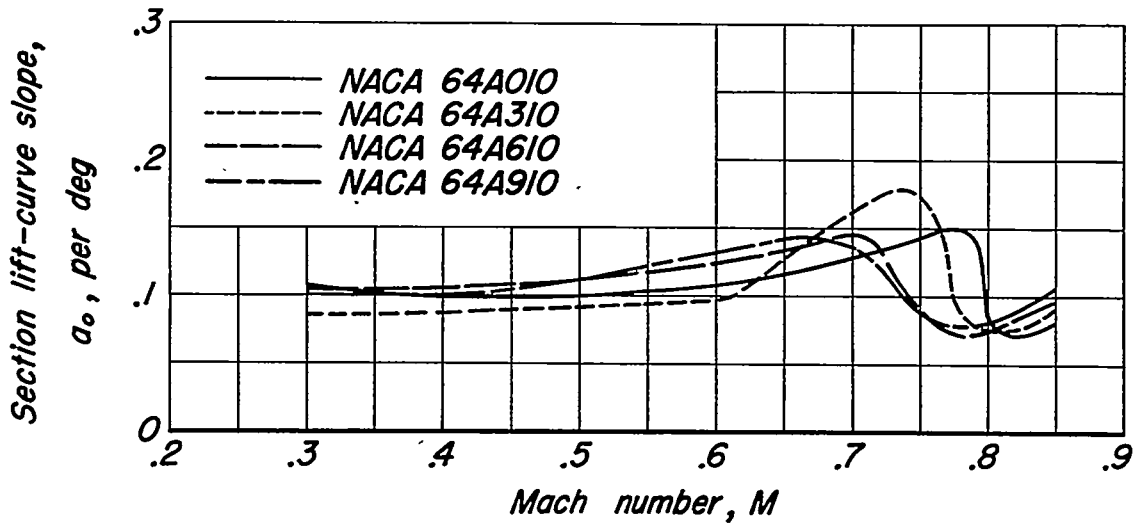
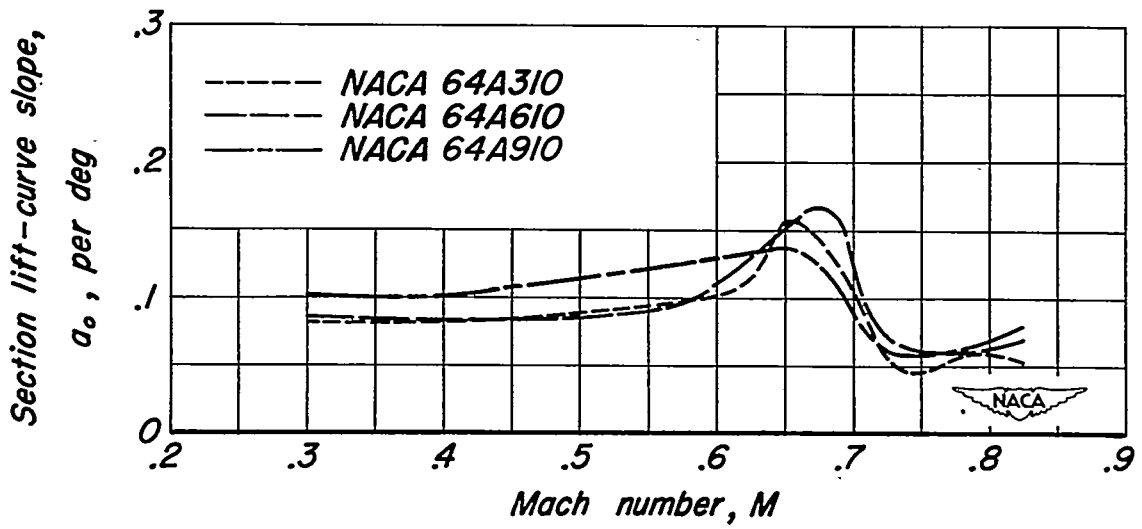
(a) $c_l, 0.$ (b) $c_l, 0.3.$

Figure 12.- The effect of the amount of camber on the variation of section lift-curve slope with Mach number.

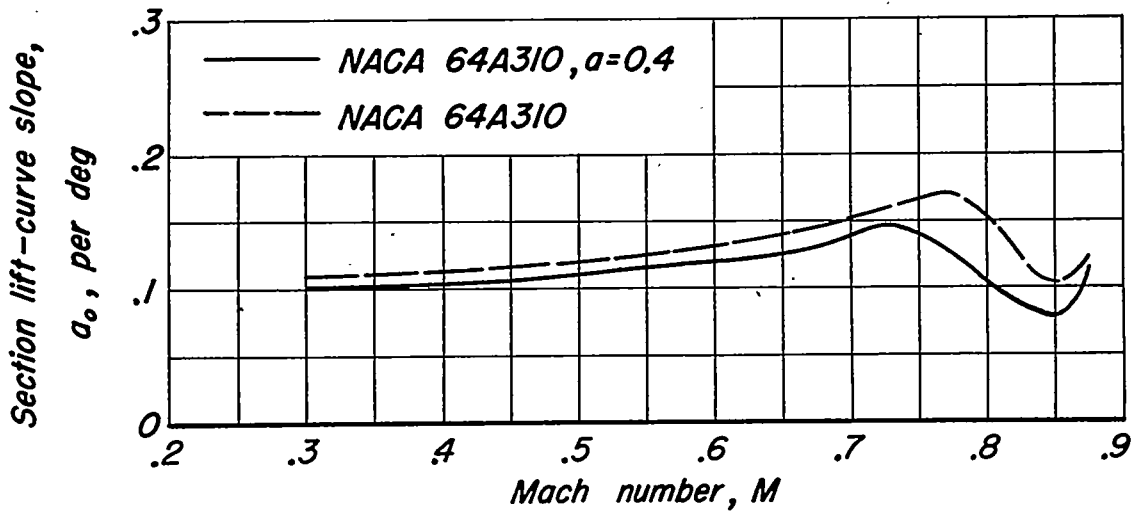


(c) $c_l, 0.6$.

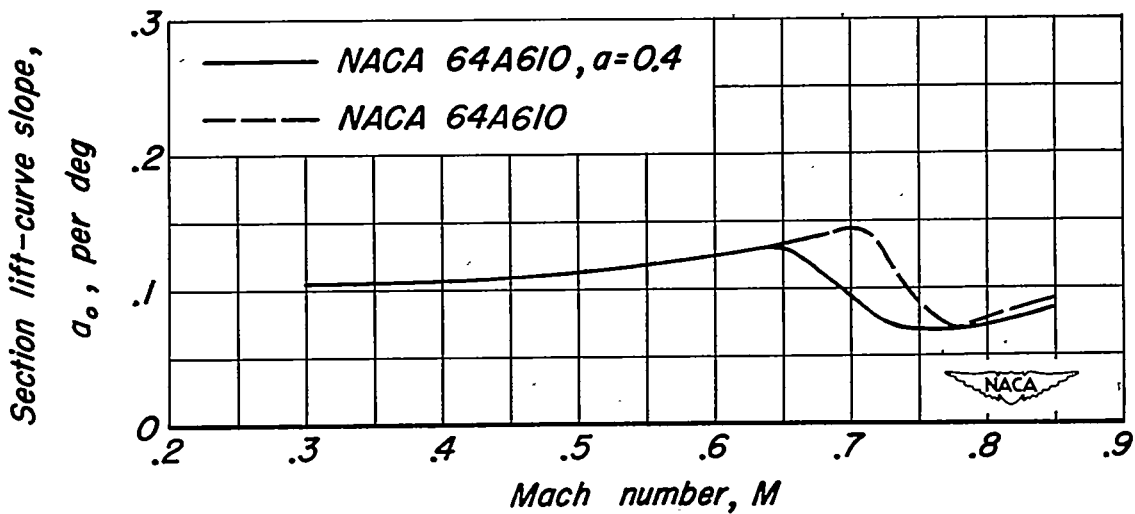


(d) $c_l, 0.9$.

Figure 12.- Concluded .

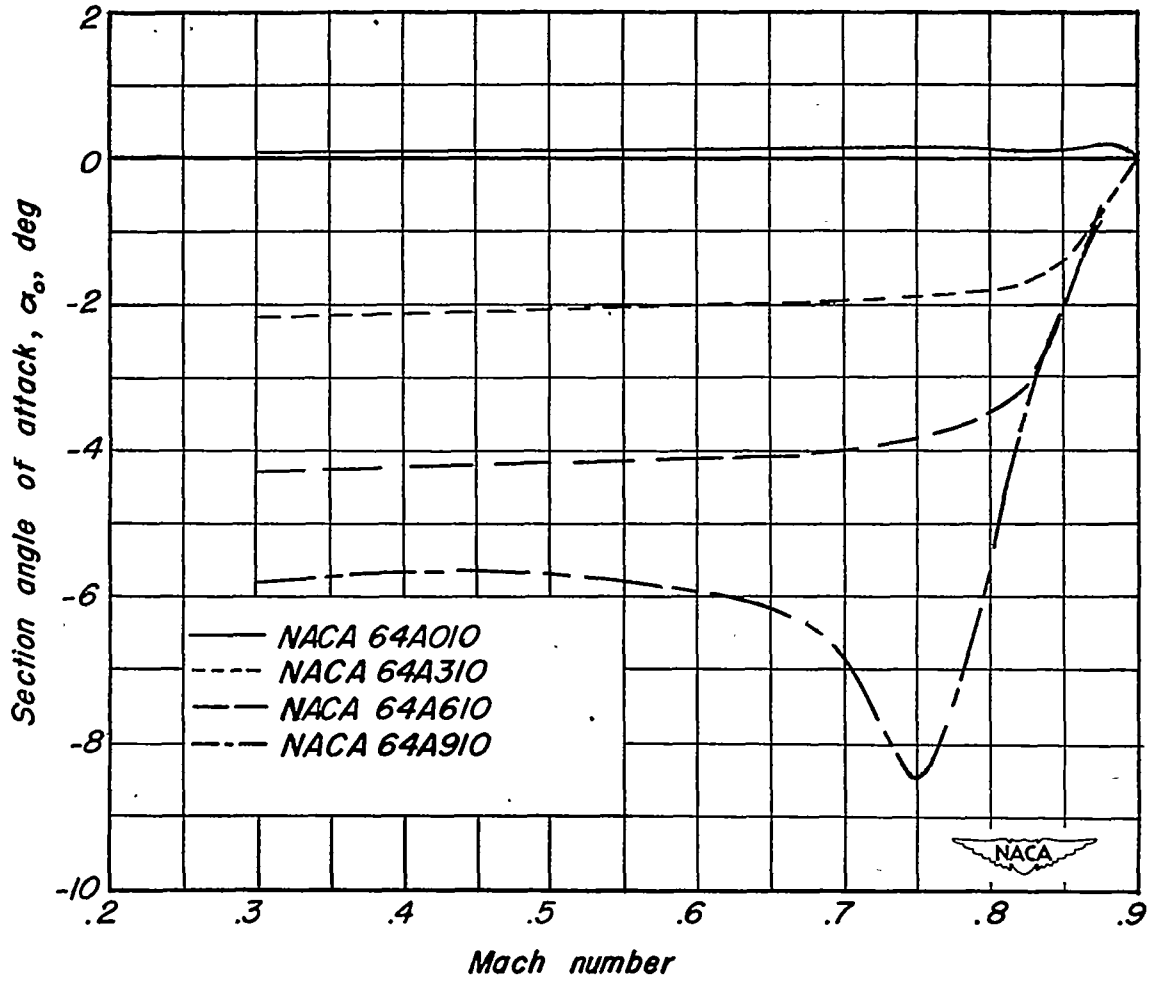


(a) $c_l, 0.3.$



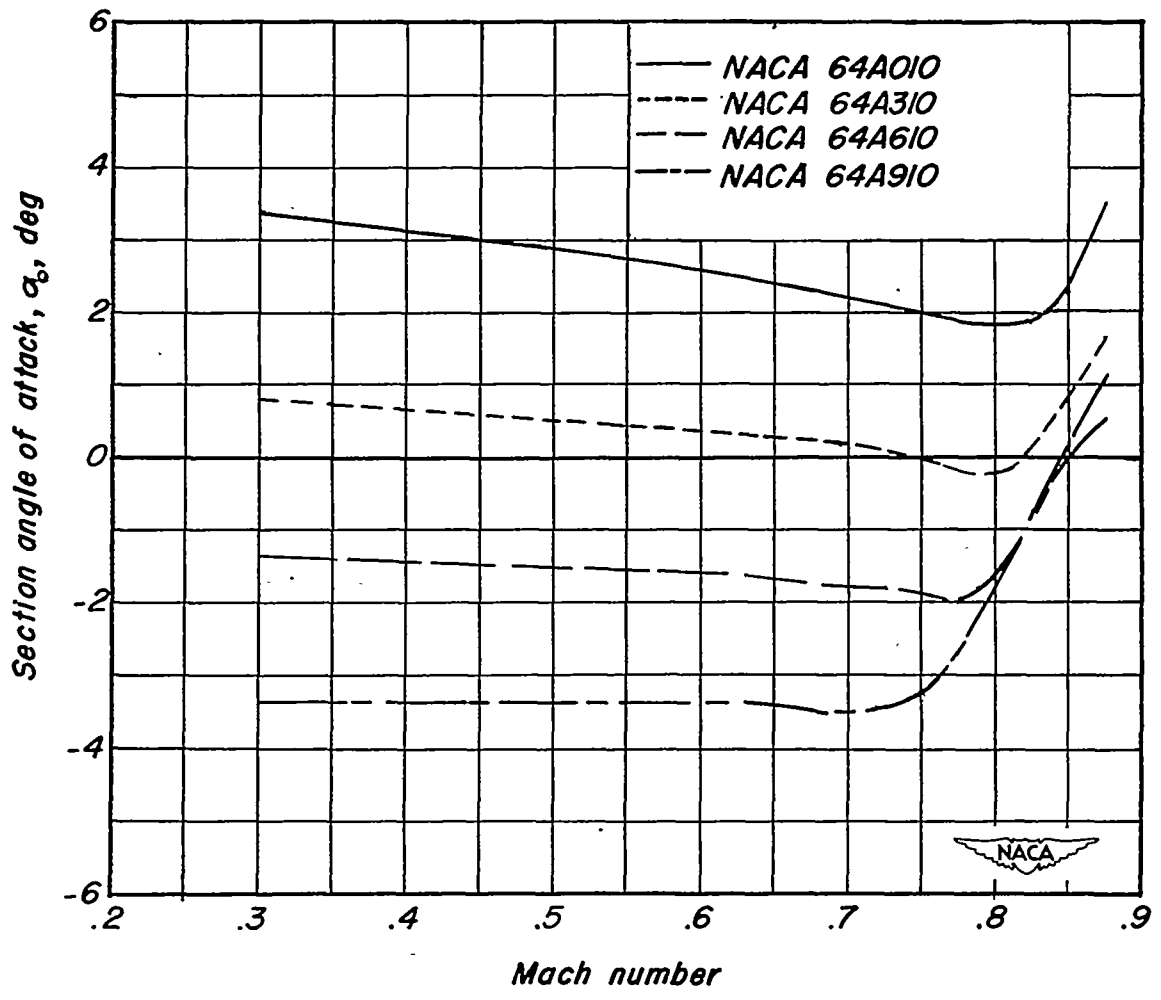
(b) $c_l, 0.6.$

Figure 13.- The effect of the type of camber on the variation of section lift-curve slope with Mach number.



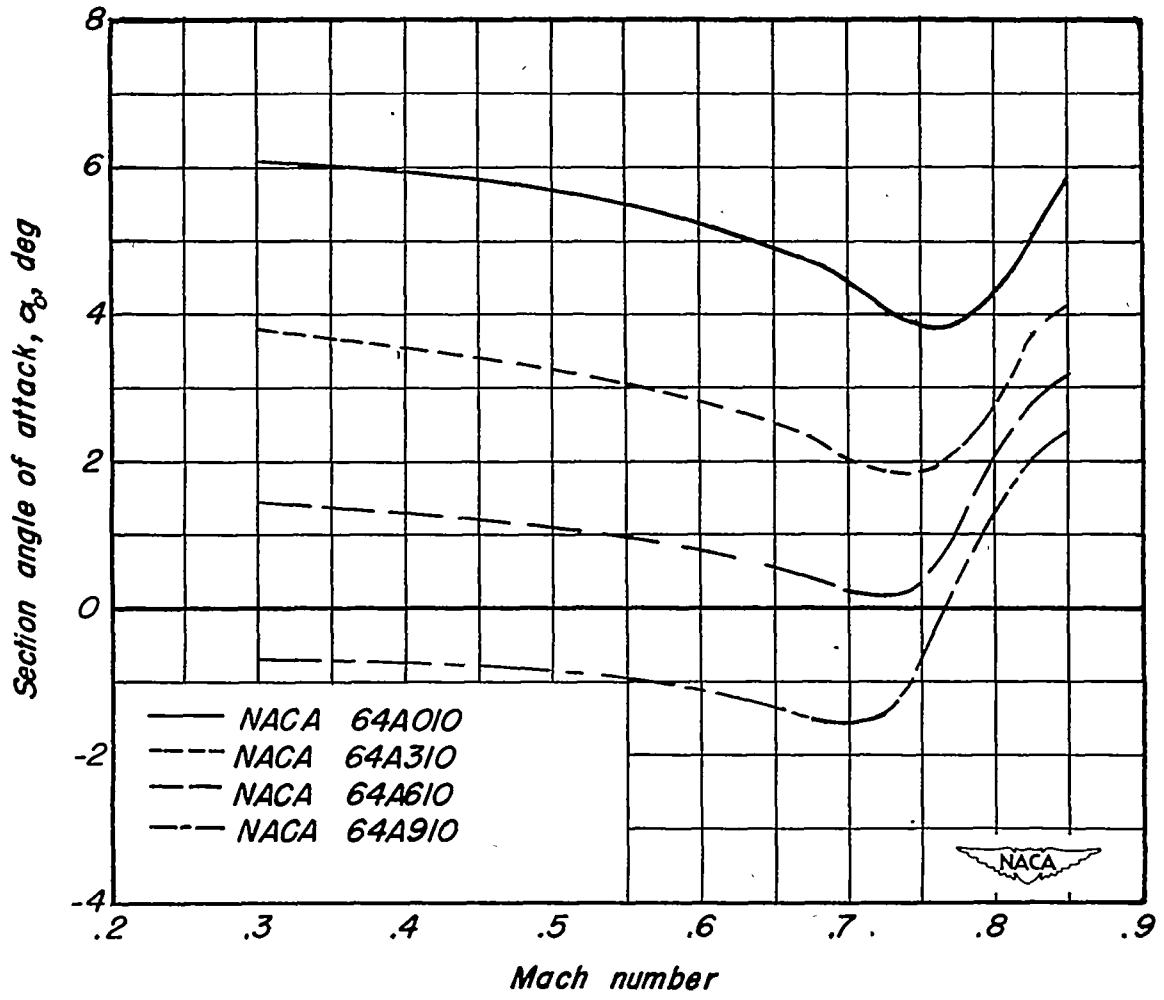
(a) $c_l, 0$.

Figure 14.- The effect of the amount of camber on the variation with Mach number of section angle of attack required at several values of section lift coefficient.



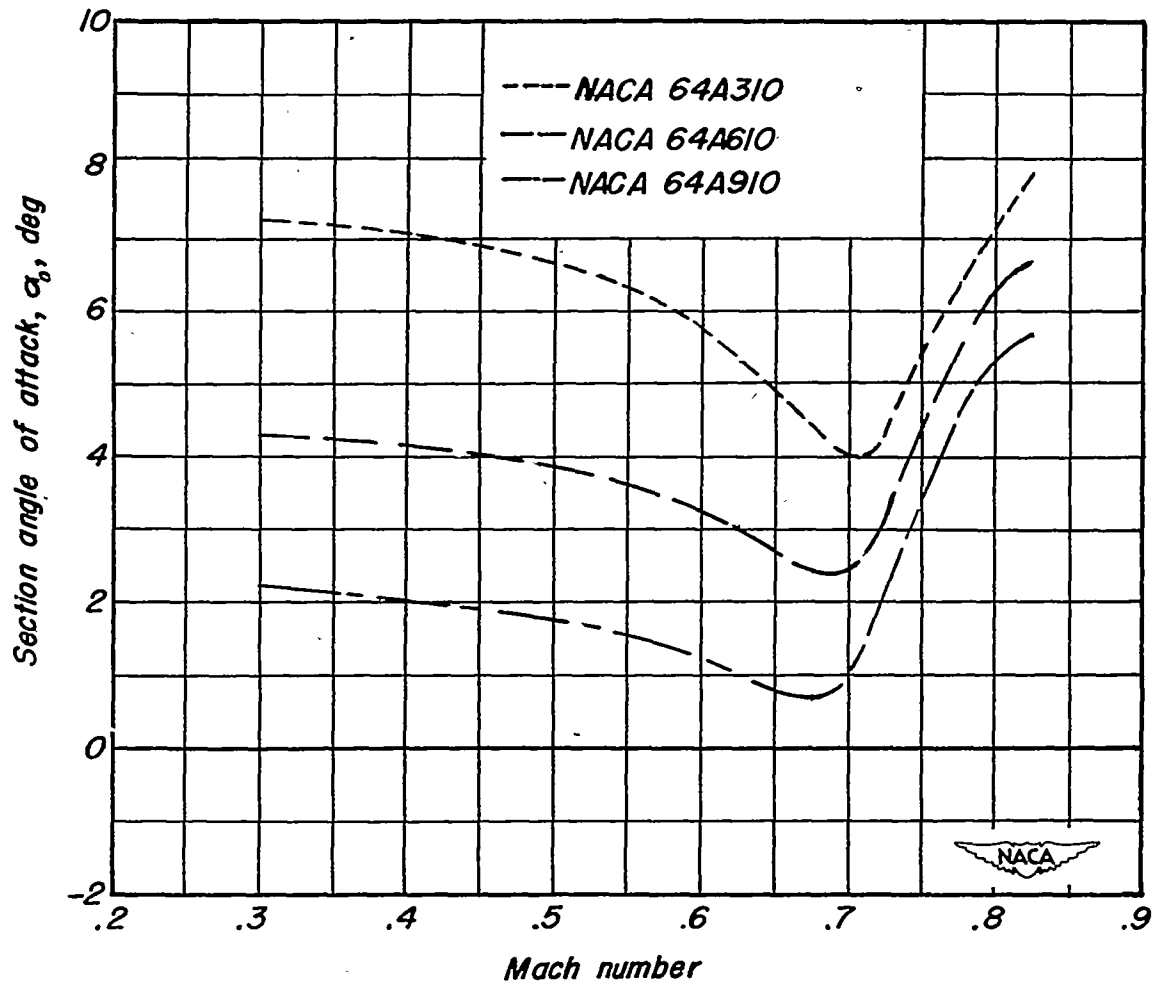
(b) c_l , 0.3 .

Figure 14.- Continued .



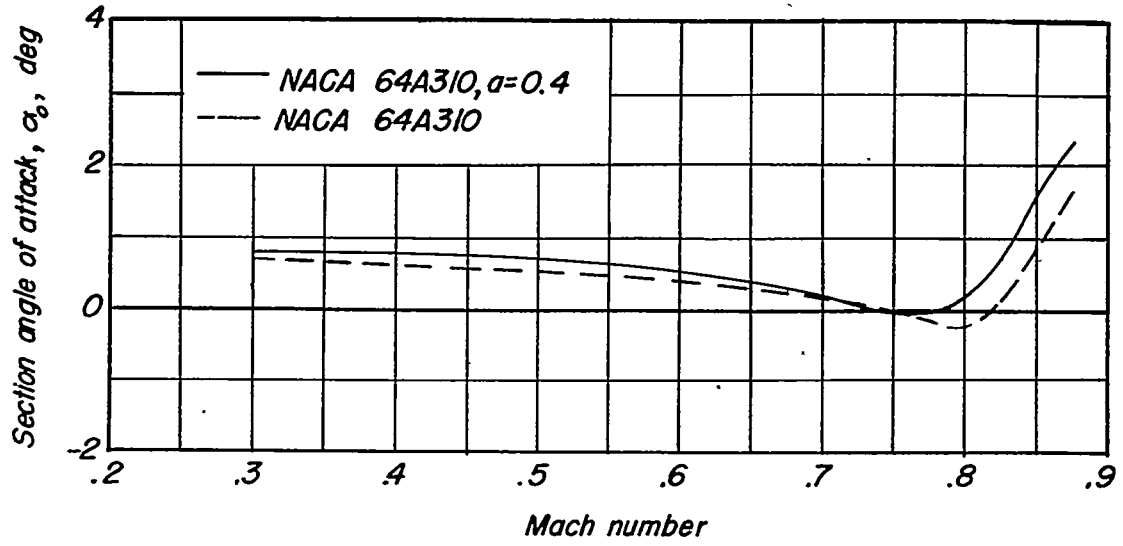
(c) c_l , 0.6.

Figure 14.- Continued.

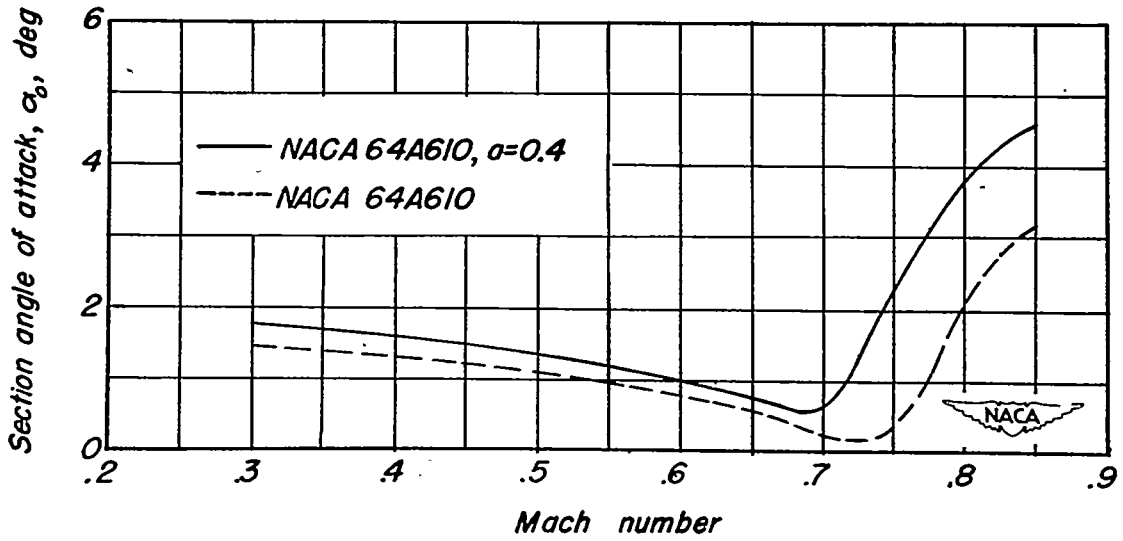


(d) c_l , 0.9.

Figure 14.- Concluded .

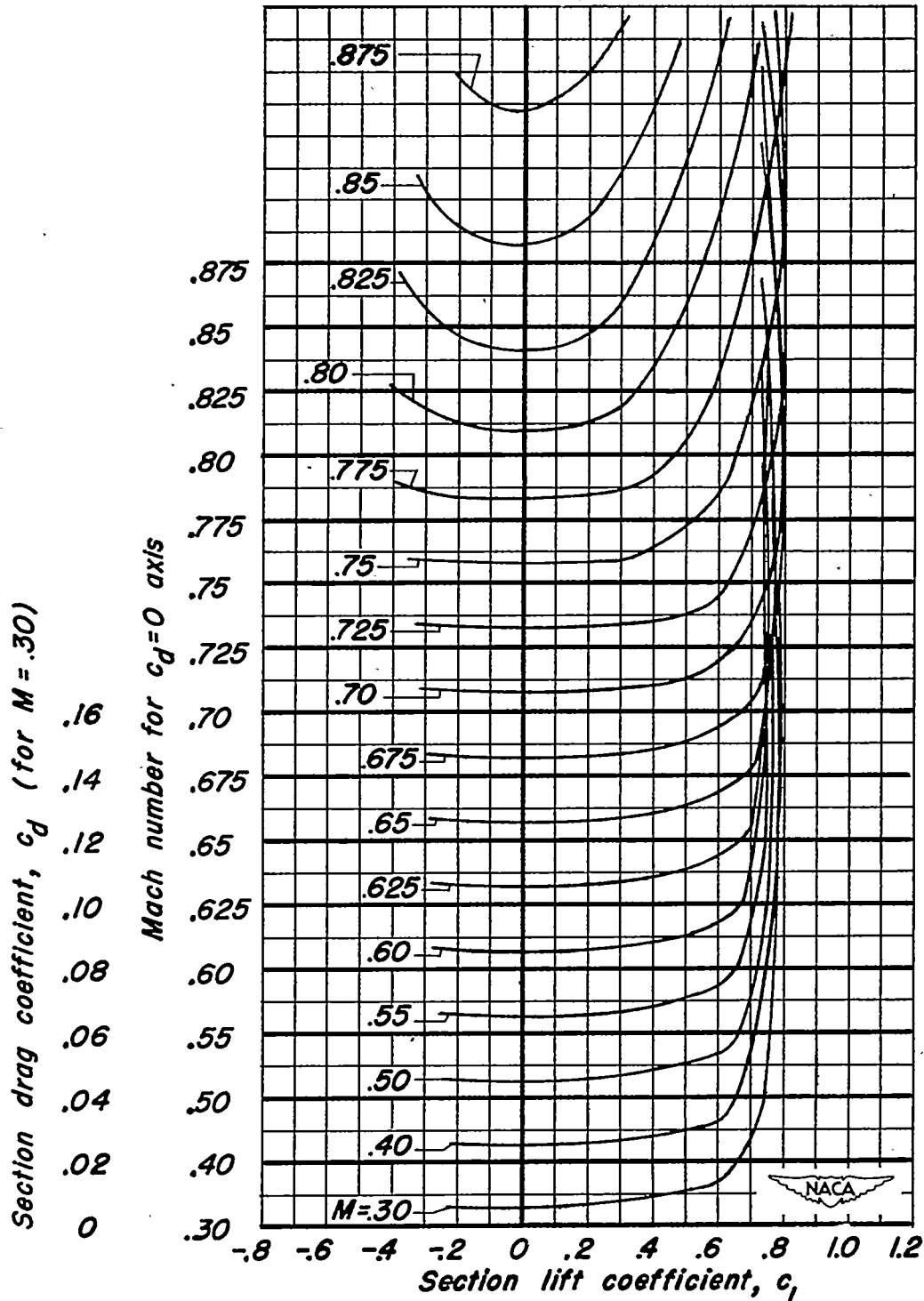


(a) $c_l, 0.3$.



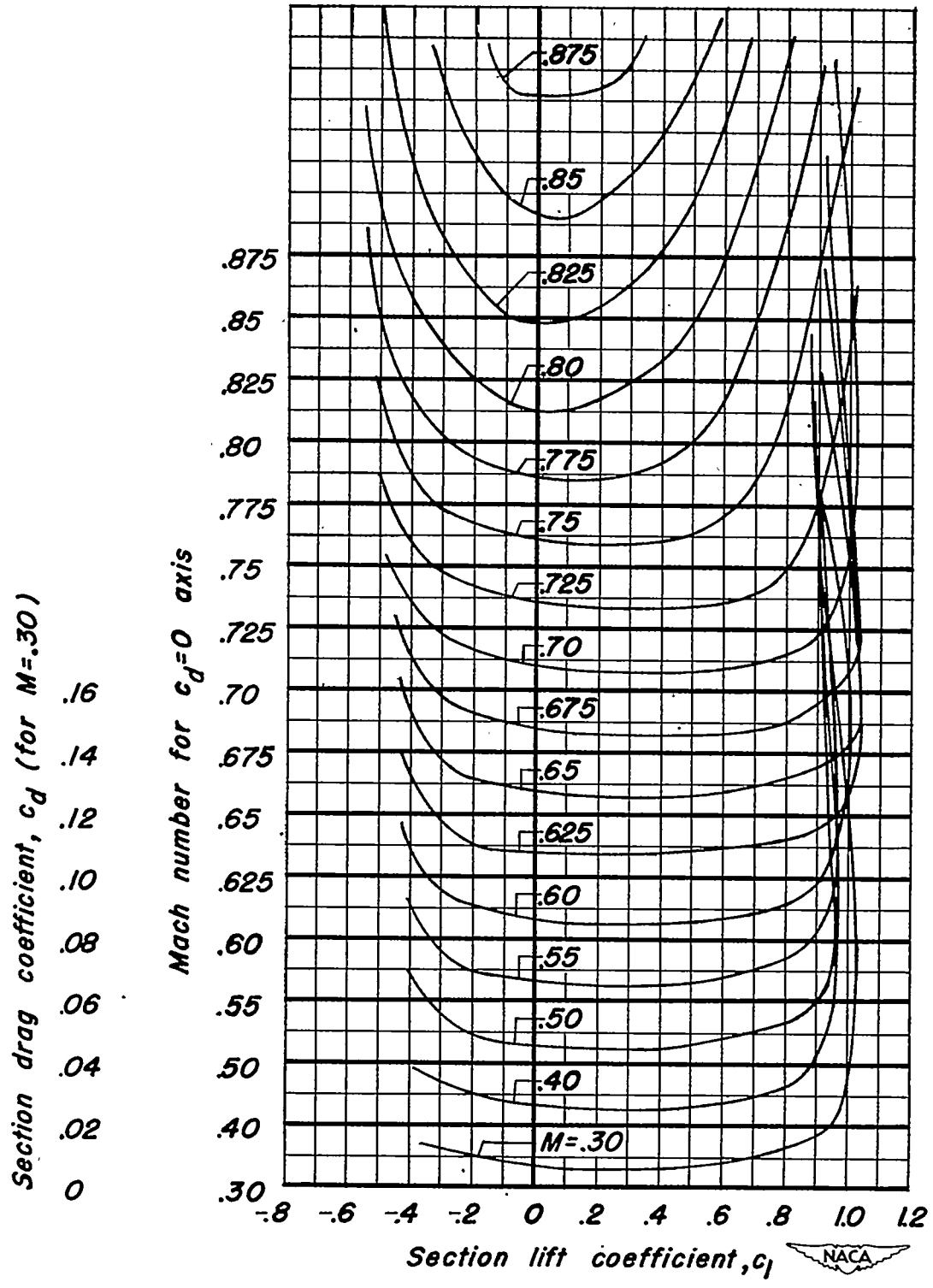
(b) $c_l, 0.6$.

Figure 15.- The effect of the type of camber on the variation with Mach number of the required section angle of attack at two values of section lift coefficient.



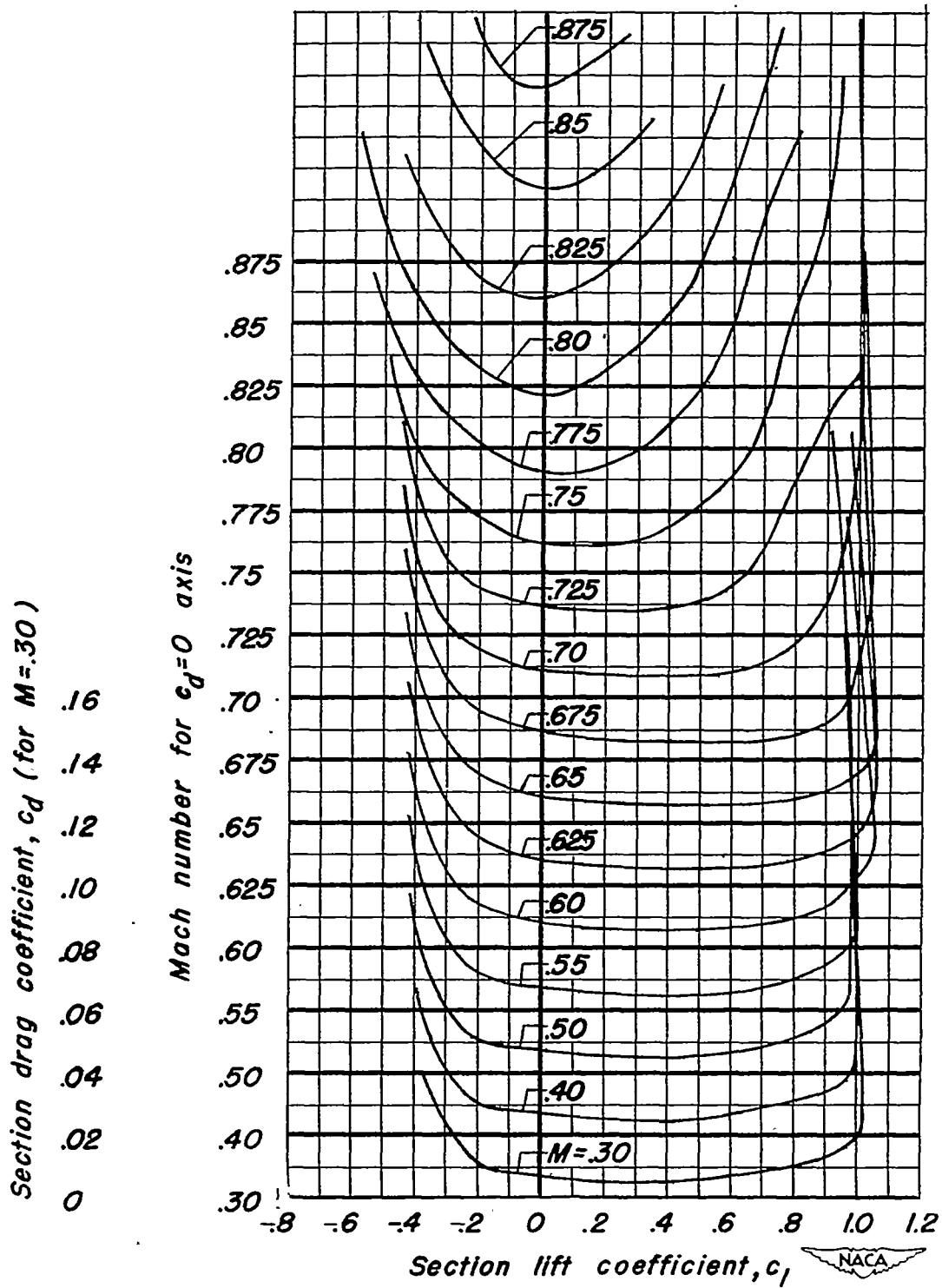
(a) NACA 64A010 airfoil section .

Figure 16.- Variation of section drag coefficient with section lift coefficient at various Mach numbers .



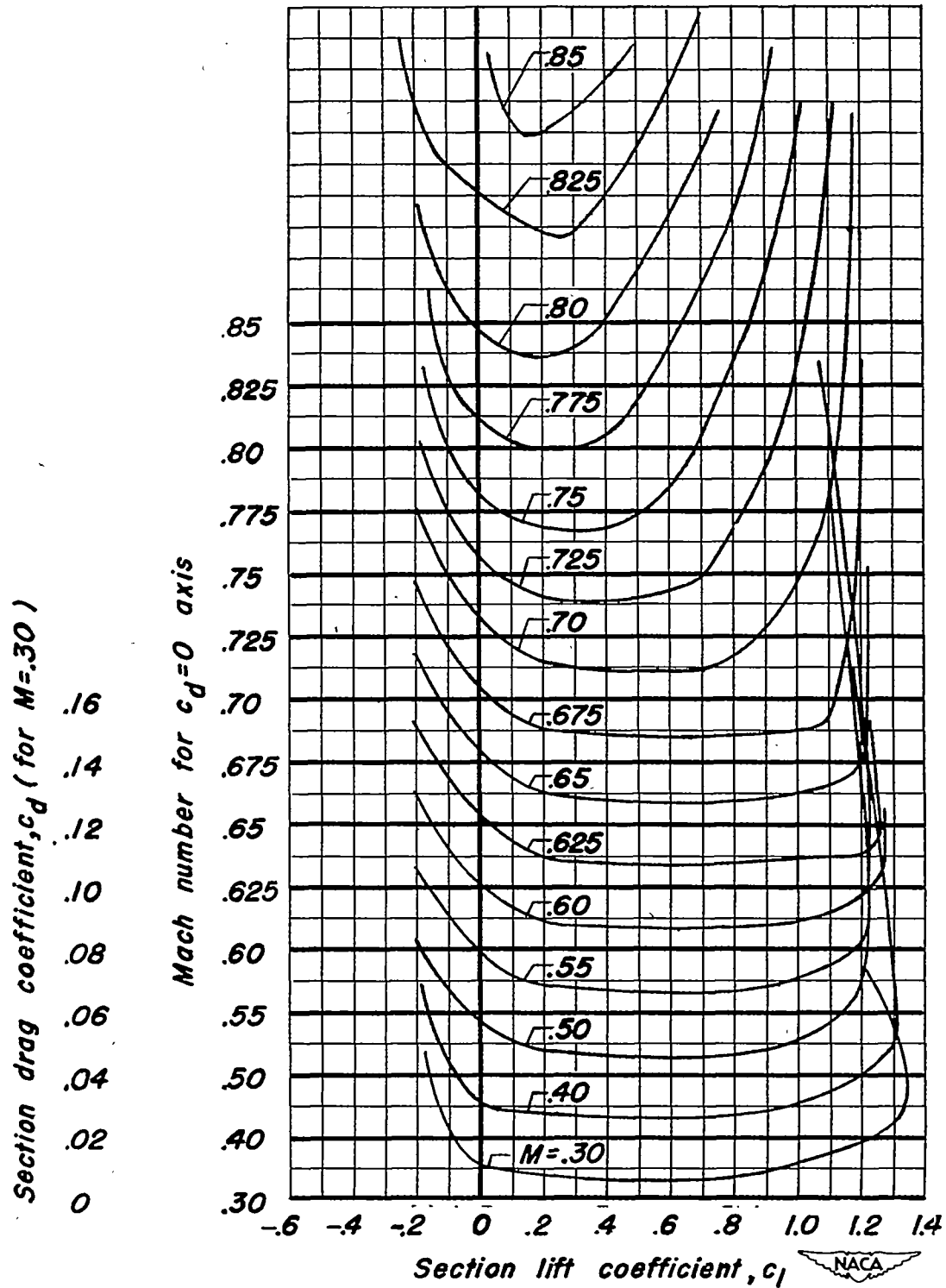
(b) NACA 64A310 airfoil section .

Figure 16.- Continued .



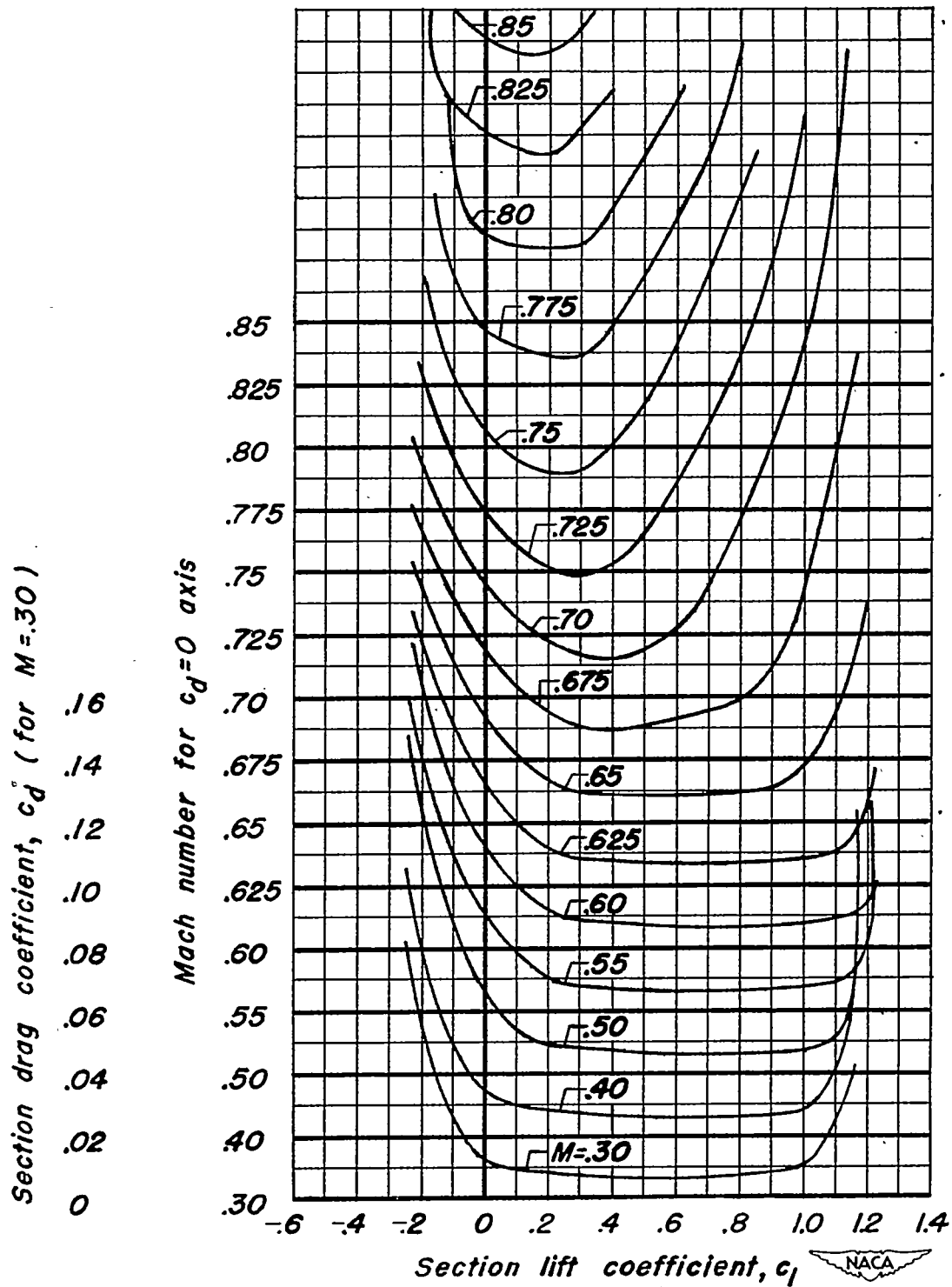
(c) NACA 64A310, $\alpha = 0.4$ airfoil section.

Figure 16.- Continued



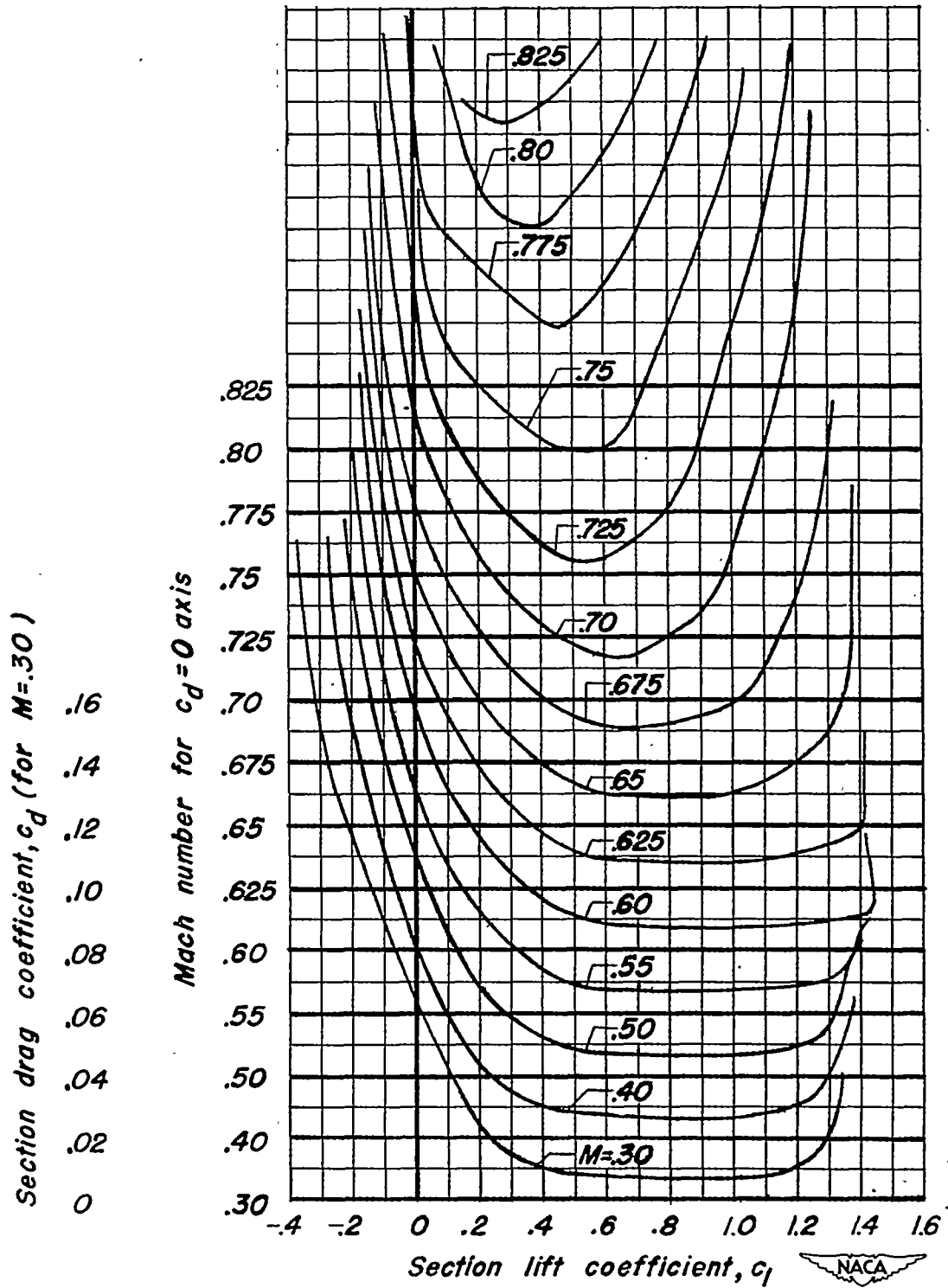
(d) NACA 64A610 airfoil section .

Figure 16.- Continued .



(e) NACA 64A610, $a=0.4$ airfoil section .

Figure 16.- Continued .



(f) NACA 64A910 airfoil section .

Figure 16.- Concluded .

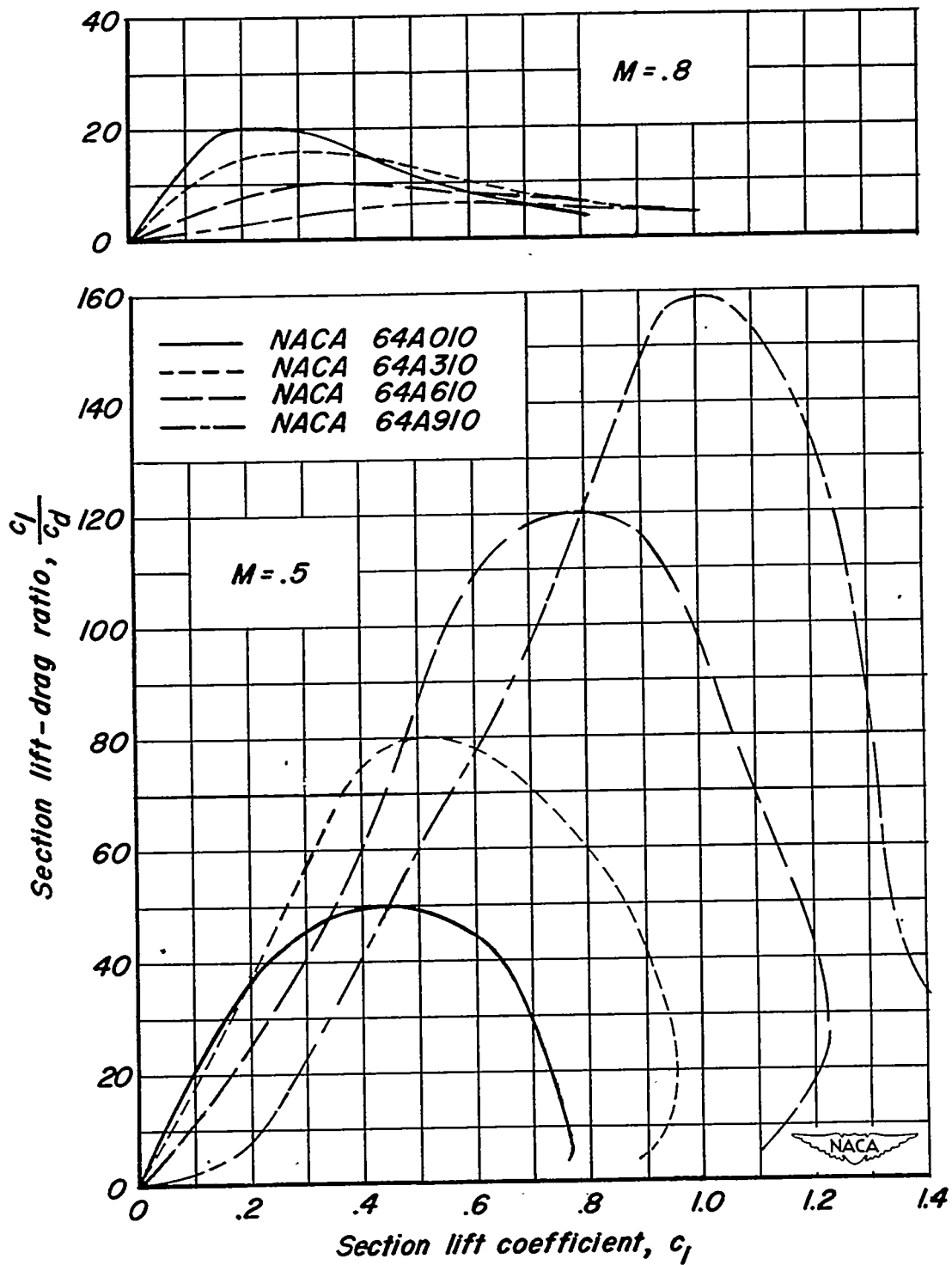
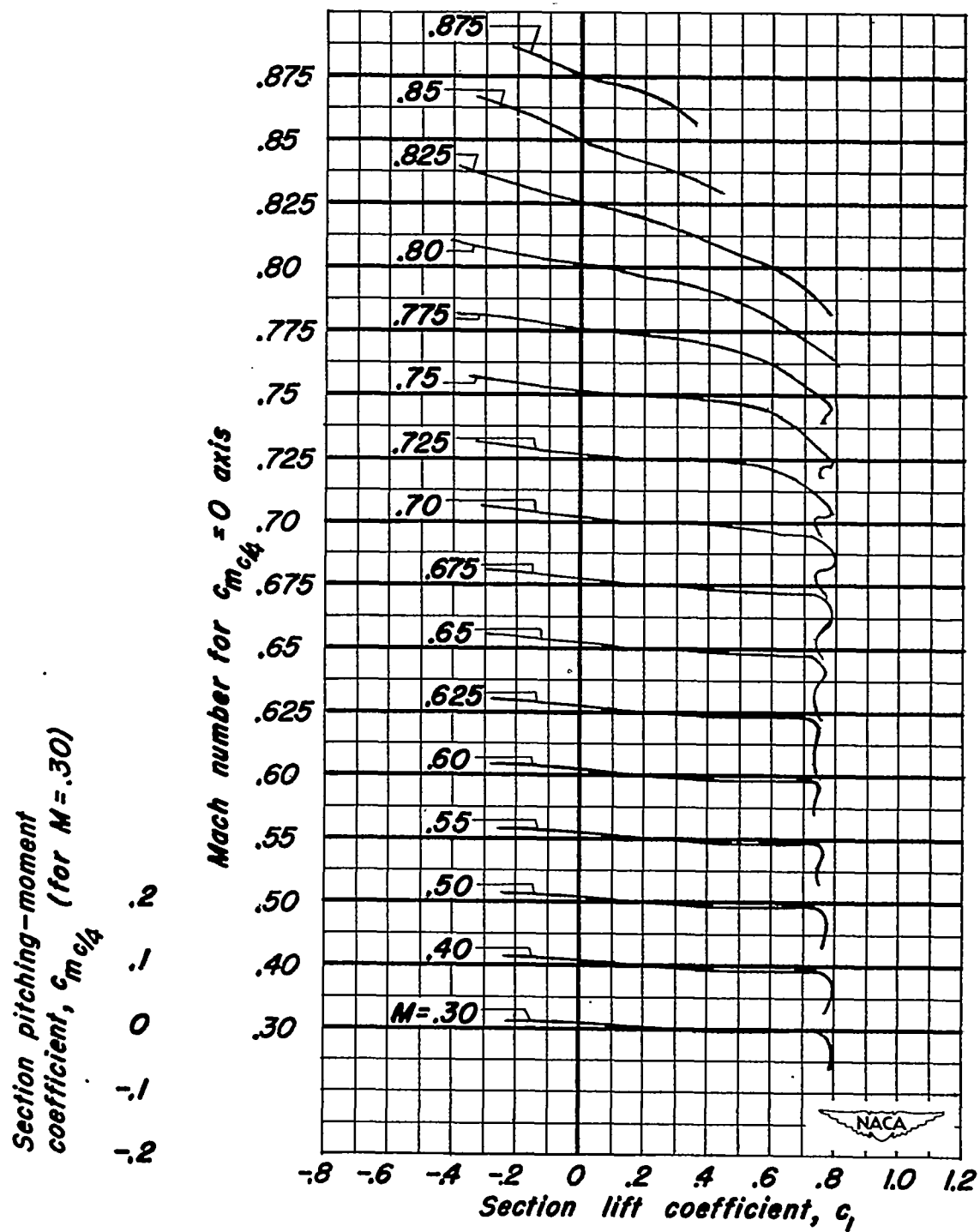
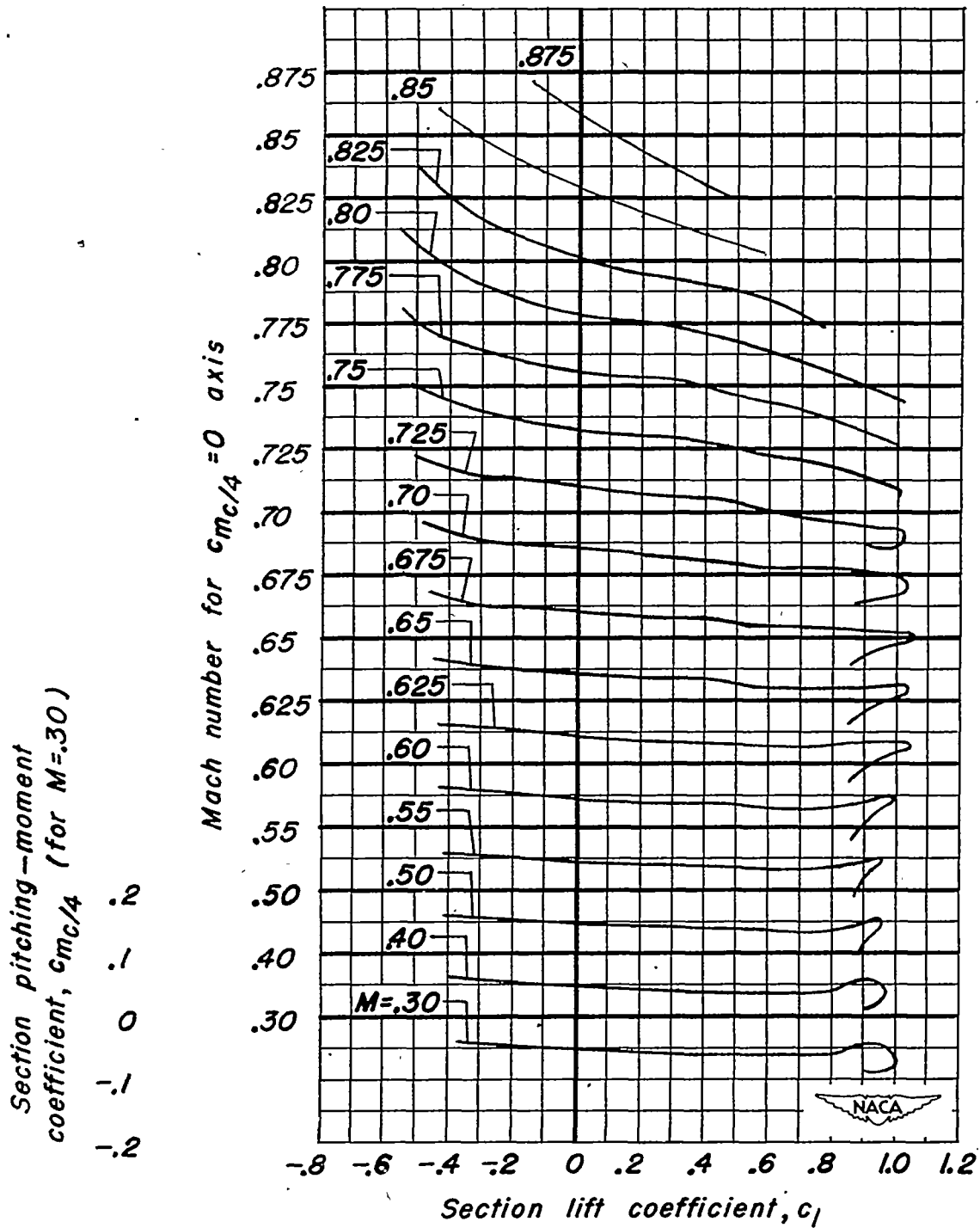


Figure 17.- The effect of the amount of camber on section lift-drag ratio .



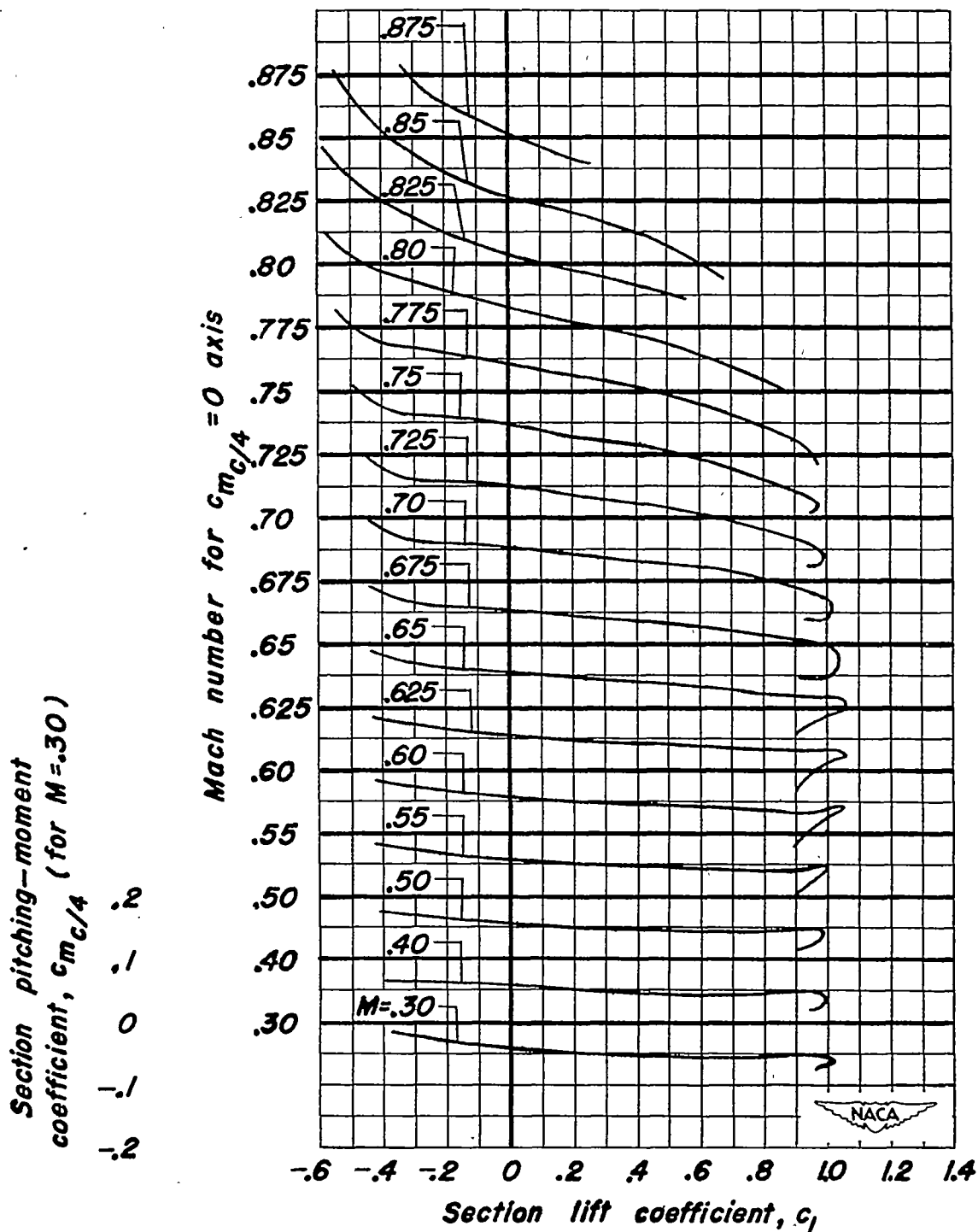
(a) NACA 64A010 airfoil section.

Figure 18.- Variation of section pitching-moment coefficient with section lift coefficient at various Mach numbers.



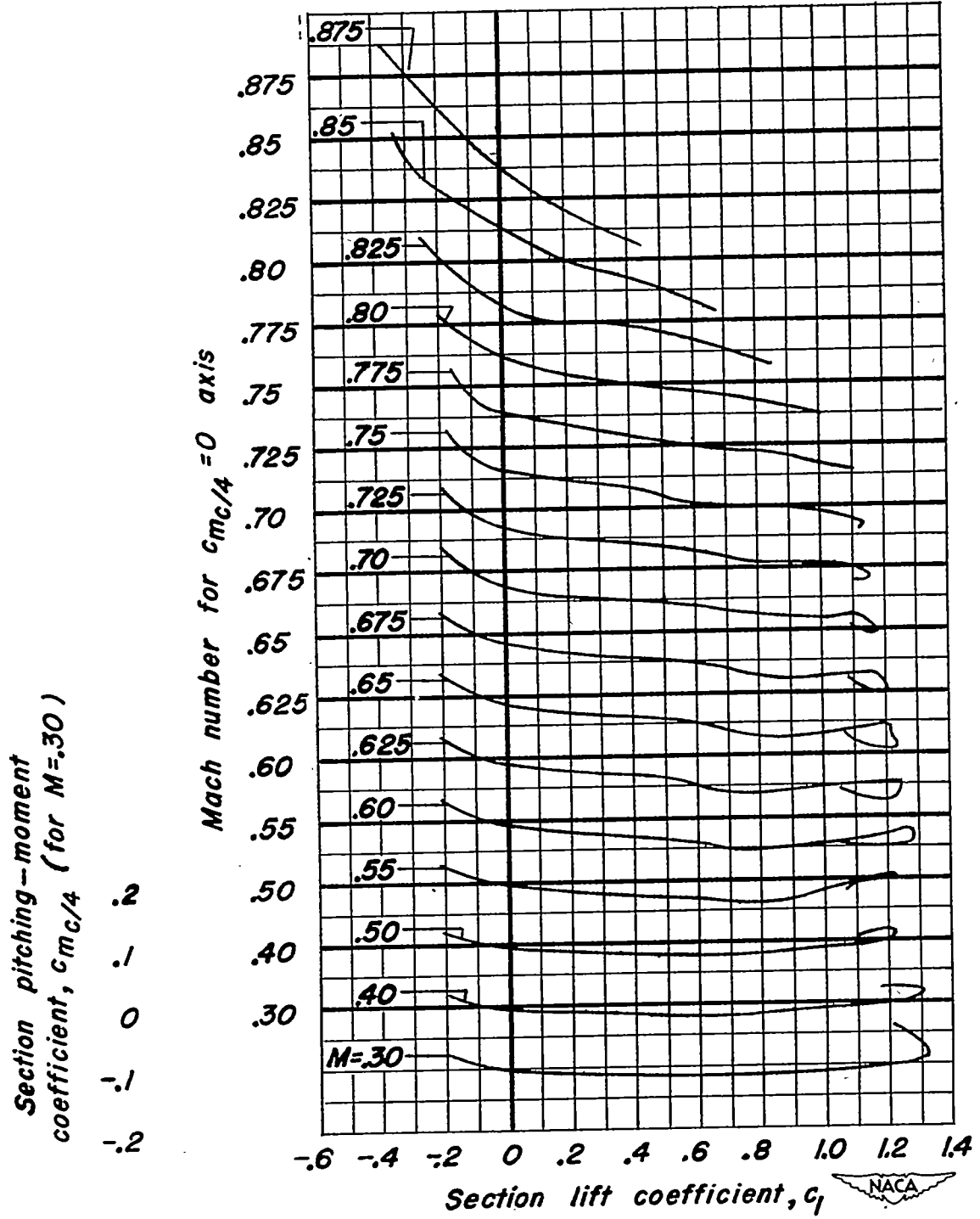
(b) NACA 64A310 airfoil section.

Figure 18.- Continued



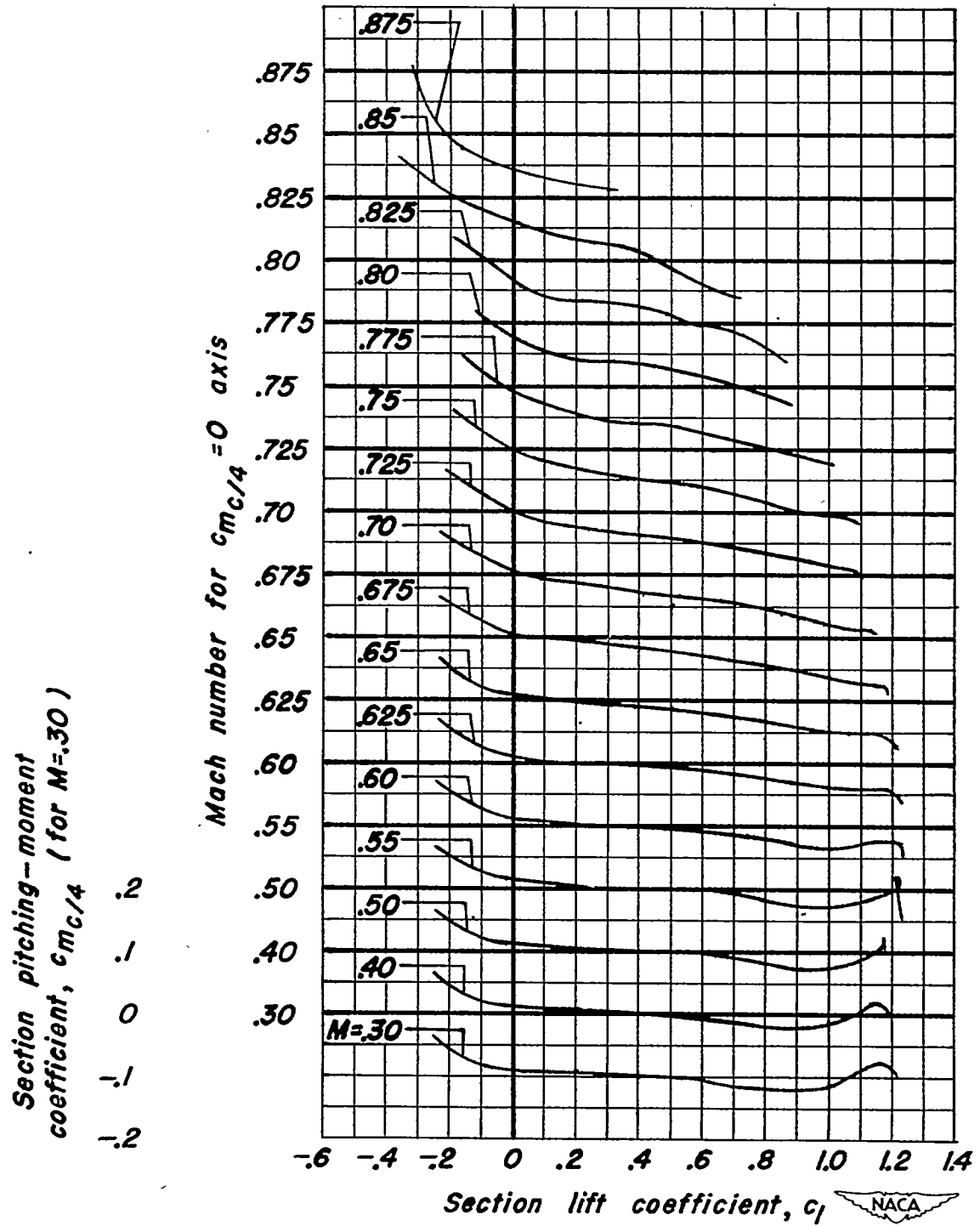
(c) NACA 64A310, $\alpha = 0.4$ airfoil section.

Figure 18.- Continued



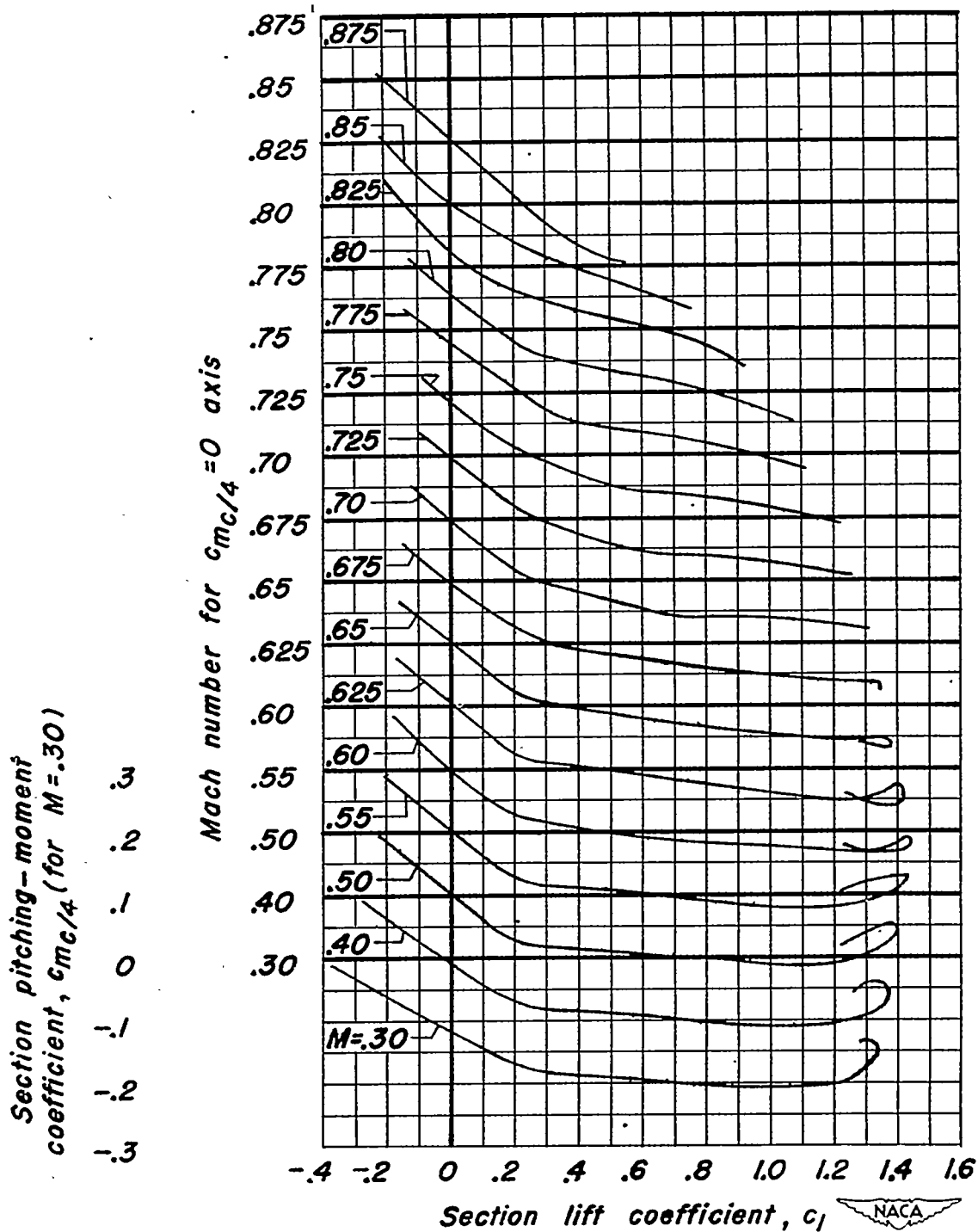
(d) NACA 64A610 airfoil section .

Figure 18.- Continued .



(e) NACA 64A610, $\alpha=0.4$ airfoil section.

Figure 18.- Continued .



(f) NACA 64A910 airfoil section.

Figure 18.- Concluded.